

**Magnetic resonance imaging
to characterize
chronic inflammatory neuropathies**

Marieke H.J. van Rosmalen

Magnetic resonance imaging to characterize chronic inflammatory neuropathies

© Marieke H.J. van Rosmalen, 2021

ISBN: 978-94-6416-763-4

All rights reserved. No part of this thesis may be reproduced or transmitted in any form or by any means without written permission of the author.

The Prinses Beatrix Spierziekten Foundation funded this work and publication of this thesis.

Cover design and layout: © evelienjagtman.com

Printing: Ridderprint | www.ridderprint.nl

Magnetic resonance imaging to characterize chronic inflammatory neuropathies

Het karakteriseren van chronische inflammatoire neuropathieën
door middel van magnetic resonance imaging (MRI)
(met een samenvatting in het Nederlands)

Proefschrift

ter verkrijging van de graad van doctor aan de Universiteit Utrecht
op gezag van de rector magnificus, prof. dr. H.R.B.M. Kummeling,
ingevolge het besluit van het college voor promoties in het openbaar te verdedigen
op donderdag 4 november 2021 des middags te 14.15 uur

door

Marieke Helena Johanna van Rosmalen
geboren op 27 maart 1990 te Rosmalen

Promotoren prof. dr. W.L. van der Pol
prof. dr. J. Hendrikse

Copromotoren dr. H.S. Goedee
dr. ir. M. Froeling

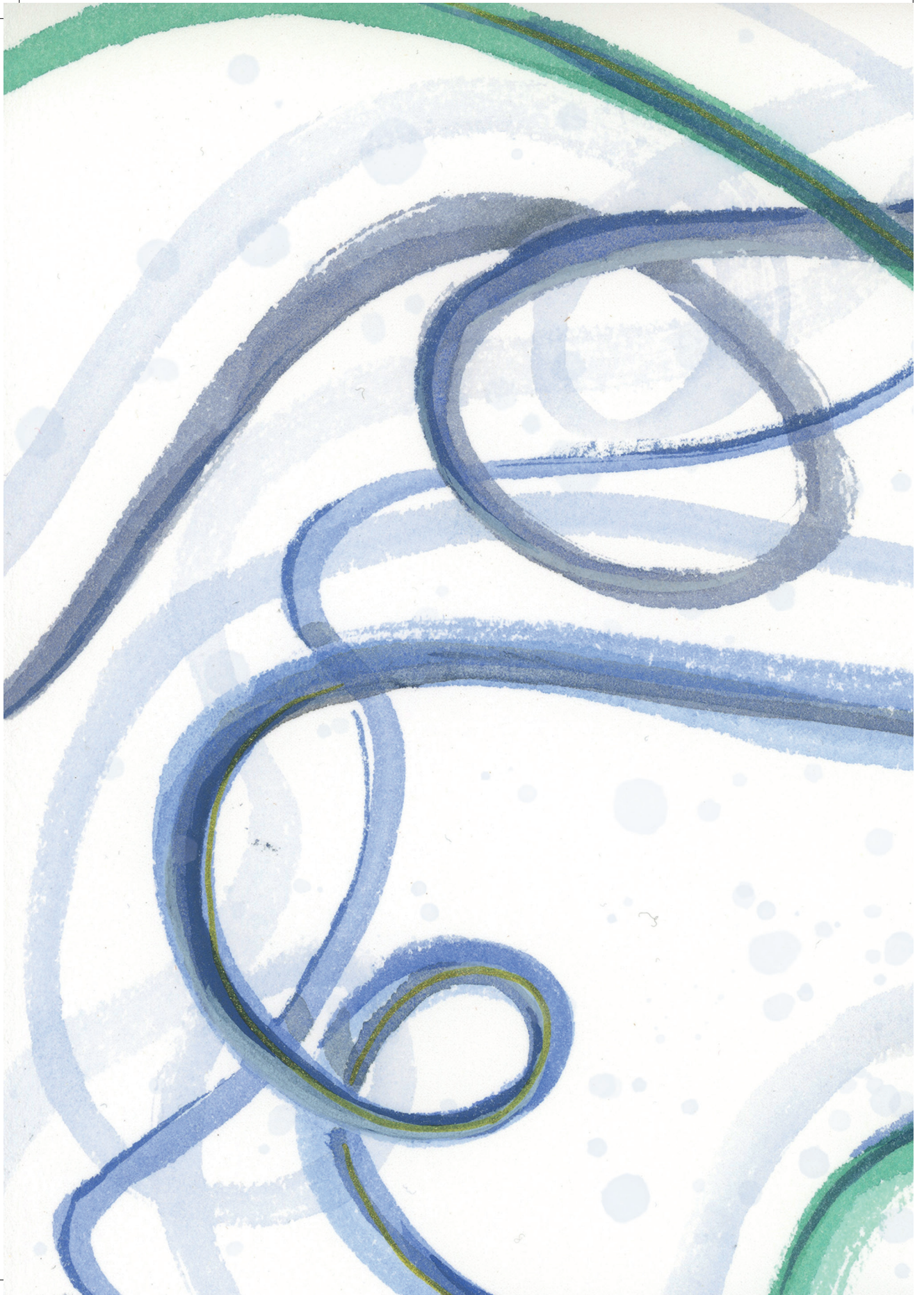
The research described in this thesis was supported by a grant of the Prinses Beatrix Spierfonds (W.OR17-21). Financial support by the Prinses Beatrix Spierfonds for the publication of this thesis is gratefully acknowledged.

Voor papa en mama



CONTENTS

Chapter 1	General introduction and thesis outline	9
Chapter 2	Clinical outcomes in multifocal motor neuropathy: a combined cross-sectional and follow-up study	25
Chapter 3	Low inter-rater reliability of brachial plexus MRI in chronic inflammatory neuropathies	43
Chapter 4	Quantitative assessment of brachial plexus MRI for the diagnosis of chronic inflammatory neuropathies	55
Chapter 5	MRI of the intraspinal nerve roots in patients with chronic inflammatory neuropathies: abnormalities correlate with clinical phenotypes	75
Chapter 6	Quantitative MRI of the brachial plexus shows specific changes in nerve architecture in CIDP, MMN and motor neuron disease	91
Chapter 7	Quantitative MRI of the brachial plexus in CIDP and MMN: a longitudinal cohort study	111
Chapter 8	General discussion	127
Addendum	Nederlandse samenvatting	157
	Review comité	165
	Dankwoord	167
	Publicatielijst	173
	Curriculum Vitae	175





Chapter 1

**General introduction
and thesis outline**



POLYNEUROPATHIES



The peripheral nervous system consists of the alpha motor neurons in the anterior horn of the spinal cord, ventral and dorsal roots, peripheral nerves, the neuromuscular junction and muscle. Peripheral nerves connect the brain and spinal cord with muscle, skin, joints and sensory organs. Dysfunction of the peripheral nerves has many causes, but is generally described as ‘polyneuropathy’. Complaints caused by polyneuropathies include weakness and sensory deficits including numbness, sensory ataxia and changed or increased pain sensations in hands and feet. Common causes for polyneuropathy are summarized in **Table 1.1** and include drugs and alcohol, diabetes, liver or renal insufficiency, (vitamin) deficiencies and idiopathic. Rare causes are of a genetic or inflammatory nature. Discriminating between these multiple causes is of great importance, as treatment opportunities and prognosis can vary between neuropathies.

In the diagnostic work-up of patients suspected to have a polyneuropathy, laboratory findings and nerve conduction studies are important tools. Rare causes may be more elusive and require special diagnostic techniques, including genetic testing and nerve imaging by means of ultrasound or magnetic resonance imaging (MRI). Imaging techniques may be particularly helpful for the identification of the rare chronic inflammatory neuropathies.

Table 1.1. Causes of polyneuropathy

Type of origin	Causes
Carcinoma	Lymphoma
Hereditary	Charcot-Marie-Tooth disease, hereditary neuropathy with liability to pressure palsies, neurofibromatosis
Idiopathic	Chronic idiopathic axonal polyneuropathy
Infectious	Leprosy, Lyme’s disease, HIV
Inflammatory	Chronic inflammatory demyelinating polyneuropathy (typical and variants), Guillain-Barré syndrome, multifocal motor neuropathy
Metabolic	Diabetes mellitus, hypothyroidism, liver insufficiency, porphyria, renal insufficiency, vitamin deficiencies
Paraneoplastic	Small cell lung cancer
Paraproteinemic	anti-MAG associated polyneuropathy, IgM-monoclonal gammopathy of unknown significance, polyneuropathy organomegaly endocrinopathy M-protein and skin changes syndrome, Waldenström
Systemic diseases	Amyloidosis, rheumatoid arthritis, sarcoidosis, Sjögren’s syndrome, systemic lupus erythematosus
Toxic	Alcohol abuse, drug associated (antimicrobials, amiodarone, chemotherapy, digoxin, immunosuppressants), toxins (botulinum toxin, lead, mercury)
Vasculitic	Microscopic polyangiitis, non-systemic vasculitic neuropathy, polyarteriitis nodosa

An overview of causes of peripheral polyneuropathy. Only some examples are shown per type of origin.

CLINICAL BACKGROUND

Chronic inflammatory neuropathies

Chronic inflammatory demyelinating polyneuropathy (CIDP) and multifocal motor neuropathy (MMN) are both rare polyneuropathies with an inflammatory cause. CIDP is characterized by slowly progressive (mostly) symmetric pure motor, pure sensory, or mixed deficits that are most pronounced in the legs, while MMN is marked by asymmetric weakness without sensory deficits that dominates in the arms. Both polyneuropathies respond to treatment.^{1,2} Early treatment can improve muscle strength or sensory symptoms, and prevents progression of symptoms and permanent axonal damage which underlines the importance of a timely diagnosis.^{1,2} Patients with CIDP and MMN both respond to treatment with immunoglobulins. Patients with CIDP, but not with MMN, also respond to treatment with corticosteroids or plasmapheresis. Another important difference between these disorders is that 26% of patients with CIDP may experience remission that allows discontinuation of treatment, while this is uncommon in MMN.³

Diagnosis of CIDP and MMN is based on diagnostic consensus criteria that use a combination of clinical phenotype, nerve conduction study results and ancillary investigations.^{4,5} The latter play an important role when nerve conduction studies do not meet the required electrodiagnostic criteria.⁴⁻⁷ They include laboratory findings and imaging abnormalities of the peripheral nerves, in particular MRI of the brachial plexus.

TECHNICAL BACKGROUND

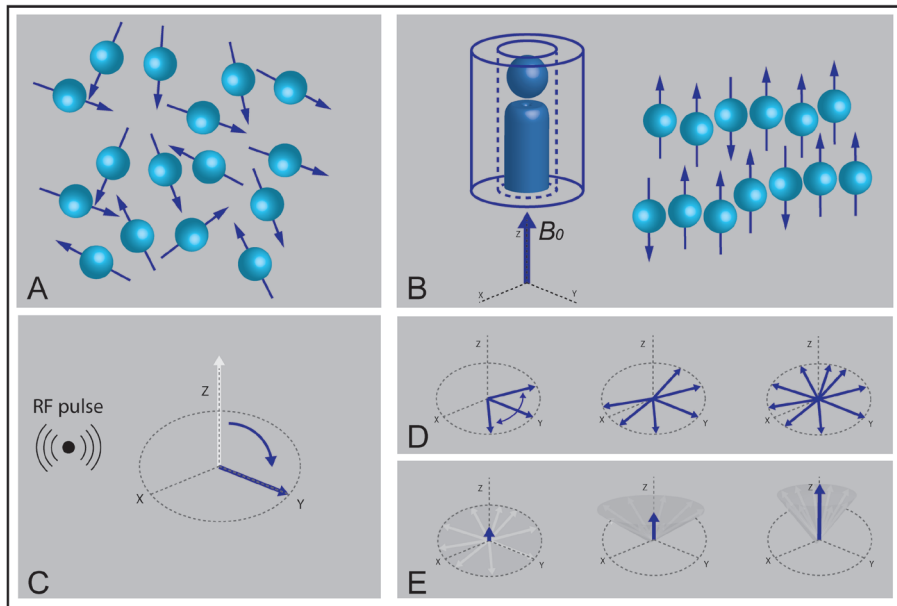
Principles of MRI physics

Magnetic resonance imaging is an imaging technique that is able to visualize pathology of the nervous system. It is widely used in clinical practice for examination of the brain, spinal cord, muscle and more recently also the peripheral nervous system. Physics of MRI is complicated but some knowledge on its principles is essential to correctly assess and interpret the images. In short, all protons in body tissue spin on their own axes (**Figure 1.1A**). After placing the patient in a static magnetic field, i.e. the MRI scanner, the resulting *magnetization* of all protons inside the patients' tissue align parallel to the magnetic field (**Figure 1.1B**). These protons rotate around the long axis of the primary magnetic field (B_0), which is called precession. Precession rate is termed as the *Larmor frequency*. The average of many protons produces the *net magnetization*. Then, a radiofrequency pulse is emitted from the scanner which creates a magnetic field perpendicular to B_0 (**Figure 1.1C**). When the radiofrequency pulse is at resonance, it creates a phase coherence in the precession of all the proton spins. The net magnetization of all protons rotating in Larmor frequency generates an electric current in the receiving coil, i.e. an electrical conductor, that is placed in the vicinity of the tissue of interest. This current is the *nuclear magnetic resonance (NMR) signal*. The NMR

signal weakens due to two simultaneous relaxation processes that cause a loss of coherence of the spin system. The NMR signal decreases (loss of transverse magnetization or dephasing) with a time constant called the *transverse relaxation time* (T_2 , **Figure 1.1D**). Concurrently, but much slower, the vector relaxes towards its equilibrium position (recovery of longitudinal magnetization) parallel to the magnetic field: this time constant is called the *spin-lattice relaxation time* (T_1 , **Figure 1.1E**).



Figure 1.1 Principles of MRI physics

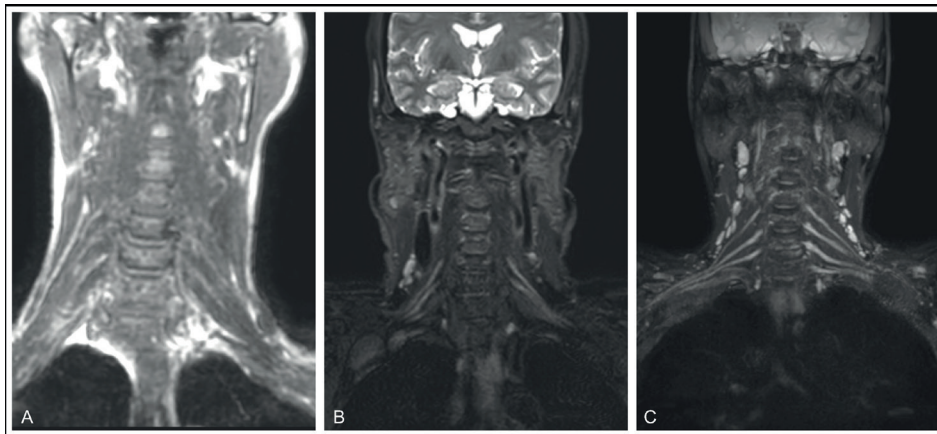


All protons in body tissue spin on their own axes (A). After placing the patient in a static magnetic field, i.e. the MRI scanner, the resulting magnetization of all protons align parallel (B) to the magnetic field (B_0). The protons rotate around B_0 at the Larmor frequency and the average of many protons produces the net magnetization. Then, a radiofrequency pulse (RF pulse) is emitted from the scanner which creates a magnetic field perpendicular to B_0 and the net magnetization moves away from the z axis (C). As soon as the RF pulse is switched off, the protons begin to relax back to their equilibrium. The two main features of relaxation are dephasing of the spins or loss of transverse magnetization (T_2 relaxation, D) and realignment along the z axis (T_1 relaxation) as an umbrella closing up (E).

Every type of body tissue has its own T_1 and T_2 relaxation times which results in different contrasts in the images. Adjustments in the MRI software enables the scanner to generate T_1 - or T_2 -weighted images of the tissues of interest. T_1 - and T_2 -weighted MRI provides qualitative information on the anatomical structures of interest. The generation of a T_1 -weighted image or a T_2 -weighted image depends on the set echo time (TE) and repetition time (TR) of the MRI sequence. T_1 -weighted images tend to have a short TE and a short TR. In T_1 -weighted images tissues that have a slow magnetization

realignment appear dark as it does not retain signal (**Figure 1.2A**). T2-weighted images require a long TE and TR and highlight differences in the T2 relaxation times of tissues. Tissues with a longer T2 relaxation time will retain signal and appear bright (**Figure 1.2B**). MRI of the peripheral nervous system, e.g. the brachial or lumbosacral plexus, is often based on T2-weighted images. T2-weighted imaging with fat suppression (e.g. spectral presaturation with inversion recovery (or SPIR)) is an excellent technique to visualize pathology of peripheral nerves, and the brachial or lumbosacral plexus (**Figure 1.2C**).⁸

Figure 1.2 Basic pulse sequences of MRI



Examples of the healthy brachial plexus visualized in a T1 weighted image (A), a T2 weighted image (B) and T2 weighted imaging with fat suppression (C).

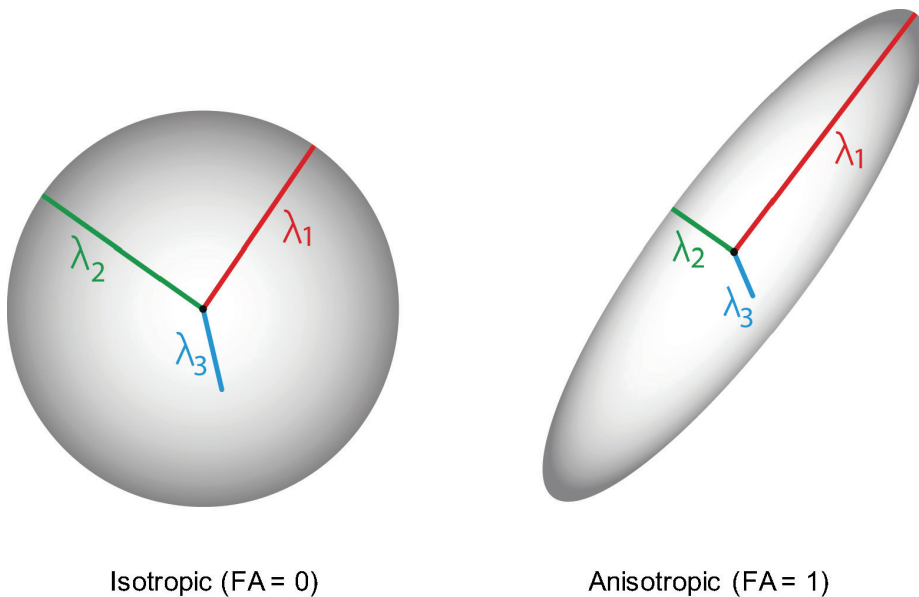
Quantitative MRI techniques

MRI is a versatile technique that can provide qualitative as well as quantitative information on (nervous) tissues. T1- and T2-weighted imaging, as described in the previous paragraph, provides qualitative information on anatomical tissues and generates an image. Advanced quantitative MRI techniques do not only produce an image, but also generate a quantitative parameter. One of these quantitative techniques is diffusion tensor imaging (DTI). DTI gives quantitative information on microstructural integrity that correlates with histological findings.⁹⁻¹¹ DTI measures diffusion of water in tissue in a number of different directions. Diffusion rates of biological tissues are not the same in every direction, which means the tissue is not isotropic but rather *anisotropic*. The direction and magnitude of the diffusion can be expressed by the diffusion tensor. From this diffusion tensor eigenvalues and eigenvectors can be derived. Eigenvectors express the direction of the diffusion, and eigenvalues express the magnitude of the diffusion. In this way, the degree of diffusion of water can be calculated along the main axis (axonal diffusivity, AD) or perpendicular to the nervous tissue (radial diffusivity, RD). AD is determined by the eigenvalue λ_1 and RD is determined by the mean of the eigenvalues λ_2 and λ_3 (**Figure 1.3**). The mean diffusivity (MD) is calculated by the mean of



the eigenvalues $(\lambda_1 + \lambda_2 + \lambda_3)/3$. Anisotropy is expressed as the ‘fractional anisotropy’ (FA) and can be calculated using a mathematical formula that contains all eigenvalues. FA is a scalar value that ranges from 0 to 1 (**Figure 1.3**). Pure water has isotropic diffusion properties, which means that the water molecules are equally likely to move in any direction, hence $FA = 0$. For tissues that have very strong anisotropy $FA = 1$, i.e. diffusion is restricted by the presence of cell membranes and there may be a preferential direction, for example along nerve fibers. As MD and FA are summary measures of the eigenvalues λ_1 , λ_2 and λ_3 , changes in MD and FA can be driven by changes in either AD or in RD. For example, an increase of AD or a decrease of RD both cause an increase of FA, and a decrease of AD or RD both cause a decrease of MD.

Figure 1.3 Principles of diffusion parameters



Isotropic diffusion (left): water molecules are equally likely to move in any direction and fractional anisotropy is 0. Anisotropic diffusion (right): water molecules move in a preferential direction and fractional anisotropy is 1.

Other quantitative MRI techniques as T2 mapping and fat fraction analysis can provide information on T2 relaxation times and fat fraction percentage of a tissue. T2 mapping relies on the principle that different echo times result in different T2 contrasts in images. By plotting the signal intensity for different echo times an exponential decay curve can be constructed. The T2 relaxation time can be calculated as a constant of the fitted curve. In this way, the T2 relaxation time can be calculated for the tissue of interest. Fat fraction analysis relies on the fact that water and fat contain protons that can be measured using Dixon imaging (chemical shift imaging). Protons in fat rotate at a different Larmor frequency than protons in water. A minimum of two images, i.e. one *in phase* and one *out of*

phase, are necessary to calculate the percentage of fat. The first image is acquired when water and fat have the same phase, i.e. they rotate in phase, and the total signal can be calculated by the sum of the signal of water and the signal of fat. Next, a second image is acquired when the protons are in opposed phase, i.e. they are out of phase, and the total signal contains the signal of water minus the signal of fat. In this way, the percentage of water and the percentage of fat of the total signal of a tissue can be calculated.

Injured or inflamed tissue may lead to changes in the diffusion parameters, for example by increasing or decreasing AD or RD, and changes in T2 relaxation times and fat fraction. Measuring and comparing quantitative MRI parameters between groups of patients and (healthy) controls, and correlating the found differences to histology or clinical data, may help in diagnosis, pathophysiology or prognosis of disease. Combined, these quantitative techniques inform on structural nerve changes due to pathophysiological processes.

CIDP, MMN & MRI

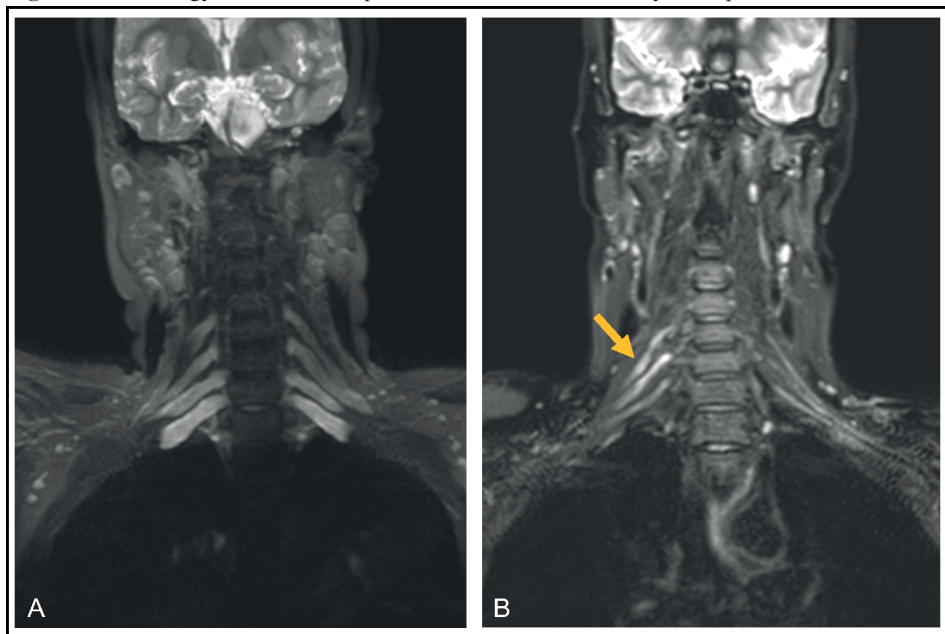
Diagnosis

In current clinical practice diagnosis of CIDP and MMN is predominantly based on the consensus criteria of the guideline of the European Federation of Neurological Societies/Peripheral Nerve Society and the Utrecht criteria.^{4,5,7} It is important to differentiate CIDP and MMN from their clinical mimics as an early start of immunomodulatory treatment in CIDP and MMN could prevent irreversible (axonal) damage and worsening of symptoms.^{1,2} Differential diagnosis of (typical and variants of) CIDP includes Guillain-Barré syndrome, motor neuron diseases, focal compression neuropathies, diabetic neuropathy and Charcot-Marie-Tooth disease.¹² MMN is an important clinical mimic of motor neuron diseases, such as amyotrophic lateral sclerosis and progressive muscular atrophy, as they all can present with an asymmetric weakness without sensory deficits. However, treatment and prognoses differ considerably and the use of diagnostic consensus guidelines may help in the differentiation. These guidelines for CIDP and MMN describe that diagnosis is primarily based on a characteristic clinical presentation and specific features on nerve conduction studies, i.e. conduction blocks. These conduction blocks are believed to be caused by demyelination, in particular in CIDP, or axolemmal changes.¹³ However, diagnosing CIDP or MMN often remains challenging as nerve conduction studies require specific expertise, cost a lot of time and are often burdensome to patients. Conduction blocks could be easily missed, which compromises diagnostic accuracy.⁶ In more elusive cases, supportive criteria may help in diagnosis. One of the additional diagnostic tools is laboratory examination which may show an increased protein in the cerebrospinal fluid or presence of anti-GM1 antibodies (MMN only).^{4,5} Second, a good response to immunomodulatory treatment may add to diagnosis although this criterium is seriously hampered by costs, the risk of adverse events in patients and the lack of a clear definition of treatment response. MRI of the brachial



plexus is in the current diagnostic guidelines the last supportive criterium and may show thickening of the cervical nerve roots (**Figure 1.4A**) or T2 hyperintensity (**Figure 1.4B**) in patients with CIDP or MMN.^{14,15} Enhancement of the nerve roots could be seen in patients with CIDP after injection with gadolinium but is less common and the diagnostic value is low.¹⁶ Abnormalities on brachial plexus MRI are more frequently present in patients with CIDP (74% of patients) than in patients with MMN (50% of patients).¹⁶ Asymmetrical thickening of the nerve roots seems to be more common in patients with MMN compared to patients with CIDP.¹⁷

Figure 1.4 Pathology of the brachial plexus in chronic inflammatory neuropathies



In the left panel (A) an example of thickening of the cervical nerve roots is shown (for example compared to figure 1.2C) using T2-weighted imaging with fat suppression. In the right panel (B) an example of T2 hyperintensity (yellow arrow) is shown using T2-weighted imaging.

A major drawback of current clinical practice is that brachial plexus MRI is qualitatively assessed by (neuro)radiologists. Obviously enlarged cervical nerve roots are easily seen but less evident thickening may result in an uncertain and subjective assessment as clear cut-off values for nerve size are lacking. Furthermore, variability and reliability of these qualitative assessments are unknown which hampers the diagnostic value of brachial plexus MRI even more. A systematic assessment with quantitative cut-off values for cervical nerve root size, and a comparison of interrater reliabilities between qualitative and quantitative assessments, is needed if we want to improve the diagnostic value of brachial plexus MRI for the diagnosis of CIDP and MMN.

More recently, nerve ultrasound has been explored as another imaging technique in diagnosis of chronic inflammatory neuropathies.^{18,19} These studies showed that a quantitative assessment, i.e. with objective cut-off values for abnormality, results in good test characteristics. Just as MRI, nerve ultrasound may show thickening of the brachial plexus and peripheral nerves. Unfortunately, nerve ultrasound is not yet widely available as its implementation in clinical practice requires experience. However, nerve ultrasound is a promising technique that might be added to the diagnostic criteria in the future. The combined role of nerve ultrasound and MRI in the diagnostic process of chronic inflammatory neuropathies should be evaluated to optimize the diagnostic performance of both imaging modalities.

Pathophysiology

Autopsy studies, sural nerve biopsy and immunostaining *in vitro* have tried to provide insight in underlying immunological mechanisms in CIDP and MMN.²⁰⁻²⁶ The scarce reports on CIDP describe moderate to severe demyelination and remyelination with onion bulbs without loss of axons.^{20-22,27} Some histological studies on MMN describe axonal loss without demyelination,^{23-25,28} while others describe de- and remyelination.²⁹⁻³¹ There is an obvious need for additional tools to study the condition of peripheral nerves of patients with a chronic inflammatory neuropathy *in vivo*. Therefore, quantitative MRI techniques that correlate to histological findings, such as DTI and T2 mapping are promising. Previous DTI studies evaluated the peripheral nerves and the brachial and lumbosacral plexus in small cohorts of patients with CIDP or MMN and healthy controls.³²⁻⁴⁰ These smaller studies already showed differences in diffusion parameters and T2 relaxation times between groups which suggests that quantitative MRI techniques could be helpful to explore pathophysiologies further. However, large and systematic studies are currently lacking.

Prognosis and treatment

Patients with CIDP and MMN both respond to immunomodulatory treatment. For patients with MMN intravenous or subcutaneous immunoglobulins is the only treatment option; patients with CIDP may also respond to treatment with corticosteroids or plasmapheresis.^{1,2} Treatment may improve motor and sensory deficits but management of treatment is challenging in current clinical practice. These challenges mainly rely on the fact that treatment response is not easily monitored as it lacks a clear definition. Therefore, it might be difficult to find the right treatment dose in some patients, which could result in over- or undertreatment.

In current clinical practice, improvement of muscle strength as measured by MRC scales, myometry or equivalent tests is assumed to be the golden standard of treatment response but strength measurements might be subject to differences between raters. Objective markers that predict course of disease and treatment response are lacking. However, these biomarkers are needed if we want to improve management of CIDP and MMN.

The value of electrophysiology and nerve ultrasound as biomarkers have been studied previously. These efforts did not result in the identification of quantitative measures that correlate to clinical outcomes or prognosis (unpublished data from our center).⁴¹⁻⁴³ Quantitative MRI techniques, such as DTI, are a potentially powerful tool to monitor tissues. DTI has been explored in several studies of the central nervous system. These studies showed differences in diffusion parameters over time and sometimes showed correlations with clinical parameters.⁴⁴⁻⁴⁹ However, there is only a very limited number of studies of the peripheral nervous system. It is therefore unknown if quantitative MRI captures relevant differences in the peripheral nervous system, for example early treatment effects.



THESIS OUTLINE

The aim of this thesis is to explore the feasibility and value of qualitative and quantitative MRI techniques in diagnosis, pathophysiology, disease course, and treatment response in chronic inflammatory neuropathies. **Chapter 2** contains a description of the natural history of MMN and an analysis of the correlates of a progressive disease course. **Chapter 3** evaluates the interrater variability of current practice, i.e. a qualitative assessment of nerve thickening on brachial plexus MRI. In **Chapter 4** we explore feasibility and diagnostic performance of a quantitative assessment of nerve thickening. In **chapter 5** we study involvement of intraspinal roots in CIDP and MMN. In **chapter 6** we assess the use of quantitative MRI techniques (i.e. DTI, T2 mapping, and fat fraction analysis) and attempts to study nerve architecture in CIDP and MMN *in vivo*. In **chapter 7** we present data of quantitative MRI after one year of follow-up. **Chapter 8** contains a summary and discussion of the main findings of this thesis and provides recommendations for clinical practice.

REFERENCES

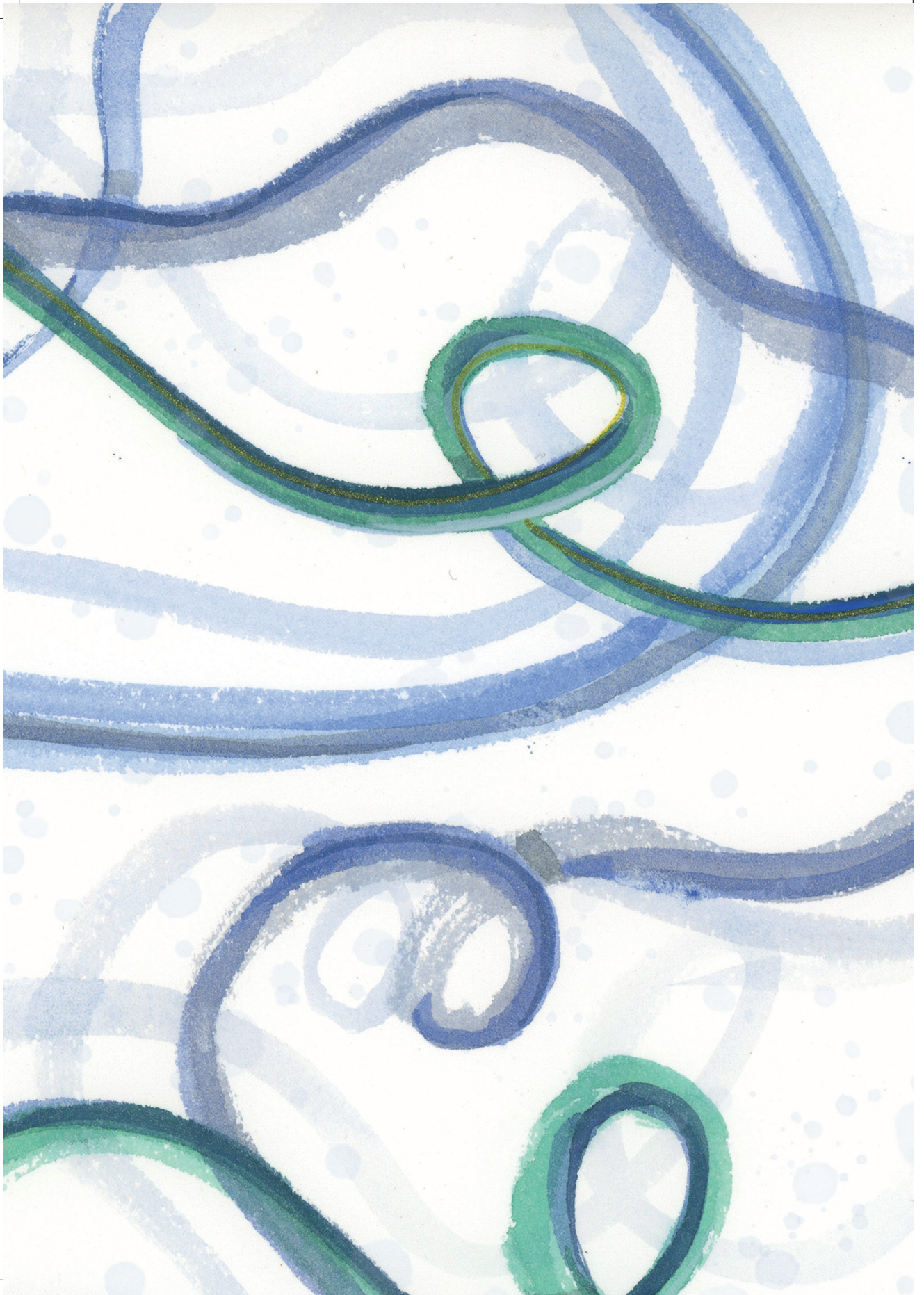
1. Oaklander A, Lunn M, Hughes R, et al. Treatments for chronic inflammatory demyelinating polyradiculoneuropathy (CIDP): An overview of systematic reviews. *Cochrane Database Syst. Rev.* 2017;13:1–33.
2. van Schaik I, van den Berg L, de Haan R, Vermeulen M. Intravenous immunoglobulin for multifocal motor neuropathy. *Cochrane Database Syst. Rev.* 2005;2:920–921.
3. Kuwabara S, Misawa S, Mori M, et al. Long term prognosis of chronic inflammatory demyelinating polyneuropathy: A five year follow up of 38 cases. *J. Neurol. Neurosurg. Psychiatry* 2006;77:66–70.
4. van den Bergh PYK, Hadden RDM, Bouche P, et al. European Federation of Neurological Societies/Peripheral Nerve Society Guideline on management of chronic inflammatory demyelinating polyradiculoneuropathy: Report of a joint task force of the European Federation of Neurological Societies and the Peripher. *Eur. J. Neurol.* 2010;17:356–363.
5. Vlam L, Van Der Pol WL, Cats EA, et al. Multifocal motor neuropathy: Diagnosis, pathogenesis and treatment strategies. *Nat. Rev. Neurol.* 2012;8:48–58.
6. Allen JA, Lewis RA. CIDP diagnostic pitfalls and perception of treatment benefit. *Neurology* 2015;85:498–504.
7. Van Schaik IN, Léger JM, Nobile-Orazio E, et al. European Federation of Neurological Societies/Peripheral Nerve Society Guideline on management of multifocal motor neuropathy. Report of a Joint Task Force of the European Federation of Neurological Societies and the Peripheral Nerve Society - First revis. *J Peripher Nerv Syst* 2010;15:295–301.
8. Chhabra A, Zhao L, Carrino JA, et al. MR Neurography: Advances. *Radiol. Res. Pract.* 2013;2013:1–14.
9. Song SK, Sun SW, Ramsbottom MJ, et al. Dysmyelination revealed through MRI as increased radial (but unchanged axial) diffusion of water. *Neuroimage* 2002;17:1429–1436.
10. Song SK, Sun SW, Ju WK, et al. Diffusion tensor imaging detects and differentiates axon and myelin degeneration in mouse optic nerve after retinal ischemia. *Neuroimage* 2003;20:1714–1722.
11. Morisaki S, Kawai Y, Umeda M, et al. In vivo assessment of peripheral nerve regeneration by diffusion tensor imaging. *J. Magn. Reson. Imaging* 2011;33:535–542.
12. Neligan A, Reilly MM, Lunn MP. CIDP: Mimics and chameleons. *Pract. Neurol.* 2014;14:399–408.
13. Van Asseldonk JTH, Van Den Berg LH, Kalmijn S, et al. Criteria for demyelination based on the maximum slowing due to axonal degeneration, determined after warming in water at 37°C: Diagnostic yield in chronic inflammatory demyelinating polyneuropathy. *Brain* 2005;128:880–891.
14. van Es HW, van den Berg LH, Franssen H, et al. Magnetic resonance imaging of the brachial plexus in patients with multifocal motor neuropathy. *Neurology* 1997;48:1218–1224.
15. Castillo M, Mukherji SK. MRI of enlarged dorsal ganglia, lumbar nerve roots, and cranial nerves in polyradiculoneuropathies. *Neuroradiology* 1996;38:516–520.
16. Goedee HS, Jongbloed BA, van Asseldonk J-TH, et al. A comparative study of brachial plexus sonography and magnetic resonance imaging in chronic inflammatory demyelinating neuropathy and multifocal motor neuropathy. *Eur. J. Neurol.* 2017;24:1307–1313.
17. Jongbloed BA, Bos JW, Rutgers D, et al. Brachial plexus magnetic resonance imaging differentiates between inflammatory neuropathies and does not predict disease course. *Brain Behav.* 2017;7:e00632.
18. Goedee HS, Van Der Pol WL, Van Asseldonk JTH, et al. Diagnostic value of sonography in treatment-naive chronic inflammatory neuropathies. *Neurology* 2017;88:143–151.

19. Herraets IJT, Goedee HS, Telleman JA, et al. Nerve ultrasound for the diagnosis of chronic inflammatory neuropathy: a multicenter validation study. *Neurology* 2020;95:e1745–e1753.
20. Matthews WB, Howell DA, Hughes RC. Relapsing corticosteroid-dependent polyneuritis. *J. Neurol. Neurosurg. Psychiatry* 1970;33:330–337.
21. Torvik A, Lundar T. A case of chronic demyelinating polyneuropathy resembling the Guillan-Barré Syndrome. *J. Neurol. Sci.* 1977;32:45–52.
22. Matsuda M, Ikeda SI, Sakurai S, et al. Hypertrophic neuritis due to chronic inflammatory demyelinating polyradiculoneuropathy (CIDP): A postmortem pathological study. *Muscle and Nerve* 1996;19:163–169.
23. Krarup C, Stewart JD, Sumne AJ, et al. A syndrome of asymmetric limb weakness with motor conduction block. *Neurology* 1990;40:118–127.
24. Adams D, Kuntzer T, Steck AJ, et al. Motor conduction block and high titres of anti-GM1 ganglioside antibodies: Pathological evidence of a motor neuropathy in a patient with lower motor neuron syndrome. *J. Neurol. Neurosurg. Psychiatry* 1993;56:982–987.
25. Veugelers B, Theys P, Lammens M, et al. Pathological findings in a patient with amyotrophic lateral sclerosis and multifocal motor neuropathy with conduction block. *J. Neurol. Sci.* 1996;136:64–70.
26. Harschnitz O, van den Berg LH, Johansen LE, et al. Autoantibody pathogenicity in a multifocal motor neuropathy induced pluripotent stem cell-derived model. *Ann. Neurol.* 2016;80:71–88.
27. Sasaki M, Ohara S, Oide T, et al. An autopsy case of chronic inflammatory demyelinating polyradiculoneuropathy with respiratory failure. *Muscle and Nerve* 2004;30:382–387.
28. Taylor B V., Dyck PJB, Engelstad JN, et al. Multifocal Motor Neuropathy: Pathologic Alterations at the Site of Conduction Block. *J. Neuropathol. Exp. Neurol.* 2004;63:129–137.
29. Auer RN, Bell RB, Lee MA. Neuropathy with Onion Bulb Formations and Pure Motor Manifestations. *Can. J. Neurol. Sci. / J. Can. des Sci. Neurol.* 1989;16:194–197.
30. Kaji R, Oka N, Tsuji T, et al. Pathological findings at the site of conduction block in multifocal motor neuropathy. *Ann. Neurol.* 1993;33:152–158.
31. Corbo M, Abouzahr MK, Latov N, et al. Motor nerve biopsy studies in motor neuropathy and motor neuron disease. *Muscle and Nerve* 1997;20:15–21.
32. Kakuda T, Fukuda H, Tanitame K, et al. Diffusion tensor imaging of peripheral nerve in patients with chronic inflammatory demyelinating polyradiculoneuropathy: A feasibility study. *Neuroradiology* 2011;53:955–960.
33. Mathys C, Aissa J, Zu Hörste GM, et al. Peripheral Neuropathy: Assessment of Proximal Nerve Integrity By Diffusion Tensor Imaging. *Muscle Nerve* 2013;48:889–896.
34. Markvardsen LH, Vaeggemose M, Ringgaard S, Andersen H. Diffusion tensor imaging can be used to detect lesions in peripheral nerves in patients with chronic inflammatory demyelinating polyneuropathy treated with subcutaneous immunoglobulin. *Neuroradiology* 2016;58:745–752.
35. Kronlage M, Pitarokoili K, Schwarz D, et al. Diffusion Tensor Imaging in Chronic Inflammatory Demyelinating Polyneuropathy: Diagnostic Accuracy and Correlation with Electrophysiology. *Invest. Radiol.* 2017;52:701–707.
36. Haakma W, Jongbloed BA, Froeling M, et al. MRI shows thickening and altered diffusion in the median and ulnar nerves in multifocal motor neuropathy. *Eur. Radiol.* 2017;27:2216–2224.
37. Lichtenstein T, Sprenger A, Weiss K, et al. MRI biomarkers of proximal nerve injury in CIDP. *Ann. Clin. Transl. Neurol.* 2018;5:19–28.
38. Oudeman J, Eftimov F, Strijkers GJ, et al. Diagnostic accuracy of MRI and ultrasound in chronic immune-mediated neuropathies. *Neurology* 2020;94:e62–e74.
39. Hiwatashi A, Togao O, Yamashita K, et al. Simultaneous MR neurography and apparent T2 mapping in brachial plexus: Evaluation



- of patients with chronic inflammatory demyelinating polyradiculoneuropathy. *Magn. Reson. Imaging* 2018;55:112–117.
40. Hiwatashi A, Togao O, Yamashita K, et al. Lumbar plexus in patients with chronic inflammatory demyelinating polyradiculoneuropathy: evaluation with simultaneous T2 mapping and neurography method with SHINKEI. *Br. J. Radiol.* 2018;91:20180501.
 41. Van Asseldonk JTH, Van den Berg LH, Van den Berg-Vos RM, et al. Demyelination and axonal loss in multifocal motor neuropathy: Distribution and relation to weakness. *Brain* 2003;126:186–198.
 42. Vucic S, Black K, Baldassari LE, et al. Long-term effects of intravenous immunoglobulin in CIDP. *Clin. Neurophysiol.* 2007;118:1980–1984.
 43. Iijima M, Yamamoto M, Hirayama M, et al. Clinical and electrophysiologic correlates of IVIg responsiveness in CIDP. *Neurology* 2005;64:1471–1475.
 44. Nowranghi M, Lyketsos C, Leoutsakos J-M, et al. Longitudinal, region-specific course of diffusion tensor imaging measures in mild cognitive impairment and Alzheimer's disease. *Bone* 2013;9:519–528.
 45. Kitamura S, Kiuchi K, Taoka T, et al. Longitudinal white matter changes in Alzheimer's disease: A tractography-based analysis study. *Brain Res.* 2013;1515:12–18.
 46. Genc S, Steward CE, Malpas CB, et al. Short-term white matter alterations in Alzheimer's disease characterized by diffusion tensor imaging. *J. Magn. Reson. Imaging* 2016;43:627–634.
 47. Mayo CD, Mazerolle EL, Ritchie L, et al. Longitudinal changes in microstructural white matter metrics in Alzheimer's disease. *NeuroImage Clin.* 2017;13:330–338.
 48. Sampedro F, Martínez-Horta S, Marín-Lahoz J, et al. Longitudinal intracortical diffusivity changes in de-novo Parkinson's disease: A promising imaging biomarker. *Park. Relat. Disord.* 2019;68:22–25.
 49. Tringale K, Nguyen T, Bahrami N, et al. Identifying early diffusion imaging biomarkers of regional white matter injury as indicators of executive function decline following brain radiotherapy: A prospective clinical trial in primary brain tumor patients. *Radiother Oncol* 2019;132:27–33.





Chapter 2

Clinical outcomes in multifocal motor neuropathy: a combined cross-sectional and follow-up study

Ingrid J.T. Herraets, Marieke H.J. van Rosmalen, Jeroen W. Bos, Ruben P.A. van Eijk, Elies A. Cats, Bas A. Jongbloed, L. Vlam, S. Piepers, J. Thies van Asseldonk, H. Stephan Goedee, Leonard H. van den Berg, W. Ludo van der Pol

Neurology, 2020 Oct; 95, e1979 - e1987

ABSTRACT

Objective: To assess the clinical course of multifocal motor neuropathy (MMN) in a large cohort of patients and to identify predictive factors of a progressive disease course.

Methods: Between May 2015 and February 2016, we collected clinical data from 100 patients with MMN of whom 60 had participated in a nationwide cross-sectional cohort study in 2007. We documented clinical characteristics using standardized questionnaires and performed a standardized neurological examination. We used multiple linear regression analysis to identify factors that correlated with worse outcome.

Results: We found that age of diagnosis (45.2 vs. 48.6 years, $p < 0.02$) significantly increased between 2007 and 2015 – 2016, whereas diagnostic delay decreased with 15 months. Seven out of ten outcome measures deteriorated over time (all $p < 0.01$). Patients who had a lower Medical Research Council (MRC) sum score and absence of one or more reflexes at the baseline visit showed a greater functional loss at follow up ($p = 0.007$ and $p = 0.016$).

Conclusion: Our study shows that MMN is a progressive disease. Although 87% of patients received maintenance treatment, muscle strength, reflexes, vibration sense, and the Self-Evaluation Scale significantly deteriorated over time. Lower MRC sum score and absence of reflexes predicted a more progressive disease course.

INTRODUCTION

Multifocal motor neuropathy (MMN) is a pure motor disorder characterized by slowly progressive asymmetric distal weakness mainly in the hands, the absence of upper motor neuron signs and presence of one or more abnormal ancillary investigations, i.e. abnormal nerve conduction or conduction block (CB), thickening or T2 hyperintensity on magnetic resonance imaging (MRI) of the brachial plexus, sonographic nerve thickening, increased protein content in the cerebrospinal fluid (CSF) or the presence of anti-GM1 IgM antibodies in serum.¹⁻⁵ Administration of intravenous or subcutaneous immunoglobulins transiently improves muscle strength and maintenance treatment is therefore needed.⁶⁻¹⁰

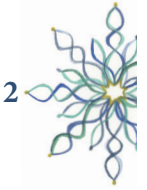
Consensus criteria have facilitated diagnosis of MMN and shortened diagnostic delays, but we know less of the disease course and outcome.^{5,11} Early case reports suggested that its course is not benign in individual patients, but few studies have longitudinally addressed natural history in larger patients cohorts.¹²⁻¹⁴ Early treatment may improve long-term outcome, but accumulating axonal damage nevertheless results in significant disability in up to one fifth of patients.^{11,15} More detailed insight in MMN's clinical course would help to identify correlates of worse outcome and thereby patients at higher risk for developing severe deficits, and eventually to investigate efficacy of other treatment approaches.

We have previously reported the characteristics of a relatively large cross sectional cohort of patients with MMN in the Netherlands.¹¹ In order to gain more insight in the clinical course of MMN, we performed a combined cross-sectional and follow-up study in a cohort of 100 patients with the aim to identify factors that predict a progressive disease course of MMN.

METHODS

Study design and patients

This cross-sectional cohort study was performed between May 2015 and February 2016 in the University Medical Center (UMC) Utrecht, a large tertiary referral center for neuromuscular disorders in The Netherlands. We invited all patients listed in the MMN database of the UMC Utrecht who met the following inclusion criteria: 1) a diagnosis of definite, probable or possible MMN according to the EFNS/PNS criteria and 2) age \geq 18 years.⁵ A subgroup of our patients previously participated in a similar cross-sectional cohort study in 2007.¹¹ The local medical ethics committee of the UMC Utrecht approved the research protocol (NL50354.041.14). All included patients gave written informed consent.



2

Neurological examination and questionnaires

We documented clinical characteristics of patients with MMN (including but not limited to site of onset and age at symptom onset) using a standardized questionnaire and collected the Overall Disability Sum Score (ODSS), the Self-Evaluation Scale (SES), the Rasch-built Overall Disability Score for MMN (MMN-RODS) and the Fatigue Severity Scale (FSS).^{16–20} All patients underwent a standardized neurological examination (**Supplemental table 2.1**). This consisted of bilateral grading of motor function of 18 muscle groups using the Medical Research Council (MRC) scale to calculate the MRC sum score with a maximum of 180 points. Sensory function was tested using a Rydell-Seiffer tuning fork to assess vibration sense in arms and legs bilaterally. Vibration sense was graded from normal (grade 0) to abnormal at the acromioclavicular joint or anterior superior iliac spine (grade 4).²¹ Tendon reflexes of biceps, triceps, knee and ankle were performed on both sides and scored as normal, brisk or absent. We used data obtained during a previous study in 2007 as baseline data.¹¹ To minimize inter-observer variability, one of the authors (EAC) who collected clinical data during the 2007 study trained the author (BAJ) who performed the clinical examination in 2015 – 2016, with special emphasis on the interpretation of MRC and Rydell-Seiffer scales.

Nerve conduction studies and other ancillary investigations

One of the authors (HSG) evaluated available nerve conduction study results using the EFNS/PNS criteria for CB and other abnormalities.⁵ All patients underwent nerve conduction studies (NCS) using a standardized protocol and stimulation was up to Erb's point.²² CB was defined as definite CB (compound muscle action potential (CMAP) area reduction of at least 50%) or probable CB (CMAP area reduction of 30-50%), and axonal loss as a decreased distal CMAP (distal CMAP amplitude below the lower limit of normal) in ≥ 1 nerves, including the median, ulnar, radial, musculocutaneous, peroneal, and tibial nerves.^{5,23} We also collected all available results of laboratory studies (in particular the presence of anti-GM1 IgM antibodies in serum and analysis of cerebrospinal fluid) and of MRI of the brachial plexus.

Statistical analyses

MMN cohort data

We stratified the patients with MMN into two groups: (1) patients diagnosed before our previous study in 2007, and (2) patients diagnosed after 2007) to explore differences in clinical characteristics. Depending on the distribution of the variable, we compared groups using the Mann-Whitney U test (for continuous data) and the χ^2 test (for categorical data). To account for right skew in time-related covariates, we log-transformed (natural) duration of treatment, months untreated and time to diagnosis. Univariate linear regression analyses were performed to identify changes in clinical characteristics over calendar time. Dependent variables were age at diagnosis, time to diagnosis (log-transformed) and age at onset of symptoms. The independent variable was the year of diagnosis. Subsequently, we calculated the mean MRC score per muscle group for patients with longer and shorter disease duration (defined as equal to or larger than the median disease duration). We corrected

the obtained p values for multiple testing using the Benjamini-Hochberg method. Multiple linear regression analysis was used with backward elimination based on p value selection to predict the MRC sum score 2015 – 2016 based on sex, symptom onset in a leg, presence of anti-GM1 IgM antibodies, FSS (0 – 63), duration of treatment in months (log-transformed), months untreated (log-transformed) and age at onset of symptoms in years).

Longitudinal follow-up data

The mean yearly rate of decline of each outcome measure was estimated between visit 1 (2007) and visit 2 (2015 – 2016) and tested using a one sample t test (i.e. assessing whether the yearly rate of decline is other than zero). Multiple linear regression analysis was performed with backward elimination based on p value selection to predict the yearly rate of decline in MRC sum score based on sex, presence of anti-GM1 IgM antibodies, symptom onset in leg, months untreated (log-transformed), age at onset of symptoms in years, ODSS (0 – 8), MRC sum score (0 – 180) and sum score of reflexes (0 – 8). The last three variables were analysed with data of the first visit (2007). Patients were asked to describe their disease course as stable, gradually but slowly progressive, gradually progressive, stepwise progressive or gradually improving.



RESULTS

Patients

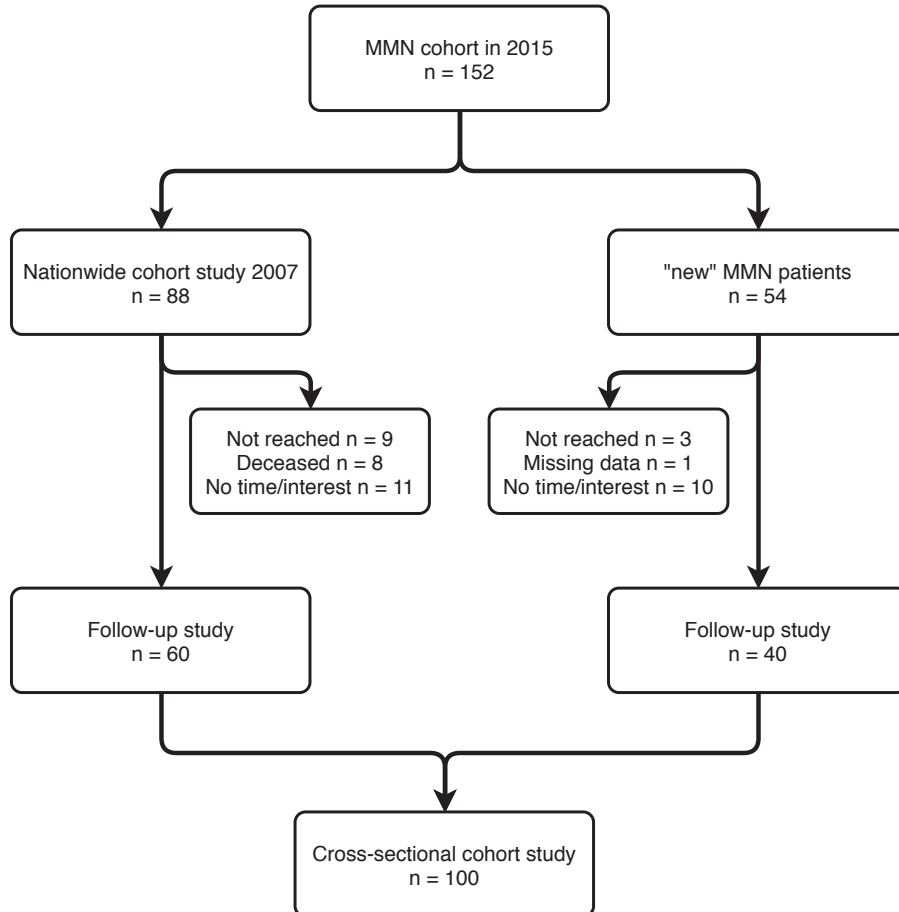
We identified a total of 142 patients with MMN. Hundred patients (70.4%) agreed to participate of whom 60 patients previously participated in a nationwide cross sectional cohort study in 2007.¹¹ Reasons for not participating are shown in **Figure 2.1**.

Clinical characteristics

Patient characteristics (sex, age at onset of symptoms, MMN diagnosis according to EFNS/PNS criteria and additional investigations i.e. NCS, MRI brachial plexus, CSF protein and presence of anti-GM1 IgM antibodies) between participants ($n = 100$) and non-participants ($n = 42$), were not significantly different, except for the onset of muscle weakness ($p = 0.04$). Median age at onset of symptoms and age of diagnosis were significantly higher in patients diagnosed after 2007 ($p < 0.01$ and $p = 0.02$; **Table 2.1**). We performed univariate linear regression analysis with year of diagnosis as independent variable. Both median age at onset of symptoms and median age of diagnosis significantly increased over time (both $p < 0.01$) (**Figure 2.2**). Median time from symptom onset to diagnosis (i.e. diagnostic delay) decreased over time (6.4 years (range 1 – 27) in period 1996 to 2000; 1.8 years (range 1 – 29) in period 2011 – 2015) but was significantly longer for patients with onset of symptoms in a leg and for patients with higher age at diagnosis ($p = 0.01$ and $p < 0.01$). We use a starting dose of 0.4 g/kg immunoglobulins per 3-4 weeks and then tailor the dose (if needed up to 1 g/kg) until patients remain stable during the treatment interval.² The starting dose

was significantly higher for patients diagnosed before 2007 ($p < 0.01$), probably due to a different treatment regime with repeated loading doses of immunoglobulins in the period before 1995 rather than lower-dosed weekly to monthly maintenance therapy. We found no significant differences in clinical characteristics between males and females.

Figure 2.1 Flowchart of study



Abbreviations: MMN = multifocal motor neuropathy.

Weakness, sensory function and tendon reflexes

The distribution of muscle weakness was distal more than proximal and more pronounced in hand than in foot or lower leg muscles (**Supplemental table 2.2**). Finger flexion and plantar foot flexion were relatively spared compared to hand and finger extension and dorsal foot flexion. Patients with longer disease duration had significantly more weakness in hand and lower leg or foot muscles

compared to patients with shorter disease duration (all $p < 0.05$) (**Figure 2.3** and **Supplemental table 2.2**). We found abnormal vibration sense on the toes in 57 patients (57.6%). Median disease duration was longer in these patients compared to those without sensory findings (median 16.1 years, range 1.3 – 46.5 vs. median 11.5 years, range 1.9 – 30.5; $p = 0.03$). We found at least one absent reflex in 79 patients (79%). Sixteen of these patients (20%) had generalized areflexia (**Supplemental table 2.3**). We did not find a relation between the presence of conduction block (definite and/or probable) and the absence of reflexes ($p > 0.10$).

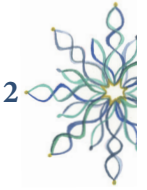
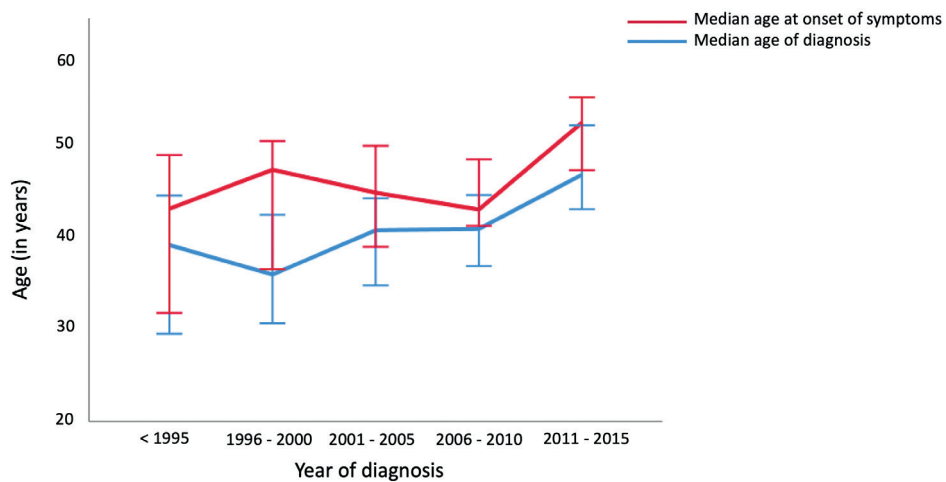


Figure 2.2 Clinical characteristics over time



Median age at onset of symptoms and median age of diagnosis over time. Error bars are 95% confidence intervals.

Nerve conduction studies and laboratory investigations

One or more definite CBs were present in 74 patients (74.0%), only probable CB in 19 patients (19.0%) and no CB in 7 patients (7.0%). The diagnosis of MMN in these 7 patients without CB was based on the presence of anti-GM1 IgM antibody titers (4 patients; 57.1%), abnormal CSF protein concentrations (protein level > 0.4 gram/litre (g/L); 2 patients; 28.6%), an abnormal MRI of the brachial plexus (3 patients; 42.9%), and response to immunoglobulin therapy in all patients. We found evidence of axonal damage during NCS in 71 patients (71.0%), the presence of anti-GM1 IgM antibodies in 55/90 patients (61.1%) and abnormal CSF protein concentrations (>0.4 g/L) in 20/26 (76.9%) patients.

Table 2.1 Clinical characteristics

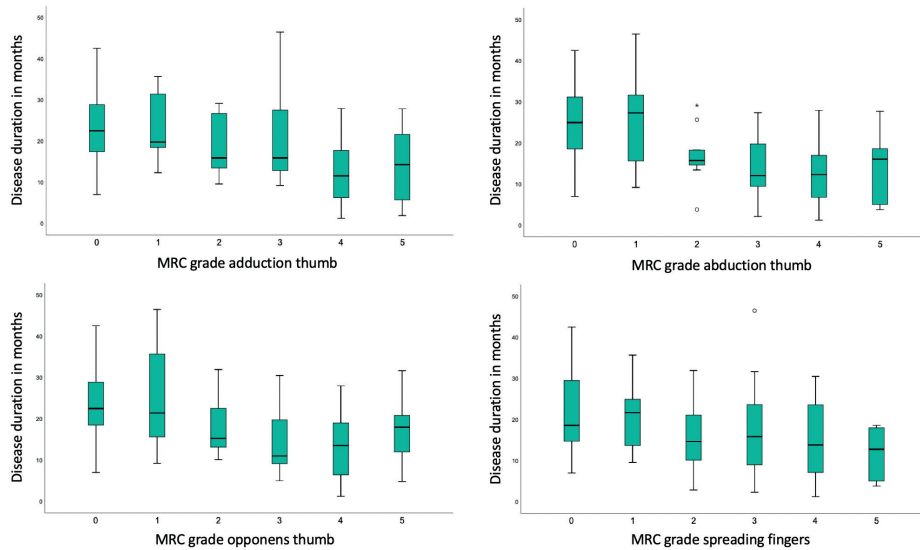
Parameter	Diagnosis before 2007 (n = 64)	Diagnosis in or after 2007 (n = 36)	p
Male	46 (72%)	29 (81%)	0.34
Age at onset of symptoms	40.3 (21.4 – 53.8)	45.2 (30.1 – 67.2)	< 0.001
Age at diagnosis	45.2 (25.2 – 71.1)	48.6 (30.9 – 73.5)	0.02
Time to diagnosis (months)*	42.0 (3.0 – 433.0)	27.0 (6.0 – 345.0)	0.10
Time from disease onset until treatment (months)	42.0 (3.0 – 435.9)	27.5 (3.9 – 346.0)	0.09
Maintenance treatment with immunoglobulins	55 (86%)	32 (89%)	0.67
Starting dose ivIg maintenance therapy per week (gram)	10.0 (5.0 – 33.0)	8.0 (4.0 – 12.0)	< 0.001
Onset of muscle weakness			
<i>Distal arm</i>	41 (64%)	25 (70%)	0.08
<i>Proximal arm</i>	3 (4%)	3 (8%)	
<i>Distal leg</i>	18 (28%)	4 (11%)	
<i>Proximal leg</i>	1 (2%)	0 (0 %)	
<i>Distal symmetrical</i>	1 (2%)	4 (11%)	
Number of affected limbs at inclusion			
0	2 (3%)	1 (3%)	0.15
1	7 (11%)	8 (22%)	
2	12 (19%)	12 (33%)	
3	18 (28%)	7 (20%)	
4	25 (39%)	8 (22%)	
Electrophysiological criteria**			
<i>Definite</i>	45 (70%)	29 (81%)	0.32
<i>Probable</i>	15 (23%)	4 (11%)	
<i>Negative</i>	4 (6%)	3 (8%)	
NCS with axonal degeneration	31 (48%)	13 (36%)	0.23
Abnormalities brachial plexus MRI	22/43 (51%)	8/17 (47%)	0.77
Laboratory findings			
<i>Increased CSF protein</i>	12/16 (75%)	8/10 (80%)	0.77
<i>Presence of anti-GM1 IgM antibodies</i>	38/61 (62%)	17/29 (59%)	0.74

Data are shown in median (range) or number of patients (%), unless stated otherwise.

* log transformed variable

** according to the EFNS/PNS criteria⁵

Abbreviations: ivIg = intravenous immunoglobulins; NCS = nerve conduction studies; MRI = magnetic resonance imaging; CSF = cerebrospinal fluid.

Figure 2.3 Correlation of MRC grade and disease duration per muscle group

The boxplots provide the variability in disease duration per MRC grade (0 – 5). Disease duration is defined as years from onset of symptoms until first study visit.

Abbreviations: MRC = Medical Research Council.

Disability questionnaires

Results of the disability questionnaires are shown in **Supplemental table 2.3**. Median ODSS of the arms was 2 (range 0 – 4), of the legs 1 (range 0 – 5) and of arms and legs combined 3 (range 0 – 8). Twelve patients (12%) reported no disability of the arms and 34 patients (34%) did not experience disability of the legs.

Correlates of outcome

Multiple linear regression analysis showed that a lower MRC sum score correlated with longer disease duration without treatment, presence of anti-GM1 IgM antibodies and lower age at onset of symptoms ($p = 0.024$, $p = 0.046$ and $p = 0.006$ respectively).

Outcome measures over time

Mean differences between visit 1 (2007) and visit 2 (2015 – 2016) of different outcome measures are shown in **Table 2.2**. Except for ODSS, FSS and vigorimetry of the left hand, all outcome measures deteriorated over time (all $p < 0.01$). The difference in MRC sum score between 2015 and 2007 was significantly larger in patients with axonal damage compared to patients without axonal damage (5.2 points vs. 13.8 points; $p = 0.014$). Most patients indicated that their disease course was stable (25.0%) or mildly progressive (61.7%). The dose of immunoglobulin treatment significantly increased over time ($p < 0.001$).

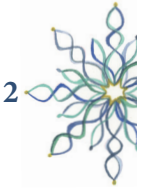


Table 2.2 Outcome measures over time

Parameter	MD per year	95% CI	<i>p</i>
ODSS (0 – 12 points)	-0.004	0.03 – -0.04	0.81
MRC sum score (0 – 180 points)	-1.361	-0.97 – -1.75	< 0.001
SES (0 – 25 points)	0.352	0.54 – 0.16	< 0.001
FSS (0 – 63 points)	-0.940	-0.25 – -1.63	< 0.001
Vibration sense (abnormal in 0 – 4 limbs)	0.121	0.15 – 0.09	< 0.001
Reflexes arm (absence in 0 – 4 reflexes)	0.055	-0.02 – -0.09	< 0.001
Reflexes leg (absence in 0 – 4 reflexes)	0.072	-0.03 – -0.11	< 0.001
Reflexes sum score (absence in 0 – 8 reflexes)	0.121	-0.06 – -0.18	< 0.001
Grip strength right (kPa)	-1.127	-0.39 – -1.87	< 0.001
Grip strength left (kPa)	-0.770	0.04 – -1.58	0.06
Number of affected muscle groups	0.465	0.36 – 0.58	< 0.001

Mean difference per year was calculated as the difference between visit 1 (2007) and visit 2 (2015-2016) divided by the follow-up duration.

Absence of reflexes arm: biceps and triceps reflexes (0 – 4). Absence of reflexes leg: knee and ankle reflexes (0 – 4). Abbreviations: MD = mean difference; CI = confidence interval; ODSS = Overall Disability Sum Score; MRC = Medical Research Council; SES = Self-evaluation Scale; FSS = Fatigue Severity Scale.

Predictors of progression

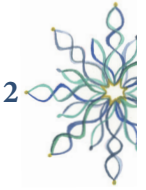
Multiple linear regression showed that faster progression, i.e. a larger difference of the MRC sum score of visit 1 (2007) and visit 2 (2015 – 2016) per year correlated with the reflexes sum score (i.e. absent reflexes) and a lower MRC sum score in 2007 ($p = 0.016$ and $p = 0.007$ respectively).

DISCUSSION

This study aimed to document clinical outcomes of patients with MMN and identify predictors of disease progression. We combined cross-sectional data with longitudinal data with a mean duration between visits of eight years. Our clinical observations confirmed that MMN is a progressive disorder in the large majority of patients even when they receive immunoglobulin maintenance treatment. Virtually all selected outcome measures significantly deteriorated over time. Factors with prognostic value of a progressive disease course were absence of reflexes and a lower MRC sum score at baseline.

A previous study described the natural history of 38 treatment-naïve patients with MMN retrospectively. Patients with longer disease duration ($n = 10$) had significantly lower MRC sum scores and a higher number of affected regions. None of the patients experienced spontaneous improvement or a relapsing remitting course.¹³ Taylor et al. longitudinally assessed 18 patients

with MMN and found a slowly worsening of muscle weakness, i.e. a change in neurological impairment score (NIS) of 1.3 points/year.¹⁴ We performed multiple linear regression analysis to determine predictors of a progressive disease course and found that absence of at least one reflex and a lower MRC sum score at baseline were associated with a larger decrease of the MRC sum score over time. This amounted to a difference of 1.36 MRC point decrease of the MRC sum score per year in patients with generalized areflexia compared to those with normal reflexes. These findings can help to identify patients with a more progressive disease course. Until the development of more effective treatment strategies for MMN, the identification of patients at greater risk may ultimately help to tailor the dosing or frequency of immunoglobulin treatment in the future.



We used two approaches to analyze cross sectional data. First, we compared patients with a diagnosis before and after 2007, and thereby with longer and shorter disease duration. The distribution pattern of muscle weakness in patients with shorter and longer disease duration was similar but the severity of weakness of hand and lower leg/foot muscles was significantly increased in the latter. This finding supports the longitudinal data and also shows that proximal muscle groups are relatively spared. The second approach consisted of multiple linear regression analysis to determine factors that were associated with more severe weakness. Previous studies showed that axonal damage is highly associated with muscle weakness and therefore we performed the analysis without axonal damage as an independent factor.¹⁵ We found that presence of anti-GM1 IgM antibodies and 'years untreated' were associated with more severe weakness, which is similar to findings of smaller previous studies.²⁴⁻²⁶ These data imply that to prevent permanent weakness, reducing time to diagnosis and providing earlier treatment are crucial. Increased awareness of MMN and possibly the extension of reliable diagnostic tools, such as nerve ultrasound might serve this goal. We think that MMN should also be actively excluded in older patients or those with asymmetric weakness in a leg.

The follow-up data showed that almost all outcome measures significantly deteriorated over time. However, there were some exceptions, most notably vigorimetry of the left hand. Although we cannot explain this finding, we previously observed that weakness is more common in the dominant hand.¹¹ This has also been reported for other inflammatory asymmetric syndromes such as neuralgic amyotrophy.²⁷ Moreover, fatigue seemed to improve over time. Fatigue is a common symptom of chronic immune-mediated disorders but without intervention, at best remains stable but often deteriorates over time.^{28,29} A possible explanation for the improvement of fatigue in MMN could be that patients get used to the feeling of fatigue or adapted by changing frequency or intensity of their daily activities (e.g. change or quit their jobs, improve their lifestyles). We do not think that immunoglobulin therapy provides an explanation for the reduction in reported fatigue, since both in 2007 and in 2015 approximately 85% of the patients received maintenance therapy.

Median age at onset of symptoms and age of diagnosis significantly increased over time. The higher median age at diagnosis could be explained by an already increased awareness of MMN, resulting in more frequent clinical suspicion in older patients presenting with asymmetric weakness. Moreover, the addition of novel diagnostic techniques other than nerve conduction studies such as nerve ultrasound or the more frequent use of immunoglobulin trials to assess response to treatment could have led to the higher median age at diagnosis. The cause of the increase of age at onset is unknown although it is not unique for MMN. Similar trends have been observed in amyotrophic lateral sclerosis (ALS) (unpublished data of ALS cohort of 2900 patients in UMC Utrecht The Netherlands).³⁰ We can therefore not exclude the possibility that this trend is caused by changes in an altered referral pattern of patients with motor neuron disorders in our center.

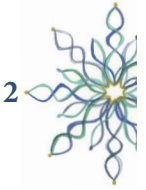
Despite the fact that MMN is considered a pure motor neuropathy, we found vibration sense abnormalities in 57% of the patients. These deficits were confined to the feet in 97% of the patients and in general occurred in patients with longer disease duration. Vibration sense also significantly deteriorated over time, which is similar to previous studies that showed reduced sensory nerve action potentials years after MMN onset.^{31,32}

Our study has some limitations. Neurological examination at both study visits was performed by different investigators. However, the authors who performed neurological examination were trained prior to the second tier of the study to minimize differences in performance, evaluation and interpretation of the MRC and Rydell-Seiffer scales. The large majority of patients received immunoglobulin maintenance treatment, which will have attenuated the true progression of MMN. Moreover, the relation of disease course with immunoglobulin therapy was not a primary aim of our study. We usually tailor treatment dose and frequency to maintain stable function between gifts. Although we found a significant increase in dose of immunoglobulin over time, possible relations between the therapy and progression should be a topic for future studies.

Our study shows that MMN is a progressive disorder in the large majority of patients despite immunoglobulin maintenance treatment. Diagnostic delays are more common in older patients or with onset of weakness in one of the legs. Absence of reflexes and lower MRC sum score at baseline predict a more progressive disease course. Whether these patients would benefit from more aggressive treatment approaches with immunoglobulins needs to be established.

REFERENCES

1. Goedee HS, Jongbloed BA, van Asseldonk J-TH, et al. A comparative study of brachial plexus sonography and magnetic resonance imaging in chronic inflammatory demyelinating neuropathy and multifocal motor neuropathy. *Eur. J. Neurol.* 2017;24:1307–1313.
2. Vlam L, Van Der Pol WL, Cats EA, et al. Multifocal motor neuropathy: Diagnosis, pathogenesis and treatment strategies. *Nat. Rev. Neurol.* 2012;8:48–58.
3. Van Asseldonk J, Franssen H, Van Den Berg-Vos R, et al. Multifocal motor neuropathy. *Lancet Neurol.* 2005;4:309–319.
4. Goedee HS, Van Der Pol WL, Van Asseldonk JTH, et al. Diagnostic value of sonography in treatment-naive chronic inflammatory neuropathies. *Neurology* 2017;88:143–151.
5. Van Schaik IN, Léger JM, Nobile-Orazio E, et al. European Federation of Neurological Societies/Peripheral Nerve Society Guideline on management of multifocal motor neuropathy. Report of a Joint Task Force of the European Federation of Neurological Societies and the Peripheral Nerve Society - First revis. *J Peripher Nerv Syst* 2010;15:295–301.
6. van Schaik I, van den Berg L, de Haan R, Vermeulen M. Intravenous immunoglobulin for multifocal motor neuropathy. *Cochrane Database Syst. Rev.* 2005;2:920–921.
7. Léger JM, Chassande B, Musset L, et al. Intravenous immunoglobulin therapy in multifocal motor neuropathy: a double-blind, placebo-controlled study. *Brain* 2001;124:145–153.
8. Eftimov F, Vermeulen M, De Haan RJ, et al. Subcutaneous immunoglobulin therapy for multifocal motor neuropathy. *J. Peripher. Nerv. Syst.* 2009;14:93–100.
9. Harbo T, Andersen H, Hess A, et al. Subcutaneous versus intravenous immunoglobulin in multifocal motor neuropathy: A randomized, single-blinded cross-over trial. *Eur. J. Neurol.* 2009;16:631–638.
10. Markvardsen LH, Harbo T. Subcutaneous immunoglobulin treatment in CIDP and MMN. Efficacy, treatment satisfaction and costs. *J. Neurol. Sci.* 2017;378:19–25.
11. Cats E, van der Pol WL, Piepers S, et al. Correlates of outcome and response to IVIG in 88 patients with multifocal motor neuropathy. *Neurology* 2011;75:818–825.
12. Lange D, Weimer L, Trojaborg W, et al. Multifocal motor neuropathy with conduction block: slow but not benign. *Arch Neurol* 2006;63:1778–1781.
13. Van den Berg-Vos RM, Franssen H, Visser J, et al. Disease severity in multifocal motor neuropathy and its association with the response to immunoglobulin treatment. *J. Neurol.* 2002;249:330–336.
14. Taylor B V., Wright RA, Harper CM, Dyck PJ. Natural history of 46 patients with multifocal motor neuropathy with conduction block. *Muscle and Nerve* 2000;23:900–908.
15. Van Asseldonk JTH, Van Den Berg LH, Kalmijn S, et al. Axon loss is an important determinant of weakness in multifocal motor neuropathy. *J. Neurol. Neurosurg. Psychiatry* 2006;77:743–747.
16. Vanhoutte EK, Faber CG, Van Nes SI, et al. Rasch-built Overall Disability Scale for Multifocal motor neuropathy (MMN-RODS®). *J. Peripher. Nerv. Syst.* 2015;20:296–305.
17. Merkies ISJ, Schmitz PIM. Getting closer to patients: the INCAT Overall Disability Sum Score relates better to patients' own clinical judgement in immune-mediated polyneuropathies. *J. Neurol. Neurosurg. Psychiatry* 2006;77:970–972.
18. Nes S Van, Vanhoutte E, van Doorn P, et al. Rasch-built Overall Disability Scale (R-ODS) for immune-mediated peripheral neuropathies. *Int. Classif.* 2011;76:337–345.
19. Rietberg MB, Van Wegen EEH, Kwakkel G. Measuring fatigue in patients with multiple sclerosis: reproducibility, responsiveness and



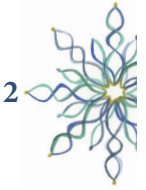
- concurrent validity of three Dutch self-report questionnaires. *Disabil. Rehabil.* 2010;32:1870–1876.
20. Krupp L, LaRocca N, Muir-Nash J, Steinberg A. The Fatigue Severity Scale: application to patients with Multiple Sclerosis and Systemic Lupus Erythematosus. *Arch Neurol* 1989;46:1121–1123.
 21. Martina ISJ, Van Koningsveld R, Schmitz PIM, et al. Measuring vibration threshold with a graduated tuning fork in normal aging and in patients with polyneuropathy. *J. Neurol. Neurosurg. Psychiatry* 1998;65:743–747.
 22. Van Den Berg-Vos RM, Franssen H, Wokke JHJ, Van Den Berg LH. Multifocal motor neuropathy: long-term clinical and electrophysiological assessment of intravenous immunoglobulin maintenance treatment. *Brain* 2002;125:1875–1886.
 23. Van Asseldonk JTH, Van den Berg LH, Van den Berg-Vos RM, et al. Demyelination and axonal loss in multifocal motor neuropathy: Distribution and relation to weakness. *Brain* 2003;126:186–198.
 24. Al-Zuhairy A, Sindrup SH, Andersen H, Jakobsen J. A population-based and cross-sectional study of the long-term prognosis in multifocal motor neuropathy. *J. Peripher. Nerv. Syst.* 2019;24:64–71.
 25. Cats EA, Jacobs BC, Yuki N, et al. Multifocal motor neuropathy: Association of anti-GM1 IgM antibodies with clinical features. *Neurology* 2010;75:1961–1967.
 26. Vlam L, Cats EA, Harschnitz O, et al. Complement activity is associated with disease severity in multifocal motor neuropathy. *Neurol. Neuroimmunol. NeuroInflammation* 2015;2:1–8.
 27. Van Alfen N, Van Engelen BGM. The clinical spectrum of neuralgic amyotrophy in 246 cases. *Brain* 2006;129:438–450.
 28. Merkies ISJ, Faber CG. Fatigue in immune-mediated neuropathies. *Neuromuscul. Disord.* 2012;22:S203–S207.
 29. Merkies IS, Schmitz PI, Samijn JP, et al. Fatigue in immune-mediated polyneuropathies. European Inflammatory Neuropathy Cause and Treatment (INCAT) Group. *Neurology* 1999;53:1648–54.
 30. Kobayashi C, Miyazaki D, Kinoshita T, et al. Increasing Incidence and Age at Onset of Amyotrophic Lateral Sclerosis in Nagano Prefecture, Japan. *Shinshu Med J* 2016;64:239–246.
 31. Delmont E, Benaïm C, Launay M, et al. Do patients having a decrease in SNAP amplitude during the course of MMN present with a different condition? *J. Neurol.* 2009;256:1876–1880.
 32. Lambrecq V, Krim E, Rouanet-Larrivière M, Laguëny A. Sensory loss in multifocal motor neuropathy: a clinical and electrophysiological study. *Muscle and Nerve* 2009;39:131–136.

SUPPLEMENTAL MATERIAL

Supplemental table 2.1 Specification of neurological examination and questionnaires

Modality	Description
MRC score	Bilateral measurement of motor function (sum score between 0 – 180 points): <i>Abduction of the arm</i> <i>Flexion and extension of the wrist and fingers</i> <i>Spreading of the fingers</i> <i>Abduction, adduction, and opposition of the thumb</i> <i>Flexion of the hip</i> <i>Flexion and extension of the knee and foot</i> <i>Extension and flexion of the toes</i>
Vibration sense	Bilateral assessment of sensory function using Rydell-Seiffer tuning fork: <i>Normal (grade 0)</i> <i>Abnormal at hallux (grade 1)</i> <i>Abnormal at ankle (grade 2)</i> <i>Abnormal at knee (grade 3)</i> <i>Abnormal at acromioclavicular joint or anterior superior iliac spine (grade 4)</i>
Vigorimetry	Bilateral measurement of grip strength in kilopascal (kPa) with the Martin Vigorimeter (Martin medizintechnik, Tuttlingen, Germany)

Abbreviations: MRC = Medical Research Council



2

Supplemental table 2.2 Mean MRC grade per muscle group

Examination site	Total cohort (n = 100)	Short disease duration (n = 50)	Long disease duration (n = 50)	<i>P</i>
Arm				
<i>Elbow flexion</i>	4.4	4.5	4.3	0.63
<i>Elbow extension</i>	4.7	4.7	4.6	0.33
<i>Shoulder abduction</i>	4.5	4.5	4.5	0.38
<i>Wrist flexion</i>	4.4	4.5	4.3	0.63
<i>Wrist extension</i>	3.9	4.1	3.6	0.20
Hand				
<i>Finger flexion</i>	4.5	4.7	4.3	0.01
<i>Finger extension</i>	3.3	3.7	3.0	0.03
<i>Finger spreading</i>	3.1	3.5	2.7	0.03
<i>Thumb adduction</i>	3.4	3.9	2.9	0.01
<i>Thumb abduction</i>	3.0	3.6	2.4	0.01
<i>Thumb opposition</i>	3.2	3.7	2.7	0.03
Leg				
<i>Hip flexion</i>	4.9	4.8	4.9	0.33
<i>Knee flexion</i>	4.9	4.9	4.9	0.73
<i>Knee extension</i>	4.9	5.0	4.9	0.38
Foot				
<i>Foot plantar flexion</i>	4.3	4.8	3.9	0.03
<i>Foot dorsal flexion</i>	3.4	4.2	2.6	0.01
<i>Toes flexion</i>	4.2	4.7	3.7	0.03
<i>Toes extension</i>	3.5	4.1	2.9	0.04

Short disease duration is defined as disease duration < 180.6 months. Long disease duration is defined as disease duration ≥ 180.6 months. Abbreviations: MRC = Medical Research Council.

Supplemental table 2.3 Overview of outcome measures

Variable	All patients (n = 100)
MRC sum score	165 (69 – 180)
Vibration sense	
<i>Normal</i>	42 (42%)
<i>Abnormal in at least one limb</i>	58 (58%)
Reflexes	
<i>Normal</i>	20 (20%)
<i>Abnormal in at least one reflex</i>	79 (79%)
<i>Generalized areflexia</i>	16 (16%)
ODSS	
<i>Arms</i>	2 (0 – 4)
<i>Legs</i>	1 (0 – 5)
<i>Total</i>	3 (0 – 8)
SES	10 (1 – 25)
FSS	37 (9 – 61)

Data are shown in median (range) or in number of patients (%).

Abbreviations: MRC = Medical Research Council; ODSS = Overall Disability Sum Scale; SES = Self-evaluation Scale; FSS = Fatigue Severity Scale.



2





Chapter 3

Low inter-rater reliability of brachial plexus MRI in chronic inflammatory neuropathies

Marieke H.J. van Rosmalen, H. Stephan Goedee, Anouk van der Gijp, Theo D. Witkamp, Martijn Froeling, Jeroen Hendrikse, W. Ludo van der Pol

Muscle and Nerve, 2020 Jun; 61, 779 - 783

ABSTRACT

Objective: Magnetic resonance imaging (MRI) of the brachial plexus shows nerve thickening in approximately half of the patients with chronic inflammatory demyelinating polyneuropathy (CIDP) and multifocal motor neuropathy (MMN). The reliability of qualitative evaluation of brachial plexus MRI has not been studied previously.

Methods: We performed an interrater study in a retrospective cohort of 19 patients with CIDP, 17 patients with MMN and 14 controls. The aim was to assess inter-rater variability between radiologists using a predefined scoring system that allowed the distinction of no, possible or definite nerve thickening.

Results: Raters agreed in 26 of 50 (52%) of all brachial plexus images. Kappa coefficient was 0.30 (SE 0.08, 95% CI 0.14 – 0.46, $p < 0.0005$).

Conclusion: Our results indicate that inter-rater reliability of qualitative evaluation of brachial plexus MRI is low. Objective criteria for abnormality are needed to optimize the diagnostic value of MRI for inflammatory neuropathies.

INTRODUCTION

Magnetic resonance imaging (MRI) of the brachial plexus can be helpful to diagnose inflammatory neuropathies such as chronic inflammatory demyelinating polyneuropathy (CIDP) and multifocal motor neuropathy (MMN). The diagnostic challenge in CIDP and MMN is to distinguish these disorders from those that do not respond to immunomodulatory treatment.

Diagnostic criteria for CIDP and MMN primarily rely on clinical phenotype and specific nerve conduction study (NCS) abnormalities.^{1,2} Brachial plexus MRI can be of diagnostic value when NCS is inconclusive despite high clinical suspicion. Magnetic imaging abnormalities associated with CIDP and MMN are thickening of roots, plexus and nerves, often combined with T2 hyperintensity.³⁻⁵ Previous MRI studies were exclusively qualitative and lacked clear definitions of abnormality.⁶⁻⁸ To clarify the value of brachial plexus MRI in the diagnostic workup of inflammatory neuropathies, we assessed interrater variability.



METHODS

Study design

We performed an interrater study in a retrospective cohort of patients with CIDP and MMN and controls.

Subjects

Patients aged 18 to 85 years with CIDP and MMN according to the European Federation of Neurological Societies/Peripheral Nerve Society criteria^{1,2}, who were seen at the University Medical Center (UMC) Utrecht and who underwent brachial plexus MRI between September 2016 and September 2018 were selected for this study. Brachial plexus MRI from patients with other causes of peripheral motor deficits were used as controls.

Clinical data

We obtained clinical data from electronic patient records, including age, sex and time from onset of symptoms to diagnosis in months, defined as disease duration. All patients gave informed consent. This study was approved by the Medical Ethical Committee of the UMC Utrecht.

MRI protocol and assessment

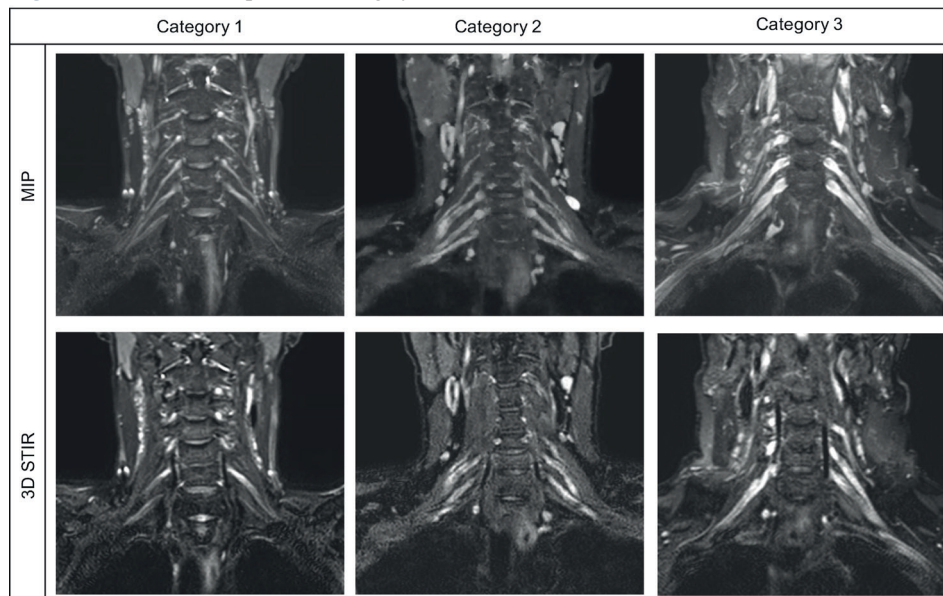
Brachial plexus MRI was performed for diagnostic purposes and was reassessed for this study. Scans were performed on 1.5 and 3.0 Tesla (T) scanners (Philips, Best, the Netherlands). The MRI protocol consisted of a fat-suppressed coronal 3D T2-weighted short-tau inversion recovery (STIR) with the following parameters: field of view = 250*320*170 mm³, matrix size = 208*269, voxel size = 0.6*0.6*1 mm³, echo time = 259 ms, repetition time = 2200 ms, turbo spin echo factor = 95, acquisition time = 06:16 minutes. In postprocessing, a coronal slab maximum intensity projection (MIP) was created.

We developed a scoring system with categories of abnormality of nerve thickening (**Figure 3.1**). Scans were scored using a 3-point scale (1 = no nerve thickening, 2 = possible nerve thickening, 3 = definite nerve thickening). Examples of abnormality were selected from a subset of all included patients by two experienced (2 years and > 30 years) neuroradiologists (AG, TW) via discussion and consensus. The examples were saved using the “Teaching Tool” in PACS IDS7 19.3.12 (Sectra AB, Linköping, Sweden). With this tool raters can scroll through images and compare them with the target image. The radiologists scored all images using PACS IDS7. The degree of abnormality was assessed by the overall impression of the entire brachial plexus. Images were presented to raters in the same order, blinded to clinical status of the subjects and on screens with similar resolution.

Statistical analysis

Statistical analyses was performed using IBM SPSS Statistics (Version 25, Armonk, New York, United States). To analyze patient characteristics we used independent samples *t* tests. The interrater variability of qualitative assessments of brachial plexus MRI was determined by Cohen’s kappa as coefficient for measure of agreement because we evaluated categorized data with limited categories. We interpreted a kappa value of 0.00 – 0.20 as no agreement, 0.21 – 0.39 as minimal, 0.40 – 0.59 as weak, 0.60 – 0.79 as moderate, 0.80 – 0.90 as strong and > 0.90 as almost perfect agreement.⁹ $p < 0.05$ was considered significant. We calculated sensitivity and specificity per rater using receiver operating characteristic curves.

Figure 3.1 The brachial plexus scoring system



Representative images of the scoring system used to define categories of abnormality, i.e. category 1 = no nerve thickening, 2 = possible nerve thickening, 3 = definite nerve thickening. Each category represents an example of a Maximum Intensity Projection (MIP) and 3D short-tau inversion recovery (STIR) image.

RESULTS

Subjects

We identified 36 patients with a chronic inflammatory neuropathy (CIDP = 19, MMN = 17) and 14 disease controls (motor neuron disease = 4, Hirayama disease = 3, ulnar neuropathy = 1, neurogenic thoracic outlet syndrome = 1, polyneuropathy in Sjögren's disease = 1, brachial plexopathy caused by alcohol abuse = 1, cervical myelopathy = 1, lumbar polyradiculopathy = 1, chronic idiopathic axonal polyneuropathy = 1). Patient characteristics are summarized in **Table 3.1**. Data was acquired for 26 subjects by using 1.5T MRI scanners and for 24 subjects by using 3.0T MRI scanners.

Table 3.1 Patient characteristics

Patient characteristics	Inflammatory neuropathy			Controls	Level of significance
	Total	CIDP	MMN		
Number of subjects	36	19	17	14	
Age, years (SD)	59.7 (14.9)	69.9 (9.0)	48.3 (11.7)	55.2 (16.5)	NS
Male (%)	26 (72%)	12 (63%)	14 (82%)	7 (50%)	NS
Disease duration, months (SD)	43.3 (47.7)	45.0 (48.7)	41.5 (48.0)	39.1 (37.0)	NS

Abbreviations: CIDP = Chronic inflammatory demyelinating polyneuropathy; MMN = Multifocal motor neuropathy; SD = standard deviation; NS = not significant. Age and disease duration are mean (SD).

Inter-rater variability

Raters agreed in 26 of 50 (52%) brachial plexus images when using three categories for abnormality (**Table 3.2**). Using the dichotomy normal – abnormal (i.e. category 1 versus categories 2 and 3) raters agreed in 36 of 50 (72%) cases. Kappa coefficient was 0.44 (SE 0.13, 95% CI 0.19 – 0.67, $p = 0.002$). Kappa coefficients for both methods indicate a minimal to weak level of agreement between raters.

In 15 of 50 (30%) cases rater 1 scored “possible nerve thickening” while rater 2 scored “no nerve thickening” or “definite nerve thickening”. Discrepancies between raters seem therefore to be caused mostly by the appreciation and distinction of subtle abnormalities (**Figure 3.2**). Sensitivity was 61% and 75% and specificity was 79% and 86% for rater 1 and 2 respectively. Area under the curve was 0.698 (95% CI 0.539 – 0.858) for rater 1 and 0.804 (95% CI 0.667 – 0.940) for rater 2 (**Figure 3.3**).



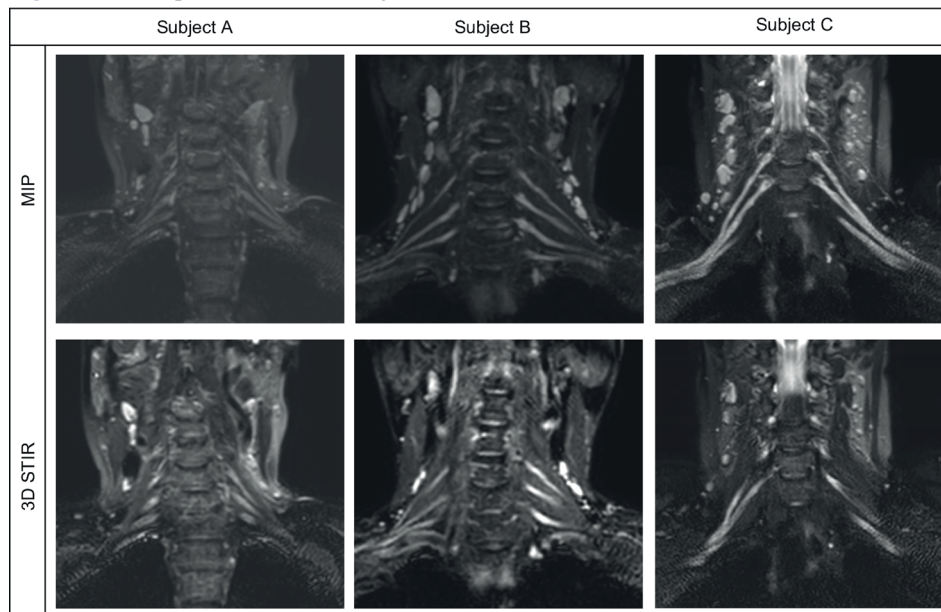
3

Table 3.2 Assessment of brachial plexus MRI by two raters.

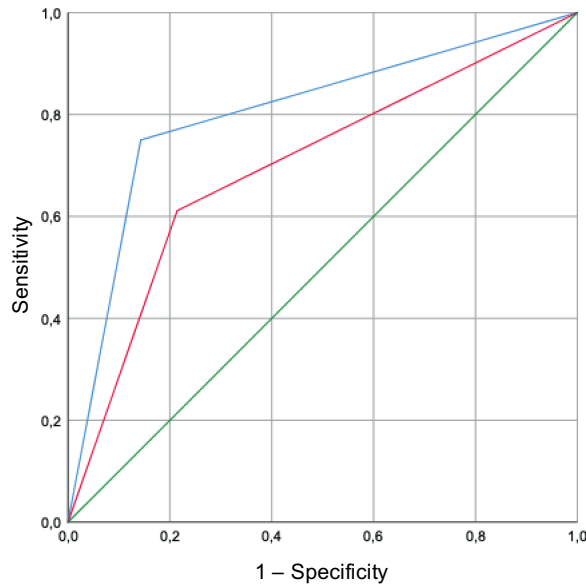
	Category 1	Category 2	Category 3	Total	Cohen's kappa (SE)	95% CI	<i>p</i> value
Rater 1 (number of cases)	25	17	8	50			
Rater 2 (number of cases)	21	4	25	50			
Cases of agreement	16	2	8	26 (52%)	0.30 (0.08)	0.14 - 0.46	< 0.0001

Abbreviations: SE = standard error; CI = confidence interval.

Kappa coefficients for assessment of images performed with 1.5T and 3.0T scanners were 0.26 (SE 0.13, 95% CI 0.00 – 0.56, $p = 0.032$) and 0.26 (SE 0.10, 95% CI 0.07 – 0.49, $p = 0.012$), respectively.

Figure 3.2 Examples of interrater disagreement

Subject A was rated as “possible nerve thickening” by rater 1 and as “no nerve thickening” by rater 2. Subject B and C were rated as “possible nerve thickening” by rater 1 and as “definite nerve thickening” by rater 2. This figure shows the difficulties in classifying subtle nerve thickening as either normal or as thickening. Each subject represents an example of a Maximum Intensity Projection (MIP) and 3D short-tau inversion recovery (STIR) image.

Figure 3.3 ROC curves per rater

Receiver operating characteristic (ROC) curve of rater 1 (red line) and rater 2 (blue line) with an area under the curve (AUC) of 0.698 (95% CI 0.539 – 0.858) and 0.804 (95% CI 0.667 – 0.940) respectively. Reference line in green.



DISCUSSION

This study shows that raters agreed in 26 of 50 (52%) images, indicating poor reliability. Although agreement was better when data were dichotomized (normal versus abnormal), our results indicate that difficulties are related mostly to distinguishing more subtle cases of nerve thickening. Objective criteria for abnormality are needed to avoid false positive and negative results and to optimize the diagnostic value of MRI for inflammatory neuropathies.

The poor agreement may have several explanations. We cannot exclude the possibility that the difference in radiological experience between raters underlies the poor reliability. However, the assessors work in the same department and had comparable training in neuroradiology. This may be an indication that interrater variability could even have been higher had we selected radiologists from different hospitals and training backgrounds. Furthermore, the gap in experience represents current clinical practice. Second, assessors of brachial plexus MRI may lack clear reference points, in particular when abnormalities are two-sided, which may have caused best-guessing particularly in cases from category 2. Third, three categories in the scoring model may have been one category too many. Analysis of dichotomized data led to a slightly higher kappa, but still indicated a poor level of

agreement. Fourth, differences between scanners may partially explain the poor level of agreement. However, despite small groups, our results showed similar agreement with overlapping confidence intervals for assessment of images performed on 1.5T and 3.0T scanners.

Earlier studies in chronic inflammatory neuropathies and plexus MRI focused on characteristics, distribution and prevalence of abnormalities.³⁻⁵ This study addresses the reproducibility of assessment of such abnormalities. Quantification of these abnormalities represents an obvious approach to improve reproducibility and reliability of assessment. Quantification of nerve size allows the identification of patients with CIDP or MMN with high sensitivity and reasonable specificity as shown in ultrasound studies.¹⁰ Few studies that have explored the use of quantitative MRI in chronic inflammatory neuropathies. One study reported cutoff values of 5.0 mm for roots C6, C7 and C8 to distinguish patients with CIDP (n = 14) from controls (n = 10).¹¹ Sensitivity and specificity were not reported, probably due to the small sample size. Another recent study used the diameter of the ganglia and nerve roots of C5 to T1 and found these to be significantly larger in patients with CIDP (n = 14) than in controls (n = 9), providing evidence to support the feasibility of this approach. However, sensitivity of ganglia measurements was only 48%, despite a specificity of 92%.¹² Sensitivity of root measurements was slightly better at 62%, with 82% specificity. Interrater agreement was good for both ganglia and root measurements. One study did not find any differences in cervical nerve root diameter between patients with CIDP (n = 15) and controls (n = 29).¹³ Three-dimensional volume measurements may be another approach. A recent study showed increased volume of peripheral nerves in patients with CIDP (n = 13) compared to controls (n = 12) using MRI with diffusion-weighted whole-body imaging with background body signal suppression.¹⁴ Combined, these studies suggest the potential of a quantitative approach to improve diagnostic reliability.

The potential of imaging techniques for diagnosis of CIDP and MMN has been demonstrated by several recent studies.¹⁵⁻¹⁸ In one of these studies MRI was abnormal in 22 of 38 (58%) patients with CIDP without definite electrodiagnostic criteria, which led to an adjustment of final diagnosis to definite CIDP in 7 patients.¹⁵ Additional studies are required to determine reproducible and reliable quantification techniques with optimal sensitivity and specificity in order to ensure proper diagnosis of treatment-responsive polyneuropathies.

REFERENCES

1. van den Bergh PYK, Hadden RDM, Bouche P, et al. European Federation of Neurological Societies/Peripheral Nerve Society Guideline on management of chronic inflammatory demyelinating polyradiculoneuropathy: Report of a joint task force of the European Federation of Neurological Societies and the Peripher. *Eur. J. Neurol.* 2010;17:356–363.
2. Van Schaik IN, Léger JM, Nobile-Orazio E, et al. European Federation of Neurological Societies/Peripheral Nerve Society Guideline on management of multifocal motor neuropathy. Report of a Joint Task Force of the European Federation of Neurological Societies and the Peripheral Nerve Society - First revis. *J Peripher Nerv Syst* 2010;15:295–301.
3. van Es HW, van den Berg LH, Franssen H, et al. Magnetic resonance imaging of the brachial plexus in patients with multifocal motor neuropathy. *Neurology* 1997;48:1218–1224.
4. Rajabally YA, Knopp MJ, Martin-Lamb D, Morlese J. Diagnostic value of MR imaging in the Lewis-Sumner syndrome: A case series. *J. Neurol. Sci.* 2014;342:182–185.
5. Castillo M, Mukherji SK. MRI of enlarged dorsal ganglia, lumbar nerve roots, and cranial nerves in polyradiculoneuropathies. *Neuroradiology* 1996;38:516–520.
6. Adachi Y, Sato N, Okamoto T, et al. Brachial and lumbar plexuses in chronic inflammatory demyelinating polyradiculoneuropathy: MRI assessment including apparent diffusion coefficient. *Neuroradiology* 2011;53:3–11.
7. Shibuya K, Sugiyama A, Ito S, et al. Reconstruction magnetic resonance neurography in chronic inflammatory demyelinating polyneuropathy. *Ann. Neurol.* 2015;77:333–337.
8. Jongbloed BA, Bos JW, Rutgers D, et al. Brachial plexus magnetic resonance imaging differentiates between inflammatory neuropathies and does not predict disease course. *Brain Behav.* 2017;7:e00632.
9. McHugh ML. Interrater reliability: the kappa statistic. *Biochem. Medica* 2012;22:276–282.
10. Goedee HS, Van Der Pol WL, Van Asseldonk JTH, et al. Diagnostic value of sonography in treatment-naive chronic inflammatory neuropathies. *Neurology* 2017;88:143–151.
11. Tazawa K-I, Matsuda M, Yoshida T, et al. Spinal Nerve Root Hypertrophy on MRI: Clinical Significance in the Diagnosis of Chronic Inflammatory Demyelinating Polyradiculoneuropathy. *Intern. Med.* 2008;47:2019–2024.
12. Hiwatashi A, Togao O, Yamashita K, et al. Evaluation of chronic inflammatory demyelinating polyneuropathy: 3D nerve-sheath signal increased with inked rest-tissue rapid acquisition of relaxation enhancement imaging (3D SHINKEI). *Eur. J. Radiol.* 2017;27:447–453.
13. Tanaka K, Mori N, Yokota Y, Suenaga T. MRI of the cervical nerve roots in the diagnosis of chronic inflammatory demyelinating polyradiculoneuropathy: a single-institution, retrospective case-control study. *BMJ Open* 2013;3:e003443.
14. Ishikawa T, Asakura K, Mizutani Y, et al. MR neurography for the evaluation of CIDP. *Muscle and Nerve* 2017;55:483–489.
15. Fargeot G, Viala K, Theaudin M, et al. Diagnostic usefulness of plexus MRI in chronic inflammatory demyelinating polyradiculopathy without electrodiagnostic criteria of demyelination. *Eur. J. Neurol.* 2019;26:631–638.
16. Jomier F, Bousson V, Viala K, et al. Prospective study of the additional benefit of plexus MRI in the diagnosis of CIDP. *Eur. J. Neurol.* 2020;27:181–187.
17. Goedee HS, Jongbloed BA, van Asseldonk J-TH, et al. A comparative study of brachial plexus sonography and magnetic



resonance imaging in chronic inflammatory demyelinating neuropathy and multifocal motor neuropathy. *Eur. J. Neurol.* 2017;24:1307–1313.

18. Goedee HS, Herraets IJT, Visser LH, et al. Nerve ultrasound can identify treatment-responsive chronic neuropathies without electrodiagnostic features of demyelination. *Muscle Nerve* 2019;60:415–419.







Chapter 4

Quantitative assessment of brachial plexus MRI for the diagnosis of chronic inflammatory neuropathies

Marieke H.J. van Rosmalen, H. Stephan Goedee, Anouk van der Gijp, Theo D. Witkamp, Ruben P.A. van Eijk, Fay-Lynn Asselman, Leonard H. van den Berg, Stefano Mandija, Martijn Froeling, Jeroen Hendrikse, W. Ludo van der Pol

Journal of Neurology, 2021 Mar; 268, 978 - 988

ABSTRACT

Objective: To develop a quantitative approach to assess abnormalities on MRI of the brachial plexus and the cervical roots in patients with chronic inflammatory demyelinating polyneuropathy (CIDP) and multifocal motor neuropathy (MMN) and to evaluate interrater reliability and its diagnostic value.

Methods: We performed a cross-sectional study in 50 patients with CIDP, 31 with MMN and 42 disease controls. We systematically measured cervical nerve root sizes on MRI bilaterally (C5, C6, C7) in the coronal (diameter (mm)) and sagittal planes (area (mm²)), next to the ganglion (G₀) and 1 cm distal from the ganglion (G₁). We determined their diagnostic value using a multivariate binary logistic model and ROC analysis. In addition, we evaluated intra- and interrater reliability.

Results: Nerve root size was larger in patients with CIDP and MMN compared to controls at all predetermined anatomical sites. We found that nerve root diameters in the coronal plane had optimal reliability (intrarater ICC 0.55–0.87; interrater ICC 0.65–0.90). AUC was 0.78 (95% CI 0.69–0.87) for measurements at G₀ and 0.81 (95% CI 0.72–0.91) for measurements at G₁. Importantly, our quantitative assessment of brachial plexus MRI identified an additional 10% of patients that showed response to treatment, but were missed by nerve conduction (NCS) and nerve ultrasound studies.

Conclusion: Our study showed that a quantitative assessment of brachial plexus MRI is reliable. MRI can serve as an important additional diagnostic tool to identify treatment responsive patients, complementary to NCS and nerve ultrasound.

INTRODUCTION

Chronic inflammatory demyelinating polyneuropathy (CIDP) and multifocal motor neuropathy (MMN) are rare disorders that often respond to treatment. Diagnostic criteria have been developed to distinguish CIDP and MMN from more common neuropathies and motor neuron disorders that rely on sets of typical clinical combined with specific electrodiagnostic features.^{1,2} Diagnosing CIDP or MMN remains challenging when nerve conduction studies (NCS) do not meet the required electrodiagnostic criteria.^{2,3}

Nerve imaging by means of qualitative MRI is recommended in diagnostic guidelines for cases without NCS abnormalities. MRI of the brachial plexus and cervical nerve roots shows nerve root thickening and increased T2 signal intensity in 45-57% of patients.⁴⁻⁷ These abnormalities have therefore been included as a supportive criterium in the diagnostic criteria for CIDP and MMN.^{1,2} However, qualitative assessments showed low interrater reliability.^{8,9} In contrast, a quantitative assessment of nerve ultrasound showed excellent test characteristics for the detection of inflammatory neuropathies.¹⁰⁻¹³ This suggests that quantification of MRI abnormalities may improve its diagnostic value.

Therefore, the aim of our study is to systematically assess nerve root sizes on MRI of the brachial plexus and cervical nerve roots in a large cohort of patients with chronic inflammatory neuropathies and relevant disease controls. Using these data, we investigated interrater reliability and the diagnostic value of MRI in addition to NCS and nerve ultrasound.

METHODS

Study design

We performed a cross-sectional study in prevalent and incident patients with CIDP and MMN, and clinically relevant controls (i.e. amyotrophic lateral sclerosis ALS) or progressive muscular atrophy (PMA)). We used a standardized protocol to systematically assess cervical nerve root sizes, determined their diagnostic value and reproducibility and developed a risk chart including objective cut-off values for abnormality.

Patients and clinical data

All prevalent and incident patients with an established diagnosis of CIDP or MMN, visiting our neuromuscular outpatient clinic at the University Medical Center Utrecht (UMCU), were eligible for inclusion. We used previously published diagnostic criteria for CIDP and MMN, in short for CIDP we used the diagnostic criteria as defined in the EFNS/PNS guideline and for MMN we used the Utrecht criteria.^{1,2} As disease controls, we enrolled a random sample of patients with motor neuron



4

disease (ALS and PMA), according to the Brooks criteria.¹⁴ We excluded patients aged < 18 years, patients with motor neuron disease that had a bulbar onset of symptoms and patients who were physically unable to undergo MRI or who met one of the routine contraindications to MRI (e.g. pacemaker, non-MRI approved surgical clips or implants, claustrophobia, a recent prosthetic operation).

We obtained demographic and clinical data, including treatment response and results from routine diagnostic work-up, i.e. diagnostic NCS and nerve ultrasound results. Treatment response was evaluated based on the discretion of the treating physician. Written informed consent was obtained from all study participants.

Routine diagnostic work-up

Nerve conduction studies

Diagnostic NCS were performed using a Nicolet Viking IV EMG machine (CareFusion Japan, Tokyo, Japan) following previously described protocols.^{10,15} The results were interpreted using the EFNS/PNS criteria for CIDP (definite, probable, possible) and the Utrecht criteria for MMN (definite motor conduction block, probable motor conduction block, slowing of conduction compatible with demyelination).^{1,2}

Nerve ultrasound

Diagnostic nerve ultrasound was performed using a Philips Affinity 70G (Philips Medical Instruments, eL 1-48 MHz linear array transducer) following a previously published protocol.¹⁰ In short, we collected nerve sizes of the median nerves (forearm and upper arm) and brachial plexus trunks bilaterally. We used the ellipse tool to measure cross sectional area (mm²) and we used cut-off values for abnormal nerve size to identify patients with a chronic inflammatory neuropathy (median nerve forearm > 10 mm² and upper arm > 13 mm²; plexus trunks > 9 mm²). Nerve ultrasound was considered abnormal if nerve enlargement was present at ≥ 1 measured sites.

Equipment and MRI parameters

All patients underwent an MRI scan of the brachial plexus and cervical nerve roots on a 3.0 Tesla MRI scanner (Philips Healthcare, Best, the Netherlands) using a 24-channel head neck coil. All participants were positioned in supine position. We performed 3D turbo spin echo spectral presaturation with inversion recovery (SPIR) in a coronal and sagittal slice orientation with the following acquisition parameters: field of view = 336*336*170 mm, matrix size = 224*223, voxel size = 0.75*0.75*1 mm³, echo time = 206 ms, repetition time = 2200 ms, turbo spin echo factor = 76, sense factor = 3 (P reduction right/left) and 1.5 (S reduction anterior/posterior), acquisition time = 03:59 minutes. A coronal slab maximum intensity projection (MIP) was created as a post-processing step (slab thickness = 10 mm, number of slabs = 75).

Nerve root measurements on MRI data

We measured cervical nerve root sizes in coronal and sagittal planes, using PACS IDS7 21.1.2 (Sectra AB, Linköping, Sweden). We used the distance tool to measure diameters (mm) of nerve roots in coronal MIP images. Nerve root diameter was measured perpendicular on the center lines of the nerve roots, bilaterally in root C5, C6 and C7 at two predetermined anatomical sites: directly next to the ganglion (G_0) and 1 cm distal from the ganglion (G_1). In addition, we used the cross-cursor tool to identify the corresponding sites of these measurements on the sagittal 3D TSE SPIR, and measured cross sectional area (mm^2) in the sagittal plane using the area tool, which is a manual tracer, resulting in 24 measurements in total per subject (duration 3-5 minutes per subject, **Figure 4.1**). Zoom magnification was standardized to 1x for all images. As anatomic variability in the brachial plexus is common, and may be even more present in more distal parts,¹⁶ we decided to not perform measurements when individual nerve roots merged, divided or showed other anatomical variances. We also did not perform measurements when image quality was poor. To determine intrarater reliability, one rater (MVR) performed all measurements twice in two sessions with an interval of 1 month between the first and second session. To determine interrater reliability a second rater (AG) scored a random sample of 20 MRI scans from our data set. Both raters were blinded to clinical status.

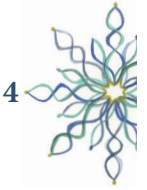
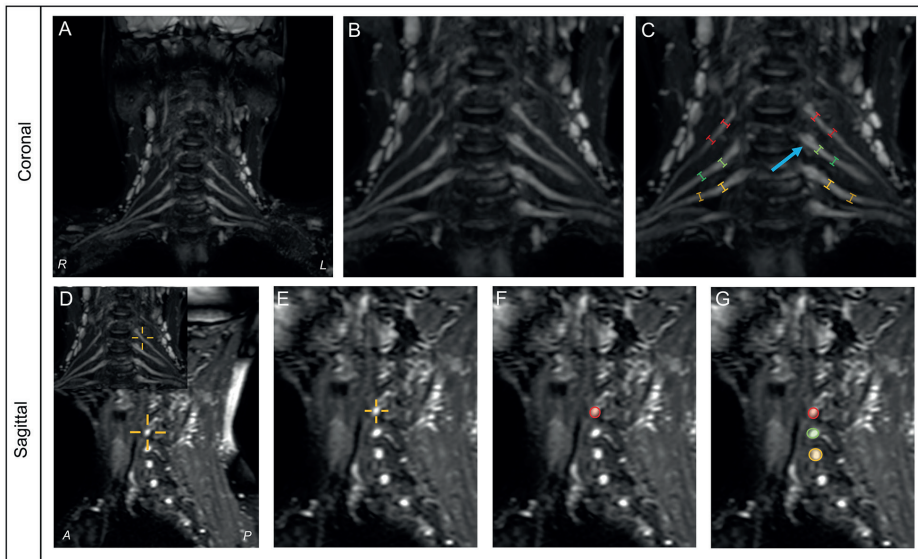


Figure 4.1 Example of nerve root measurements in coronal and sagittal planes.



Method of measurements in coronal (upper) and sagittal (lower) planes. Coronal measurements in maximum intensity projection images (A) using 1x zoom (B) and callipers placed in nerve root C5 (red), C6 (green) and C7 (yellow) next to the ganglion (blue arrow) and 1 cm distal of the ganglion (C). Sagittal measurements in T2 weighted fat-suppressed images using a cross-cursor to identify corresponding measurement sites (D) and 1x zoom (E). Measurements were then performed at these corresponding measurement sites (F, G). *R* = right; *L* = left; *A* = anterior; *P* = posterior.

Statistical analysis

IBM SPSS Statistics (Version 25, Chicago, Illinois, United States) was used for statistical analysis. To compare patient characteristics between cases and controls, we used one-way analysis of variance (ANOVA) for numerical data and Chi-squared test for categorical data. To evaluate the feasibility of our method we compared numbers of successfully performed measurements between the coronal and sagittal plane and between G_0 and G_1 using an independent samples t test. To determine mean nerve root size we also used an independent samples t test. Results with a p value < 0.05 were considered significant. To evaluate intra- and interrater reliability we used the intraclass correlation coefficient (ICC). We calculated a mean ICC of the right and left side per measurement site. We considered an ICC < 0.50 as poor reliability, $0.50 - 0.75$ as moderate, $0.75 - 0.90$ as good and > 0.90 as excellent reliability.¹⁷

ROC analysis and development of risk chart

We used receiver operating characteristic (ROC) analysis to determine area under the curve (AUC) per nerve root (C5, C6, C7) and for two different combinations of measurement: 1. mean of all three nerve roots bilaterally next to the ganglion (3 variables) and 2. mean of all three nerve roots 1 cm distal from the ganglion (3 variables). We then used a multivariate binary logistic model for both combinations separately with measurement sites as covariates. With the results of this model we calculated the log odds for having an inflammatory neuropathy using the following equation (Eq. 1):

$$\log\left(\frac{p}{1-p}\right) = \beta_0 + \beta_1 C5 + \beta_2 C6 + \beta_3 C7 \quad (\text{Eq. 1})$$

Where β_0 is the constant, b_1 , b_2 and b_3 the logistic regression coefficients of nerve roots C5, C6 and C7 respectively and C5, C6 and C7 the diameters of the nerve roots in millimetres. Subsequently, we took the inverse logit to obtain p , i.e. the absolute probability of having an inflammatory neuropathy, using the following equation (Eq. 2):

$$p = \frac{1}{1 + e^{-(\beta_0 + \beta_1 C5 + \beta_2 C6 + \beta_3 C7)}} \quad (\text{Eq. 2})$$

To develop a risk chart, we calculated p for different combinations of C5, C6 and C7 and for both combinations of measurement sites. Finally, we obtained a cut-off value for p obtaining 95% specificity, i.e. we determined at which p we considered MRI to be abnormal.

RESULTS

Patients

We included a total of 123 patients (CIDP = 50, MMN = 31, disease controls = 42). Patient characteristics are summarized in **Table 4.1**. Patients with MMN were younger than patients with CIDP and disease controls ($p < 0.001$). We found no significant differences in other baseline characteristics between groups.

Table 4.1 Patient characteristics

Parameter	Inflammatory neuropathy		Motor neuron disease	Level of significance
	CIDP	MMN		
Number of patients	50	31	42	-
Age, years (SD)	63.8 (9.4)	52.5 (11.7)	63.1 (11.2)	< 0.001*
Male (%)	42 (84.0%)	29 (93.5%)	31 (73.8%)	0.083
Disease duration, months (SD)	33.6 (65.2)	61.8 (80.5)	45.4 (38.1)	0.143
Nerve conduction study				
Inconclusive (%)	14 (28.0%)	7 (22.6%)	-	
Possible (CIDP)/Slowing of conduction (MMN) (%)	9 (18.0%)	3 (9.6%)	-	
Probable (%)	2 (4.0%)	3 (9.6%)	-	
Definite (%)	25 (50.0%)	18 (58.1%)	-	
Ultrasound				
Normal (%)	10 (20.0%)	6 (19.4%)	5 (11.9%)	
Abnormal (%)	35 (70.0%)	25 (80.6%)	3 (7.1%)	
Missing (%)	5 (10.0%)	0 (0.0%)	34 (81.0%)	

* Age differs significantly between patients with MMN and patients with CIDP, and between patients with MMN and disease controls.

Nerve root measurements on MRI

Feasibility of measuring method

Table 4.2 summarizes the number of measurements per nerve root that could be performed successfully. We obtained more measurements at G_0 compared to G_1 ($p < 0.001$). Measurements in the coronal plane were more often successful than in the sagittal plane ($p < 0.001$). We established that this was mostly related to early merging or dividing nerve roots and the fact that images showed lower image quality more distally.



4

Table 4.2 Rate of overall successful measurements per nerve root on brachial plexus MRI performed by one rater

Nerve root		Coronal		Sagittal	
		Ganglion	1 cm	Ganglion	1 cm
C5	Right	120 (97.5%)	100 (81.3%)	115 (93.5%)	74 (60.2%)
	Left	119 (96.7%)	85 (69.1%)	110 (89.4%)	56 (45.5%)
C6	Right	120 (97.5%)	96 (78.0%)	120 (97.5%)	89 (72.4%)
	Left	122 (99.2%)	87 (70.7%)	118 (95.9%)	66 (53.7%)
C7	Right	118 (95.6%)	73 (59.3%)	116 (94.3%)	68 (55.2%)
	Left	119 (96.7%)	70 (56.9%)	114 (92.7%)	60 (48.8%)

Number of measurements performed per nerve root differed between coronal and sagittal plane due to lower image quality, and between measurement site (next to ganglion or 1 cm distal from ganglion) due to merging or dividing of nerve roots.

Intra- and interrater reliability

Table 4.3 shows the intraclass correlation coefficients (ICC) within and between raters. We found moderate to good intrarater reliability in both plane orientations (ICC 0.55 – 0.87 in coronal plane, and 0.63 – 0.86 in sagittal plane). We found moderate to good interrater reliability in the coronal plane (ICC 0.65 – 0.90) but a poor to good reliability in the sagittal plane (ICC 0.47 – 0.84). Overall, we found higher consistency in measurements performed in the coronal plane orientation.

Table 4.3 Reliability of nerve root measurements on brachial plexus MRI

Site		Intrarater reliability		Interrater reliability	
		Coronal	Sagittal	Coronal	Sagittal
C5	Ganglion	0.81 (0.74 – 0.86)	0.69 (0.58 – 0.77)	0.81 (0.58 – 0.92)	0.52 (0.09 – 0.78)
	1 cm	0.55 (0.41 – 0.67)	0.63 (0.47 – 0.74)	0.78 (0.51 – 0.91)	0.62 (0.14 – 0.87)
C6	Ganglion	0.77 (0.69 – 0.84)	0.68 (0.58 – 0.77)	0.77 (0.37 – 0.89)	0.47 (0.04 – 0.75)
	1 cm	0.84 (0.77 – 0.89)	0.83 (0.74 – 0.88)	0.82 (0.58 – 0.93)	0.79 (0.50 – 0.92)
C7	Ganglion	0.78 (0.70 – 0.84)	0.75 (0.67 – 0.82)	0.65 (0.13 – 0.87)	0.73 (0.44 – 0.89)
	1 cm	0.87 (0.81 – 0.91)	0.86 (0.79 – 0.91)	0.90 (0.60 – 0.97)	0.84 (0.35 – 0.96)

Intraclass correlation coefficient (ICC) with 95% confidence interval for every measurement site in coronal and sagittal planes.

Mean nerve root size

Mean nerve root sizes are summarized in **Table 4.4**. Nerve root sizes in patients with CIDP and MMN were larger compared to disease controls, at all predetermined anatomical sites (p varied from < 0.001 to 0.026).

Table 4.4 Mean nerve root sizes per measurement site

Nerve root		Inflammatory neuropathy (n = 81)	Control (n = 42)	MD (95% CI)	Level of significance
CORONAL					
C5	<i>Ganglion</i>	3.0 (0.8)	2.5 (0.6)	0.5 (0.3 – 0.7)	< 0.001
	<i>1 cm</i>	2.8 (0.9)	2.2 (0.5)	0.6 (0.3 – 0.8)	< 0.001
C6	<i>Ganglion</i>	3.8 (0.9)	3.3 (0.6)	0.5 (0.2 – 0.8)	< 0.001
	<i>1 cm</i>	3.6 (1.1)	2.9 (0.7)	0.7 (0.3 – 1.1)	< 0.001
C7	<i>Ganglion</i>	4.0 (0.9)	3.4 (0.7)	0.7 (0.3 – 1.0)	< 0.001
	<i>1 cm</i>	3.7 (1.1)	2.8 (0.6)	0.9 (0.4 – 1.4)	< 0.001
SAGITTAL					
C5	<i>Ganglion</i>	21.6 (6.8)	18.5 (5.7)	3.1 (0.7 – 5.6)	0.013
	<i>1 cm</i>	20.3 (7.2)	16.7 (4.4)	3.6 (1.1 – 6.1)	0.005
C6	<i>Ganglion</i>	27.2 (9.1)	23.4 (5.2)	3.8 (0.8 – 6.8)	0.013
	<i>1 cm</i>	25.3 (11.5)	19.2 (6.5)	6.1 (2.0 – 10.2)	0.004
C7	<i>Ganglion</i>	26.4 (10.4)	22.0 (5.4)	4.4 (1.5 – 7.2)	0.003
	<i>1 cm</i>	23.1 (14.7)	16.1 (4.3)	7.1 (0.9 – 13.3)	0.026

Nerve root sizes are mean (standard deviation). Coronal measurements are in millimetres (mm). Sagittal measurements are square millimetres (mm²). Abbreviations: MD = mean difference; CI = confidence interval; SD = standard deviation.

ROC analysis and development of risk chart

Sagittal measurements were less often successful because of lower data quality and overall lower reliability (**Table 4.2 and 4.3**). We therefore decided to exclude the measurements in the sagittal plane from further analysis. Results from the ROC analysis are shown in **Figure 4.2**. We found a comparable AUC for both predetermined anatomical sites in the coronal plane (G_0 and G_1). We developed a risk chart (**Figure 4.3**) that predicts the absolute chance of having a chronic inflammatory neuropathy, based on different combinations of nerve root sizes of C5, C6 and C7.

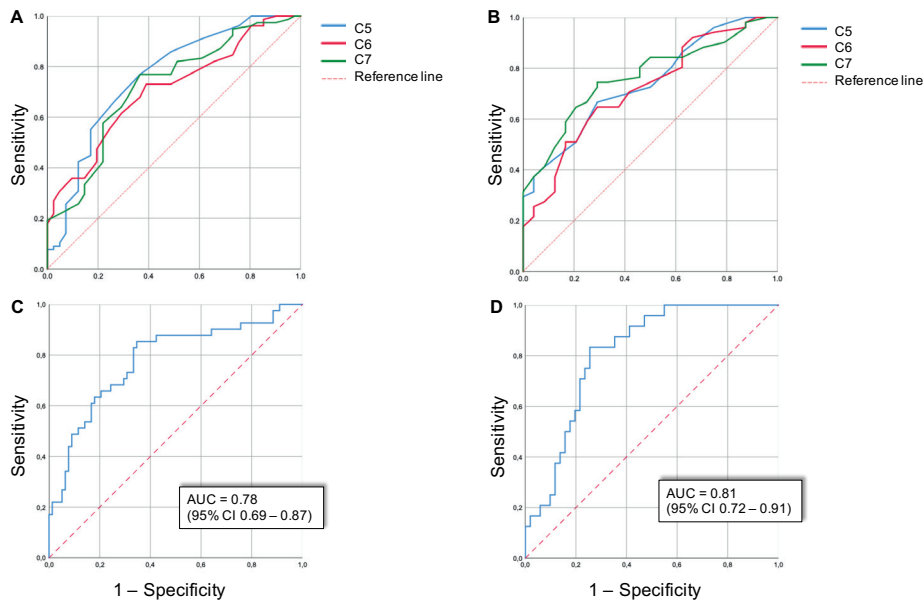


4

The added value of MRI

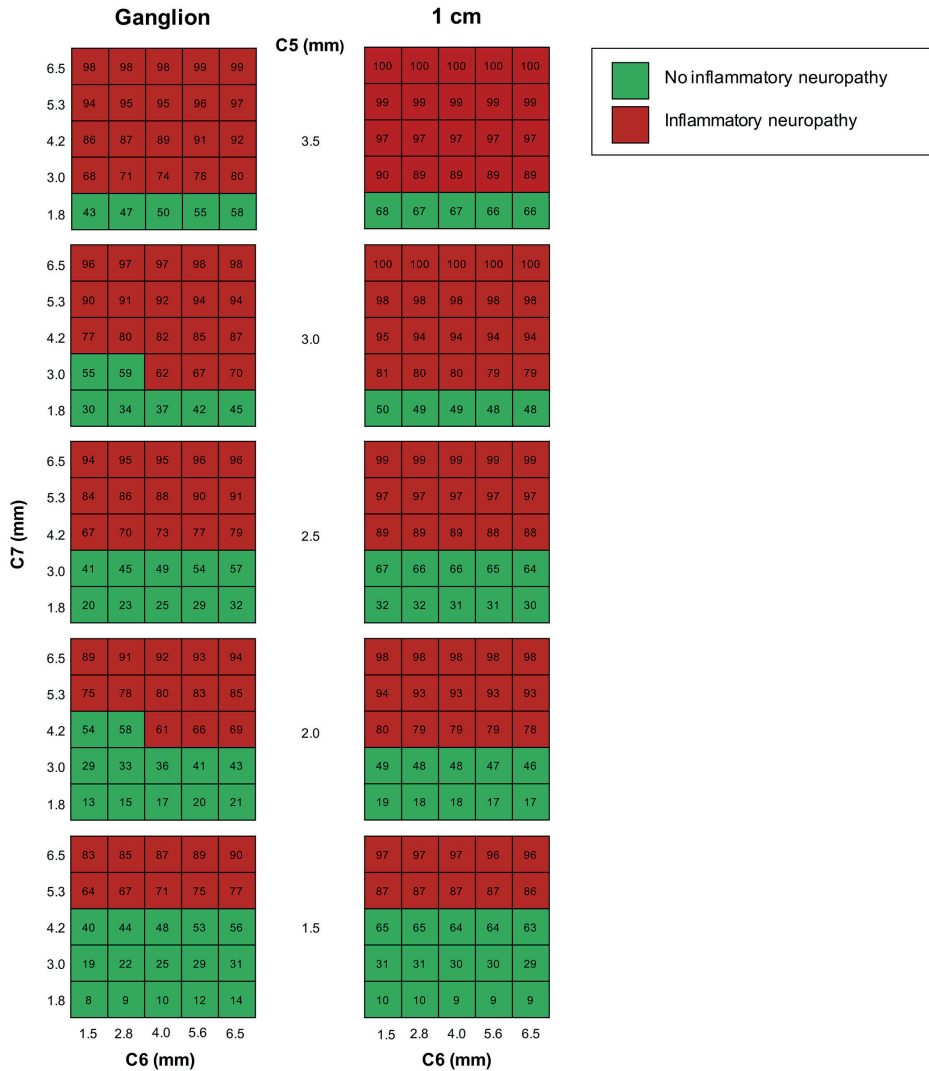
ROC analysis showed that at a set specificity of 95%, the sensitivities are 27% for G_0 and 17% at G_1 . With this specificity, a probability of $\geq 61\%$ for measurements at G_0 and $\geq 69\%$ at G_1 in the risk chart were considered abnormal or likely to have a chronic inflammatory neuropathy (**Figure 4.3**). With these cut-off values, we determined which patients in our data set had an abnormal MRI and we investigated the added value of brachial plexus MRI in addition to NCS and nerve ultrasound. We found that NCS combined with nerve ultrasound identified most patients with an inflammatory neuropathy. The majority of patients with abnormal ultrasound findings also had abnormal MRI findings (**Figure 4.4A and B**). However, 5/50 (10%) patients with CIDP had an abnormal MRI result, while NCS did not fulfill the criteria for CIDP and ultrasound did not show abnormalities. All patients had a good response to treatment. Clinical symptoms and laboratory findings of these 5 patients are summarized in **Table 4.5**. MRI did not have any added diagnostic value for MMN.

Figure 4.2 ROC analysis of nerve root size measurements on MRI



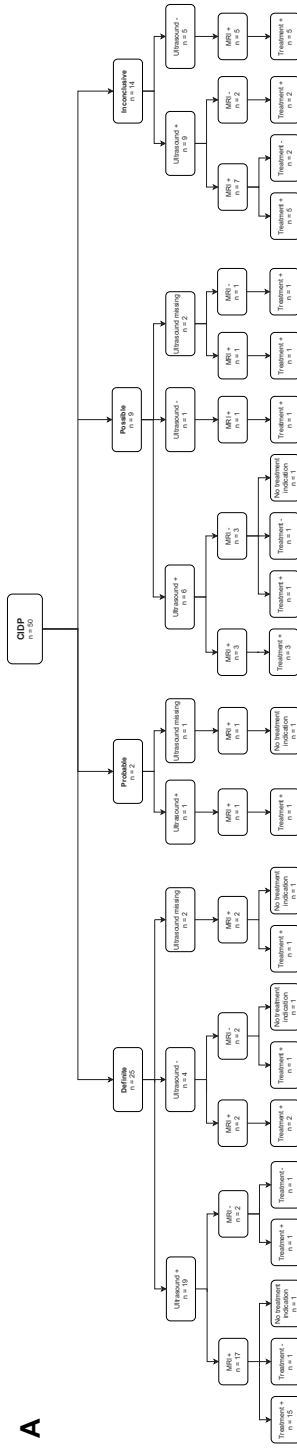
ROC curves of measurements per nerve root next to the ganglion (A) and 1 cm distal of the ganglion (B) are shown in the upper panels. Combined ROC curves of measurements next to the ganglion (C) and 1 cm distal of the ganglion (D) are shown in the lower panels. Combined measurements are expressed as area under the curve (AUC) and 95% confidence interval (CI).

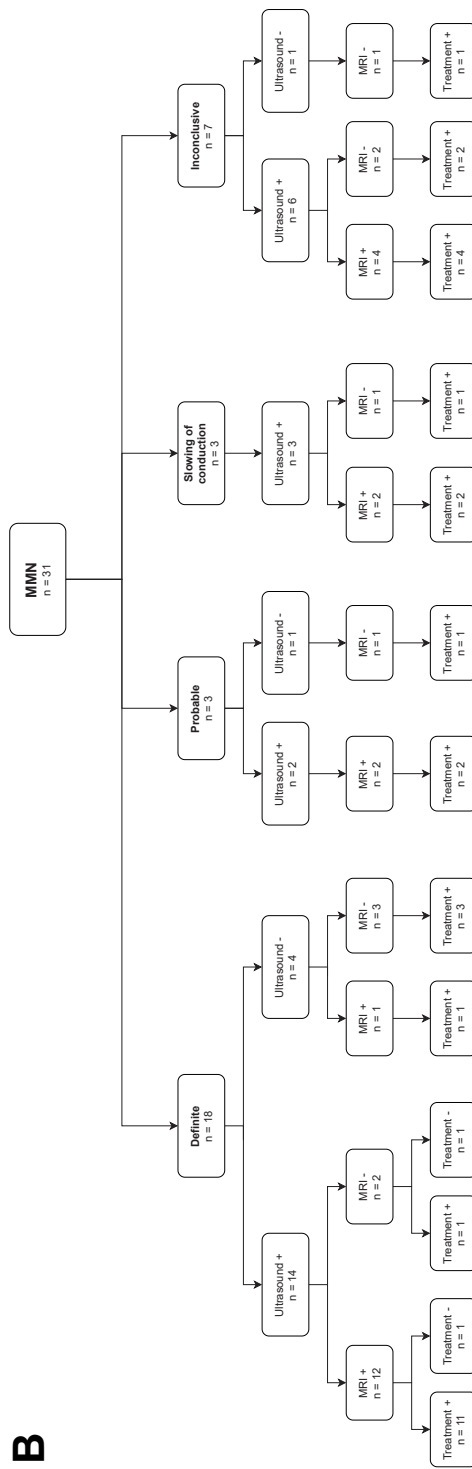
Figure 4.3 Risk chart for predicting CIDP or MMN based on nerve root sizes



Risk charts for measurements next to the ganglion (left panels) and 1 cm distal from the ganglion (right panels). The risk chart provides the absolute risk of having CIDP or MMN based on different combinations of nerve root thickness of nerve root C5, C6 and C7. Every cell of the table contains the probability of having CIDP or MMN (e.g. for measurements next to the ganglion (left panels): if C5 is 1.5 mm, C6 is 1.5 mm and C7 is 1.8 mm, the probability of having CIDP or MMN is 8%). A probability of $\geq 61\%$ for measurements next to the ganglion and $\geq 69\%$ for measurements 1 cm distal from the ganglion were considered abnormal (cells in red). The axes range between the 95% lowest and highest measurements.

Figure 4.4 Results of NCS, ultrasound and MRI in patients with CIDP and MMN





Flow chart of patients with CIDP (A) and MMN (B) showing outcome of nerve conduction studies, nerve ultrasound of the brachial plexus and median nerve, MRI of the brachial plexus and cervical nerve roots and treatment response.

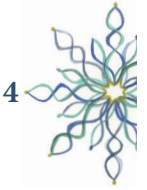


Table 4.5 Patient characteristics of patients with CIDP who did not fulfil diagnostics criteria on NCS and without ultrasound abnormalities

Patient	Male/female	Clinical presentation	NCS
1	Male	Symmetrical weakness in proximal and distal arm and leg muscles; loss of vibration, touch and position sense in arms and legs; areflexia	CMAP↓ right median, right peroneal and left tibial nerve. ↑DML bilateral median nerves. ↓SNAP bilateral median, ulnar, radial and sural nerves.
2	Male	Asymmetrical weakness in proximal and distal right arm muscles and right leg muscles; loss of vibration sense distal from knees; low reflexes in the arms, areflexia in the legs	CMAP↓ bilateral median, right ulnar, bilateral peroneal and left tibial nerve. ↑DML bilateral median nerves. Normal SNAP's.
3	Male	Asymmetrical weakness in proximal and distal right arm; tremor; loss of vibration sense in feet; areflexia.	CMAP↓right median nerve. ↑DML left median nerve. ↓SNAP bilateral median and sural nerves.
4	Male	Symmetrical weakness in proximal and distal leg muscles; fluctuating pain in legs; loss of vibration sense in feet; areflexia	CMAP↓ right peroneal and left tibial nerve. ↑DML right median and left ulnar nerve. ↓SNAP bilateral sural nerves.
5	Male	Symmetrical weakness in extensor hallucis longus muscle; loss of vibration and touch sense in feet up to the knees; low reflexes in the arms, areflexia in the legs.	CMAP↑ left median, bilateral ulnar and peroneal, right tibial nerve. ↑DML right median nerve. ↓SNAP bilateral median, right ulnar, left tibial, bilateral sural.

Electrodiagnostic criteria	Liquor protein in g/L (normal 0.00 – 0.40)	Treatment and dosage	Response to treatment
Not compatible	0.39	Intravenous immunoglobulins, 40 gram every 3 weeks.	Improvement of pinch force right hand from 55 kPa to 100 kPa, improvement pinch force left hand of 30 kPa to 98 kPa, measured with Martin vigorimeter.
Not compatible	0.48	Intravenous immunoglobulins, 30 gram every 3 weeks.	Improvement of dorsal flexion of right foot, measured with myometry by physiotherapist.
Not compatible	0.61	Intravenous immunoglobulins, 40 gram every 4 weeks.	Improvement of MRC 4 to 5 in right arm, measured by treating physician.
Not compatible	0.70	Methylprednisolone 1000 mg every 4 weeks.	Improvement of MRC 3 to 4 (right) and MRC 4 to 5 (left) in quadriceps muscles, improvement of MRC 0 to 4 in left anterior tibial muscle, measured by treating physician.
Not compatible	0.42	Single therapy of intravenous immunoglobulins, 40 gram during 5 days.	Improvement of touch sense, better balance, observed by treating physician.



4

DISCUSSION

Quantitative assessment of brachial plexus MRI has acceptable interrater reliability and can be used in the diagnostic workup of patients who may have an inflammatory neuropathy. It can complement NCS and nerve ultrasound for the diagnosis of CIDP, but not MMN. A quantitative assessment of MRI of the brachial plexus and cervical nerve roots with high specificity identified 10% additional patients who responded to treatment but had not been identified by NCS and nerve ultrasound.

MRI is part of the current diagnostic criteria for CIDP and MMN and is recommended in particular for the identification of elusive cases, i.e. those without clear NCS abnormalities.^{1,2,18-21} This is based on several MRI studies that showed cervical nerve root thickening and increased signal intensity on brachial plexus MRI in a subgroup of patients with chronic inflammatory neuropathies.^{7,20} A clear limitation of qualitative assessment of brachial plexus MRI as it is used nowadays is its low interrater reliability.^{8,9} Few studies have explored the feasibility and use of a quantitative MRI assessment and only in small groups of patients and healthy controls.^{9,22-25} Estimates of the upper limit of normal for cervical nerve root size in healthy controls ranged between 4-5 mm. Analysis of our data from a large cohort of patients with CIDP and MMN showed that combinations of nerve root size are probably more useful than a fixed cut-off. This may be explained by the patchy nature of inflammatory changes. We found that 6 bilateral measurements close to the ganglion of root C5, C6 and C7 in coronal plane was easy to implement in routine practice (3 minutes per subject) and resulted in optimal test characteristics with high specificity levels. Sensitivity levels of quantitative assessment of brachial plexus MRI were lower than those reported in qualitative studies.^{23,24} This may be explained by some inclusion bias in earlier studies, as shown by another recent prospective cohort study that also reported a relatively low sensitivity of qualitative brachial and lumbosacral plexus MRI in patients with suspected CIDP.²¹ Importantly, test-retest reliability for quantitative measurements was good, which is supported by data from another recent study.²³

We analyzed the diagnostic value of a quantitative assessment of MRI next to NCS and nerve ultrasound studies.^{10,12,13} MRI helped to identify patients with a clinical phenotype compatible with CIDP but who did not fulfil the diagnostic criteria of NCS and who did not have ultrasound abnormalities. In this sense, MRI complements nerve ultrasound, which has an excellent sensitivity as shown in previous studies.^{10,13} Quantitative assessment of brachial plexus MRI identified an additional 10% of patients who responded to treatment, which is clinically relevant. MRI should therefore be considered as an additional diagnostic tool when there is a strong clinical suspicion of CIDP, particularly when NCS and nerve ultrasound results are normal. Nerve ultrasound, and especially the required expertise, is not always available in all medical centres. In these centres MRI could be used as an additional tool to NCS and laboratory findings, although physicians should always consider the poor sensitivity of MRI when interpreting results.

Our study comprises a relatively large number of patients with MMN and CIDP, although we acknowledge that the group sizes in studies on rare neuropathies are almost always a limitation. Our control group was homogeneous and did not include a spectrum of mimics as in previous studies. This was a deliberate choice since ultrasound studies showed that it is unlikely that nerve root sizes are enlarged in patients with axonal neuropathies.¹⁰ We also acknowledge that both nerve imaging and NCS may fail to discriminate CIDP from certain rare mimics, such as hereditary demyelinating polyneuropathies, paraproteinemic polyneuropathies and amyloidosis. However, clinical phenotypes and laboratory findings in these rare mimics will often guide a clinician to the right diagnosis without the use of nerve imaging techniques.

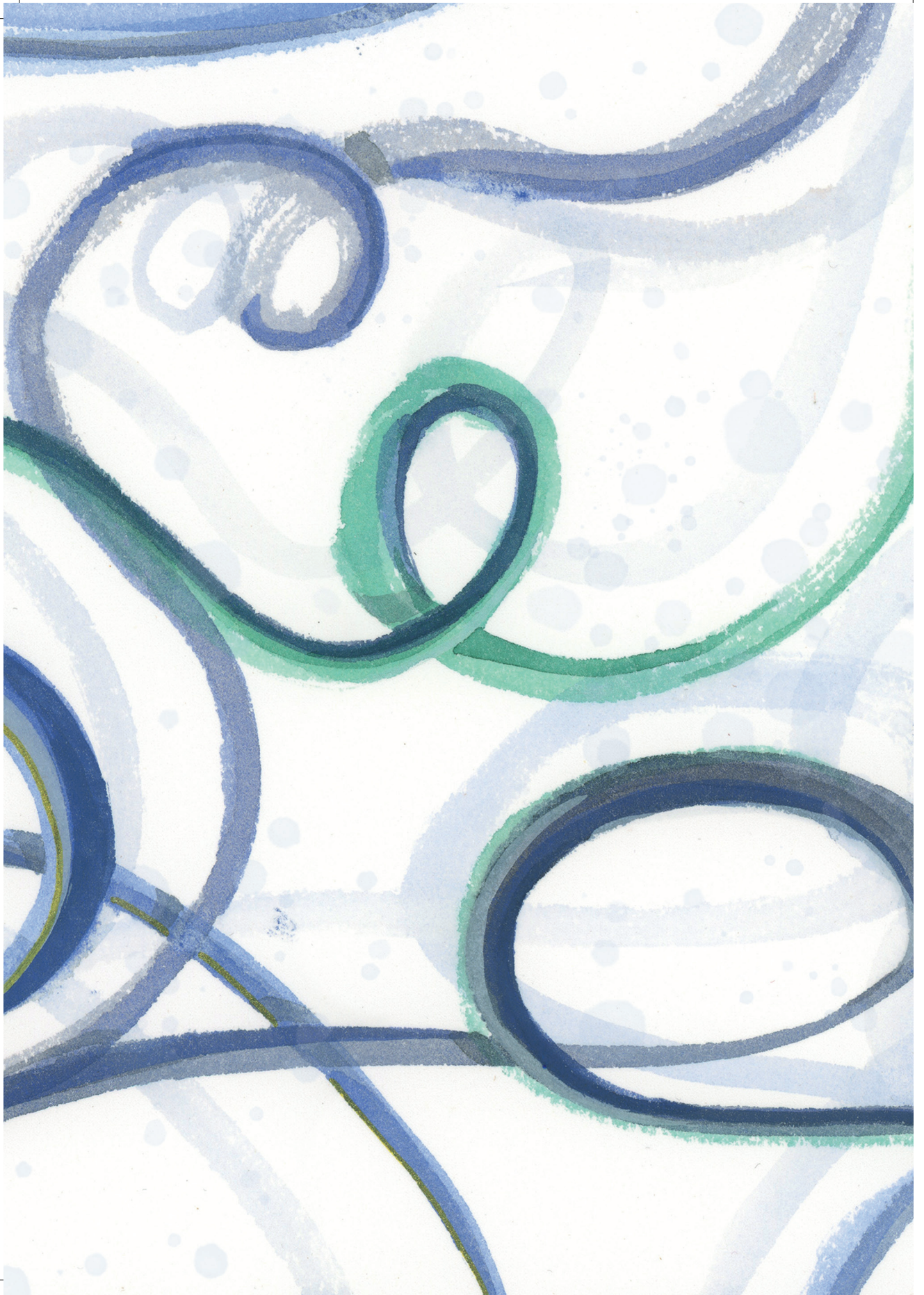
We show that quantitative assessment of MRI of the brachial plexus and cervical nerve roots is a reliable and useful tool for the diagnostic workup of patients who may have a chronic inflammatory neuropathy. A quantitative approach is feasible and does not have the limitation of high interrater variability of the currently used qualitative assessments.

REFERENCES

1. van den Bergh PYK, Hadden RDM, Bouche P, et al. European Federation of Neurological Societies/Peripheral Nerve Society Guideline on management of chronic inflammatory demyelinating polyradiculoneuropathy: Report of a joint task force of the European Federation of Neurological Societies and the Peripher. *Eur. J. Neurol.* 2010;17:356–363.
2. Vlam L, Van Der Pol WL, Cats EA, et al. Multifocal motor neuropathy: Diagnosis, pathogenesis and treatment strategies. *Nat. Rev. Neurol.* 2012;8:48–58.
3. Allen JA, Lewis RA. CIDP diagnostic pitfalls and perception of treatment benefit. *Neurology* 2015;85:498–504.
4. Castillo M, Mukherji SK. MRI of enlarged dorsal ganglia, lumbar nerve roots, and cranial nerves in polyradiculoneuropathies. *Neuroradiology* 1996;38:516–520.
5. van Es HW, van den Berg LH, Franssen H, et al. Magnetic resonance imaging of the brachial plexus in patients with multifocal motor neuropathy. *Neurology* 1997;48:1218–1224.
6. Goedee HS, Jongbloed BA, van Asseldonk J-TH, et al. A comparative study of brachial plexus sonography and magnetic resonance imaging in chronic inflammatory demyelinating neuropathy and multifocal motor neuropathy. *Eur. J. Neurol.* 2017;24:1307–1313.
7. Jongbloed BA, Bos JW, Rutgers D, et al. Brachial plexus magnetic resonance imaging differentiates between inflammatory neuropathies and does not predict disease course. *Brain Behav.* 2017;7:e00632.
8. Rosmalen MHJ, Goedee HS, Gijp A, et al. Low interrater reliability of brachial plexus MRI in chronic inflammatory neuropathies. *Muscle Nerve* 2020;61:779–783.
9. Oudeman J, Eftimov F, Strijkers GJ, et al. Diagnostic accuracy of MRI and ultrasound in chronic immune-mediated neuropathies. *Neurology* 2020;94:e62–e74.
10. Goedee HS, Van Der Pol WL, Van Asseldonk JTH, et al. Diagnostic value of sonography in treatment-naïve chronic inflammatory neuropathies. *Neurology* 2017;88:143–151.
11. Goedee HS, Van Der Pol WL, Hendrikse J, Van Den Berg LH. Nerve ultrasound and magnetic resonance imaging in the diagnosis of neuropathy. *Curr. Opin. Neurol.* 2018;31:526–533.
12. Herraets IJT, Goedee HS, Telleman JA, et al. Nerve ultrasound improves detection of treatment-responsive chronic inflammatory neuropathies. *Neurology* 2020;94:e1470–e1479.
13. Herraets IJT, Goedee HS, Telleman JA, et al. Nerve ultrasound for the diagnosis of chronic inflammatory neuropathy: a multicenter validation study. *Neurology* 2020;95:e1745–e1753.
14. Brooks BR, Miller RG, Swash M, Munsat TL. El Escorial revisited: Revised criteria for the diagnosis of amyotrophic lateral sclerosis. *ALS Mot. neuron Disord.* 2000;1:293–299.
15. Van Asseldonk JTH, Van Den Berg LH, Kalmijn S, et al. Criteria for demyelination based on the maximum slowing due to axonal degeneration, determined after warming in water at 37°C: Diagnostic yield in chronic inflammatory demyelinating polyneuropathy. *Brain* 2005;128:880–891.
16. Johnson EO, Vekris M, Demesticha T, Soucacos PN. Neuroanatomy of the brachial plexus: Normal and variant anatomy of its formation. *Surg. Radiol. Anat.* 2010;32:291–297.
17. Koo TK, Li MY. A Guideline of Selecting and Reporting Intraclass Correlation Coefficients for Reliability Research. *J. Chiropr. Med.* 2016;15:155–163.
18. Gasparotti R, Lucchetta M, Cacciavillani M, et al. Neuroimaging in diagnosis of atypical polyradiculoneuropathies: report of three cases and review of the literature. *J. Neurol.* 2015;262:1714–1723.

19. Lozeron P, Lacour MC, Vandendries C, et al. Contribution of plexus MRI in the diagnosis of atypical chronic inflammatory demyelinating polyneuropathies. *J. Neurol. Sci.* 2016;360:170–175.
20. Fargeot G, Viala K, Theaudin M, et al. Diagnostic usefulness of plexus MRI in chronic inflammatory demyelinating polyradiculopathy without electrodiagnostic criteria of demyelination. *Eur. J. Neurol.* 2019;26:631–638.
21. Jomier F, Bousson V, Viala K, et al. Prospective study of the additional benefit of plexus MRI in the diagnosis of CIDP. *Eur. J. Neurol.* 2020;27:181–187.
22. Tazawa K-I, Matsuda M, Yoshida T, et al. Spinal Nerve Root Hypertrophy on MRI: Clinical Significance in the Diagnosis of Chronic Inflammatory Demyelinating Polyradiculoneuropathy. *Intern. Med.* 2008;47:2019–2024.
23. Hiwatashi A, Togao O, Yamashita K, et al. Evaluation of chronic inflammatory demyelinating polyneuropathy: 3D nerve-sheath signal increased with inked rest-tissue rapid acquisition of relaxation enhancement imaging (3D SHINKEI). *Eur. J. Radiol.* 2017;27:447–453.
24. Tanaka K, Mori N, Yokota Y, Suenaga T. MRI of the cervical nerve roots in the diagnosis of chronic inflammatory demyelinating polyradiculoneuropathy: a single-institution, retrospective case-control study. *BMJ Open* 2013;3:e003443.
25. Su X, Kong X, Liu D, et al. Multimodal magnetic resonance imaging of peripheral nerves: Establishment and validation of brachial and lumbosacral plexi measurements in 163 healthy subjects. *Eur. J. Radiol.* 2019;117:41–48.





Chapter 5

MRI of the intraspinal nerve roots in patients with chronic inflammatory neuropathies: abnormalities correlate with clinical phenotypes

Marieke H.J. van Rosmalen, Martijn Froeling, Stefano Mandija, Jeroen Hendrikse, W. Ludo van der Pol*, H. Stephan Goedee*

* These authors contributed equally to the manuscript

Accepted in Journal of Neurology

ABSTRACT

Objective: Chronic inflammatory demyelinating polyneuropathy (CIDP) and multifocal motor neuropathy (MMN) are caused by inflammatory changes of peripheral nerves. It is unknown if the intraspinal roots are also affected. This MRI study systematically visualized intraspinal nerve roots, i.e. the ventral and dorsal roots, in patients with CIDP, MMN, motor neuron disease (MND) and healthy controls.

Methods: We performed a cross-sectional study in 40 patients with CIDP, 27 with MMN, 34 with MND and 5 healthy controls. All patients underwent an MRI scan of the cervical intraspinal roots. We systematically measured intraspinal nerve root sizes bilaterally in the transversal plane at C5, C6 and C7 level. We calculated mean nerve root sizes and compared them between study groups and between different clinical phenotypes using a univariate general linear model.

Results: Cervical intraspinal nerve root size was larger in patients with CIDP, MMN and MND compared to healthy controls ($p < 0.001 - 0.003$). Patients with a motor phenotype had thicker ventral roots compared to patients with a sensorimotor phenotype ($p = 0.018$) and with MND ($p = 0.002$), while patients with a sensory phenotype had thicker dorsal roots compared to patients with a sensorimotor phenotype ($p = 0.001$) and with MND ($p = 0.006$).

Conclusion: We here show changes in the morphology of intraspinal nerve roots in patients with chronic inflammatory neuropathies, compatible with their clinical phenotype.

INTRODUCTION

Multifocal motor neuropathy (MMN) and chronic inflammatory demyelinating polyneuropathy (CIDP) are chronic inflammatory neuropathies that respond to treatment. CIDP is characterized by pure motor, pure sensory or, most often, mixed deficits in arms or legs, while MMN is characterized by weakness without sensory deficits. Nerve conduction studies (NCS) are the main diagnostic tool for both disorders. They show motor conduction blocks in MMN with normal sensory nerve conduction. NCS in CIDP can also show blocks or a multifocal pattern of conduction slowing.

Imaging studies showed thickened peripheral nerves in both MMN and CIDP that is sometimes more widespread than NCS suggest.¹⁻⁵ Nerve ultrasound has become a flexible diagnostic tool that can be used to examine the entire nerve and brachial plexus in one session. Magnetic resonance imaging (MRI) of the brachial plexus is also used for diagnostic purposes. Ultrasound and MRI abnormalities correlate in the forearm and brachial plexus.⁶ Imaging abnormalities do not correlate with phenotype or clinical characteristics.⁷

The more recently developed advanced MRI techniques allow assessment of the morphology of the intraspinal roots (i.e. motor ventral roots and sensory dorsal roots) and provide the opportunity to correlate morphological with functional changes.⁸ In this MRI study we therefore used a quantitative approach to systematically evaluate the sizes of intraspinal nerve roots of patients with chronic inflammatory neuropathies, disease controls and healthy controls.



METHODS

Study design

We performed a cross-sectional MRI study to assess cervical intraspinal nerve root sizes in patients with CIDP and MMN, disease controls with lower motor neuron syndromes and healthy controls. We systematically measured and compared the cervical intraspinal nerve roots by manually measuring the nerve root diameter.

Patients and clinical data

We enrolled all prevalent and incident patients with an established diagnosis of CIDP or MMN according to the EFNS/PNS criteria who visited our neuromuscular outpatient clinic at the University Medical Center Utrecht (UMCU).^{4,9} We enrolled a group of patients with motor neuron disease (MND) as disease controls, according to the Brooks criteria.¹⁰ Healthy controls were eligible for inclusion if they had no history of neuromuscular disorders, neuropathy or spinal (nerve root) injuries. We excluded patients aged < 18 years, patients with MND with a bulbar onset of symptoms and who were physically unable to undergo MRI or with a contraindication to MRI.

We obtained demographic and clinical data, including age, sex and time from onset of symptoms to research MRI (i.e. disease duration) in months. We performed a clinical examination and analyzed results from the diagnostic NCS of patients with CIDP and MMN to determine their clinical phenotype. We defined the following categories: sensorimotor, pure motor (i.e. no sensory involvement on clinical examination and NCS), and pure sensory or ataxic (i.e. no motor involvement on clinical examination and only demyelinating motor conduction abnormalities allowed). All participants gave informed consent. This study was approved by the Medical Ethical Committee of the UMCU.

Equipment and MRI parameters

We used a 3.0 Tesla MRI scanner (Philips Healthcare, Best, the Netherlands) with a 24-channel head-neck coil to image the cervical intraspinal roots. All participants were positioned in a supine position and scans were performed in a transversal slice orientation. We performed 3D balanced fast field echo with the following parameters: field of view = 250*250*39.90 mm³; matrix size = 416*249; voxel size = 0.35*0.35*0.35 mm³; echo time = 3.3 ms; number of echoes = 1; repetition time = 6.6 ms; flip angle = 55°; sense factor = 1.20 (P reduction foot/head) and 1 (S reduction anterior/posterior); acquisition time = 02:52 minutes. Additionally, we used coronal 3D TSE SPIR scans as anatomical reference, collected from a previously published MRI study.¹¹ The 3D TSE SPIR had the following parameters: field of view = 336*336*170 mm, matrix size = 224*223, voxel size = 0.75*0.75*1 mm³, echo time = 206 ms, repetition time = 2200 ms, turbo spin echo factor = 76, sense factor = 3 (P reduction right/left) and 1.5 (S reduction anterior/posterior), acquisition time = 03:59 minutes.

Intraspinal root measurements on MRI

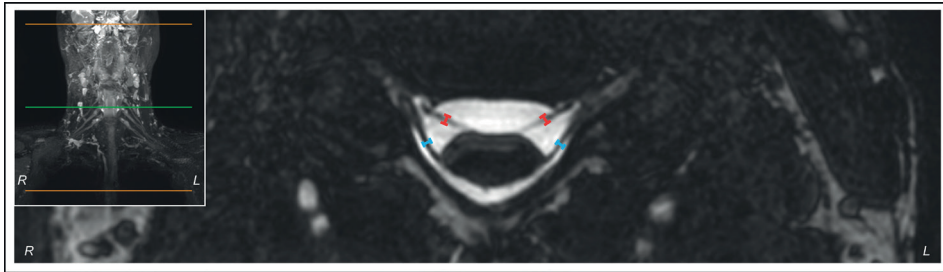
We measured diameters of intraspinal nerve roots using Horos medical image viewer (version 3.3.6, www.horosproject.org). To determine nerve root levels accurately we used reference lines in the coronal 3D TSE SPIR. We used zoom magnification (standardized to 250% for all images) and subsequently used the length tool to measure diameters (mm) of ventral and dorsal intraspinal nerve roots. Diameters were measured in the transversal plane perpendicular to the center lines of the nerve roots and in the middle of the intraspinal nerve root, bilaterally in nerve roots C5, C6 and C7 (**Figure 5.1**), resulting in 12 measurements per subject. All measurements were performed thrice at each measurement site (approximately 7-10 minutes per subject) by one rater (MVR), who was blinded to the clinical status. We used the mean of these three measurements for further statistical analysis. We did not perform measurements when image quality was poor, when intraspinal nerve roots borders could not be accurately defined or when banding artifacts hindered an accurate measurement.

Statistical analysis

IBM SPSS Statistics (version 26, Chicago, Illinois, United States) was used for statistical analysis. To compare patient characteristics, we used a one-way ANOVA on numerical data, with post-hoc Tukey HSD to correct for multiple testing, and a Chi-squared test on categorical data. To evaluate the feasibility of our method we compared numbers of successfully performed measurements using

independent samples *t* test between ventral and dorsal nerve roots, and a paired *t* test to compare successfully performed measurements between the right and left side of one patient. We evaluated intrarater reliability of our measurements using the intraclass correlation coefficient (ICC). We considered an ICC < 0.50 as poor reliability, 0.50 – 0.75 as moderate, 0.75 – 0.90 as good and > 0.90 as excellent reliability.¹² To calculate means of intraspinal nerve root sizes per study group (CIDP, MMN, disease controls and healthy controls) we used a univariate general linear model with the measurements as dependent variable and diagnosis as fixed factor. Tukey HSD was used to correct for multiple testing. Additionally, we used a second univariate general linear model to calculate mean intraspinal root sizes per clinical phenotype (sensorimotor, pure motor, and sensory or ataxic) with again the measurements as dependent variable. Results with a *p* value < 0.05 were considered significant.

Figure 5.1 Example of intraspinal nerve root measurements



Method of measurements with calipers are placed in transversal plane in the ventral (red) and dorsal (blue) intraspinal nerve root at C5 to C7 level, here at C6 level. In the upper left corner the 3D TSE SPIR (anatomical reference) with the reference line (green). Abbreviations: *R* = right; *L* = left.



RESULTS

Patients and clinical data

We included a total of 106 participants (CIDP = 40, MMN = 27, disease controls = 34, healthy controls = 5). There were 31 patients with a sensorimotor phenotype, 29 with a pure motor and 7 with a pure sensory or ataxic phenotype. Patient characteristics are summarized in **Table 5.1**. We found no differences in the baseline characteristics between groups, other than a younger age in patients with MMN compared to patients with CIDP and MND (*p* = 0.003).

Table 5.1 Patient characteristics

Parameter	Inflammatory neuropathy		Controls		Level of significance
	CIDP	MMN	Disease (MND)	Healthy	
Number of patients	40	27	34	5	-
Age, years (SD)	62.9 (9.7)	53.4 (11.8)	61.7 (11.3)	54.4 (7.3)	0.003*
Male (%)	34 (85.0%)	25 (92.6%)	26 (76.5%)	3 (60.0%)	0.189
Disease duration, months (SD)	37.3 (70.8)	69.1 (83.7)	46.0 (40.3)	NA	0.156
Phenotype					
Sensorimotor	31	0			
Pure motor	2	27			
Pure sensory or ataxic	7	0			

* Patients with MMN were younger compared to patients with CIDP and MND. Abbreviations: CIDP = chronic inflammatory demyelinating polyneuropathy; MMN = multifocal motor neuropathy; MND = motor neuron disease; SD = standard deviation.

Intraspinal nerve root measurements on MRI

Feasibility of measuring method

Table 5.2 summarizes the number of measurements per nerve root and per measurement location, i.e. ventral and dorsal roots (C5-C7). The number of successful measurements did not differ between right and left sides ($p = 0.120$). We obtained more measurements in dorsal roots compared to ventral roots ($p < 0.001$). We established that ventral nerve roots were occasionally found very close to the ventral border of the vertebral column, which complicated or even precluded the definition of the ventral roots. Dorsal intraspinal roots were frequently surrounded by more cerebrospinal fluid that provided more contrast and facilitated the identification and measurements of nerve roots.

Table 5.2 Rate of overall successful measurements per root

Root level (n = 106)		Ventral	Dorsal
C5	Right	81 (76.4%)	96 (90.6%)
	Left	85 (80.2%)	96 (90.6%)
C6	Right	57 (53.8%)	75 (70.8%)
	Left	55 (51.9%)	76 (71.7%)
C7	Right	45 (42.5%)	68 (64.2%)
	Left	52 (49.1%)	71 (67.0%)
Total (max. 1272)		887 (69.7%)	

Number of measurements per root differed between ventral and dorsal roots ($p < 0.001$), but did not differ between right and left side ($p = 0.120$). Maximum number of measurements per measurement site is 106 (total included participants = 106).

Intrarater reliability

Table 5.3 shows the intrarater reliability. We found moderate to excellent intrarater reliability for measurements in ventral roots (ICC 0.71 – 0.91) as well as for measurements in dorsal roots (ICC 0.72 – 0.94).

Table 5.3 Reliability of intraspinal nerve root measurements

Site		Intrarater reliability (95% CI)	
		Ventral	Dorsal
C5	Right	0.84 (0.77 – 0.89)	0.83 (0.76 – 0.88)
	Left	0.80 (0.71 – 0.87)	0.72 (0.61 – 0.81)
C6	Right	0.77 (0.64 – 0.86)	0.86 (0.80 – 0.91)
	Left	0.71 (0.54 – 0.82)	0.78 (0.68 – 0.85)
C7	Right	0.91 (0.85 – 0.95)	0.89 (0.82 – 0.93)
	Left	0.83 (0.73 – 0.90)	0.94 (0.92 – 0.96)

Interclass correlation coefficient (ICC) with 95% confidence interval (CI) per measurement location, i.e. at C5, C6 or C7 level, left or right, and ventral or dorsal.

Mean intraspinal nerve root size per study group

Mean intraspinal nerve root sizes are summarized in **Table 5.4**. Nerve root sizes in patients with CIDP, MMN and MND were larger compared to healthy controls, at all predetermined sites (p varied from < 0.001 to 0.003 , **Figure 5.2**). We found no differences in the intraspinal nerve root sizes between patients with CIDP, MMN and MND, other than the right ventral root C6 patients with MMN compared to patients with CIDP ($p = 0.03$). **Figure 5.3** shows examples of patients with thickened intraspinal nerve roots. We established that patients with thickened intraspinal nerve roots did not necessarily have thickened cervical nerve roots in the brachial plexus (**Figure 5.3**).

Mean intraspinal nerve root sizes per clinical phenotype

Mean intraspinal nerve root sizes per phenotype are summarized in **Table 5.5**. In healthy controls ventral (0.53, (standard deviation (SD) 0.12)) and dorsal nerve roots (0.56 (SD 0.12)) did not differ ($p = 0.149$). Dorsal nerve roots were thicker (0.67 (SD 0.16)) than ventral nerve roots (0.64 (SD 0.14); $p < 0.001$) in all clinical phenotypes of the chronic inflammatory neuropathies, except for patients with a pure motor presentation ($p = 0.248$).

Between groups we found thicker ventral nerve roots in patients with a motor phenotype compared to patients with a sensorimotor phenotype ($p = 0.018$) and patients with MND ($p = 0.002$). In contrast, we found thicker dorsal nerve roots in patients with a sensory or ataxic phenotype compared to patients with a sensorimotor phenotype ($p = 0.001$) and patients with MND ($p = 0.006$).



Table 5.4 Mean intraspinal nerve root sizes in patients with CIDP, MMN and controls

	Inflammatory neuropathy		Controls		Level of significance
	<i>CIDP</i> (<i>n</i> = 40)	<i>MMN</i> (<i>n</i> = 27)	<i>MND</i> (<i>n</i> = 34)	<i>Healthy control</i> (<i>n</i> = 5)	
Ventral					
C5	0.66 (0.13)	0.68 (0.17)	0.65 (0.11)	0.56 (0.13)	0.001 ^a
Right	0.69 (0.13)	0.69 (0.15)	0.67 (0.13)	0.60 (0.14)	0.076
Left	0.63 (0.12)	0.67 (0.20)	0.64 (0.10)	0.53 (0.11)	0.004 ^a
C6	0.62 (0.10)	0.66 (0.14)	0.63 (0.11)	0.50 (0.12)	<0.001 ^a
Right	0.61 (0.10)	0.68 (0.14)	0.62 (0.10)	0.48 (0.11)	<0.001 ^{a,b}
Left	0.62 (0.10)	0.64 (0.13)	0.64 (0.12)	0.54 (0.15)	0.222
C7	0.67 (0.16)	0.67 (0.15)	0.61 (0.09)	0.52 (0.10)	<0.001 ^a
Right	0.70 (0.19)	0.67 (0.17)	0.60 (0.08)	0.55 (0.07)	<0.001 ^c
Left	0.65 (0.14)	0.67 (0.14)	0.61 (0.10)	0.48 (0.11)	<0.001 ^a
Dorsal					
C5	0.67 (0.13)	0.67 (0.14)	0.65 (0.12)	0.58 (0.12)	0.003 ^a
Right	0.68 (0.15)	0.67 (0.15)	0.66 (0.12)	0.52 (0.08)	0.001 ^a
Left	0.67 (0.12)	0.67 (0.12)	0.65 (0.12)	0.64 (0.13)	0.504
C6	0.68 (0.14)	0.69 (0.14)	0.66 (0.13)	0.52 (0.11)	<0.001 ^a
Right	0.67 (0.15)	0.70 (0.15)	0.65 (0.13)	0.52 (0.12)	0.001 ^a
Left	0.69 (0.13)	0.67 (0.13)	0.66 (0.12)	0.52 (0.11)	0.003 ^a
C7	0.69 (0.18)	0.73 (0.27)	0.73 (0.18)	0.56 (0.11)	0.001 ^a
Right	0.68 (0.20)	0.68 (0.16)	0.72 (0.16)	0.56 (0.14)	0.046 ^d
Left	0.70 (0.15)	0.77 (0.34)	0.73 (0.20)	0.55 (0.06)	0.016 ^e

Nerve root sizes are mean in millimeters with standard deviation.

^a Significant difference between healthy controls compared to CIDP, MMN and MND patients.

^b Significant difference between patients with MMN and CIDP

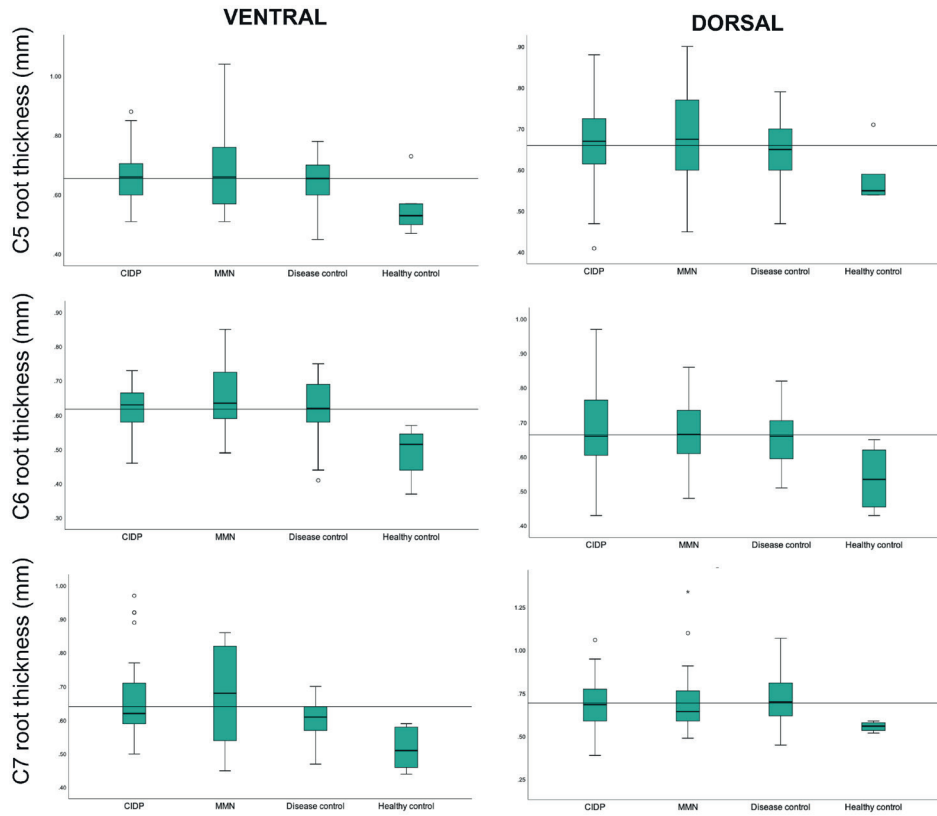
^c Significant difference between patients with CIDP and healthy controls

^d Significant difference between patients with MND and healthy controls

^e Significant difference between patients with MMN and healthy controls

Abbreviations: CIDP = chronic inflammatory demyelinating polyneuropathy; MMN = multifocal motor neuropathy; MND = motor neuron disease.

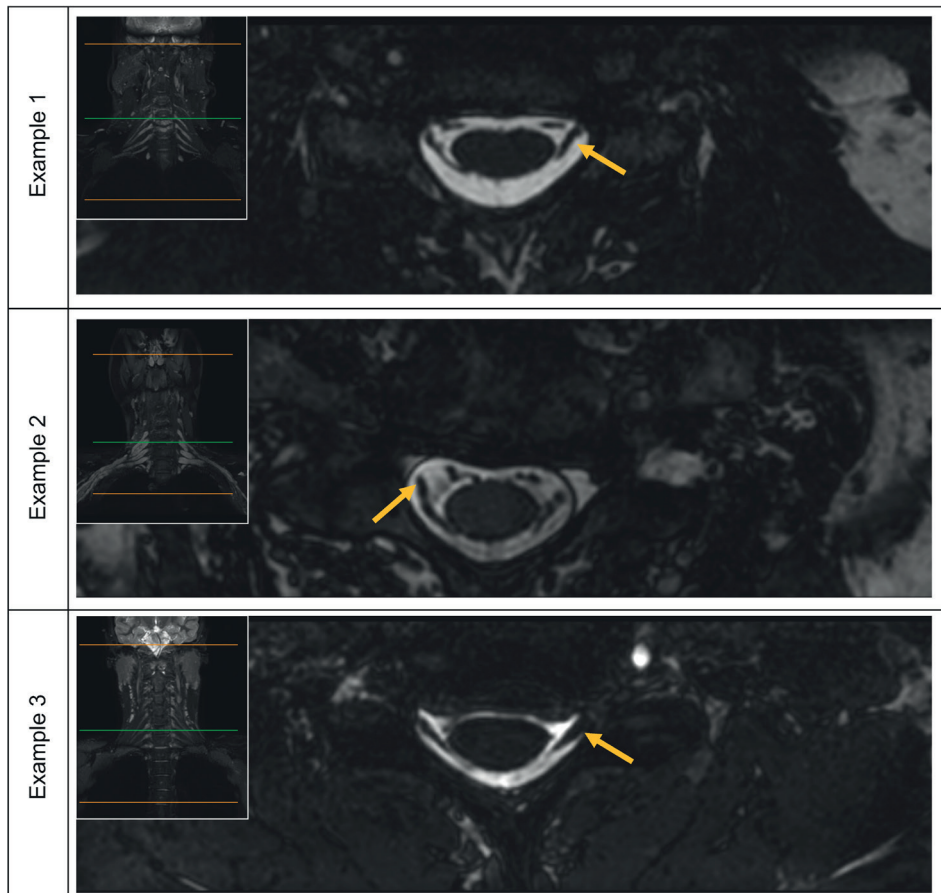
Figure 5.2 Boxplots of mean intraspinal nerve root size per measurement location



Mean of intraspinal nerve root size at C5, C6 and C7 level. Measurements were performed in ventral (left panels) and dorsal (right panels) intraspinal nerve roots. Healthy controls had lower mean nerve root sizes compared to patients with CIDP, MMN and MND (disease controls). Abbreviations: CIDP = chronic inflammatory demyelinating polyneuropathy; MMN = multifocal motor neuropathy; MND = motor neuron disease; mm = millimeters.



5

Figure 5.3 Examples of thickened intraspinal nerve roots

Three examples of patients (MND, CIDP and MMN respectively) with thickening (yellow arrows) of the intraspinal nerve roots. The nerve roots imaged here measured over 1 mm diameter. Thickening is evident when the examples are compared with the image in **Figure 5.1** In the upper left corner the 3D TSE SPIR (anatomical reference) with the reference line (green). Example 2 had obviously thickened cervical nerve roots in the brachial plexus (upper left panel of example 2), while example 1 and 3 did not have these thickened cervical nerve roots. Abbreviations: CIDP = chronic inflammatory demyelinating polyneuropathy; MMN = multifocal motor neuropathy; MND = motor neuron disease.

Table 5.5 Mean intraspinal nerve root sizes per clinical phenotype and controls

	Ventral	Dorsal	MD	95% CI	p_1
OVERALL	0.64 (0.14)	0.67 (0.16)	0.03 (SE 0.01)	0.02 – 0.04	< 0.001
Sensorimotor	0.64 (0.13)	0.67 (0.15)	0.02 (SE 0.01)	0.01 – 0.04	0.018
Motor	0.67 (0.16)	0.69 (0.18)	0.02 (SE 0.01)	-0.04 – 0.11	0.248
Sensory/ataxic	0.68 (0.13)	0.73 (0.17)	0.53 (SE 0.02)	0.01 – 0.09	0.011
MND	0.63 (0.11)	0.67 (0.14)	0.04 (SE 0.01)	0.02 – 0.06	<0.001
Healthy	0.53 (0.12)	0.56 (0.12)	0.03 (SE 0.02)	-0.01 – 0.07	0.149
p_2	< 0.001 ^{a,b,c}	< 0.001 ^{a,d,e}			

Nerve root sizes are mean in millimeters with standard deviation. Mean differences (MD) are shown with standard error (SE) and 95% confidence intervals (CI).

$p_1 = p$ values concerning ventral vs. dorsal roots

$p_2 = p$ values concerning ventral roots between phenotypes, and dorsal roots between phenotypes.

^a $p < 0.001$ for healthy vs. sensorimotor, motor, and sensory or ataxic phenotype, and MND

^b $p = 0.018$ for motor vs. sensorimotor phenotype

^c $p = 0.002$ for motor phenotype vs. MND

^d $p = 0.001$ for sensory or ataxic phenotype vs. sensorimotor

^e $p = 0.006$ for sensory or ataxic phenotype vs. MND

Abbreviations: MND = motor neuron disease.



DISCUSSION

This study shows that MRI of the intraspinal nerve roots shows changes in patients with an inflammatory neuropathy and that the location of these changes corresponds with the nature of neurological deficits. Ventral intraspinal nerve roots were thicker in patients with a pure motor phenotype (i.e. MMN and pure motor CIDP) compared to patients with a sensorimotor phenotype and patients with MND. Dorsal intraspinal nerve roots were thicker in patients with a pure sensory or ataxic phenotype (i.e. sensory CIDP). These findings for the first time show that anatomical abnormalities correspond with clinical deficits in inflammatory neuropathies.

Previously used imaging techniques for chronic inflammatory neuropathies focused on the peripheral nerves and nerve roots in arms or legs outside the vertebral foramen.^{2,3,11} Since these nerves almost always have a mixed composition (i.e. motor and sensory), it was impossible to detect preferential involvement of motor or sensory nerves. Nerve conduction studies often show normal sensory conduction in pure motor neuropathies and vice versa, but assessing involvement of the most proximal parts is challenging. F-waves could provide information on the most proximal parts of the peripheral nervous system, but this information is unspecific and does not localize the exact site of injury. Previous NCS studies did not show a clear relation between nerve function and nerve

morphology.^{13,14} MRI of the intraspinal nerve roots allowed us to image the most proximal parts of the peripheral nervous system, and provided the unique opportunity to study the motor and sensory roots separately. MRI of the intraspinal nerve roots has been previously used to assess the intraspinal nerve root integrity in traumatic brachial plexus injuries.¹⁵⁻¹⁷ A few smaller studies describe MRI results of the intraspinal nerve roots in patients with Guillain-Barré syndrome (GBS).¹⁸⁻²² These studies report nerve root enhancement in the spinal roots, with preferential involvement of the ventral spinal roots in patients with pure motor GBS and enhancement of the ventral and dorsal spinal roots in patients with a sensorimotor phenotype. We here corroborate these results in a much larger patient sample.

Our data seem to indicate that motor and sensory nerves can be specific targets in inflammatory neuropathies. We think that it is likely that the widespread thickening of peripheral nerves is caused by specific isolated changes in motor or sensory nerves in MMN and sensory CIDP.

Our study has limitations. We included a small group of healthy controls, but the variability in spinal nerve root sizes in this group was limited. Absolute nerve root size differences between groups were small and in terms of hundredth of a millimeter. The fact that intrarater reliability was good indicates that the methodology is sound and that the resolution is high. An even higher resolution is probably technically feasible and could result in even more accurate measurements and less artifacts, in particular of ventral roots.

This study contributes to our understanding of inflammatory neuropathies. This high-resolution technology might have biomarker value in the future.

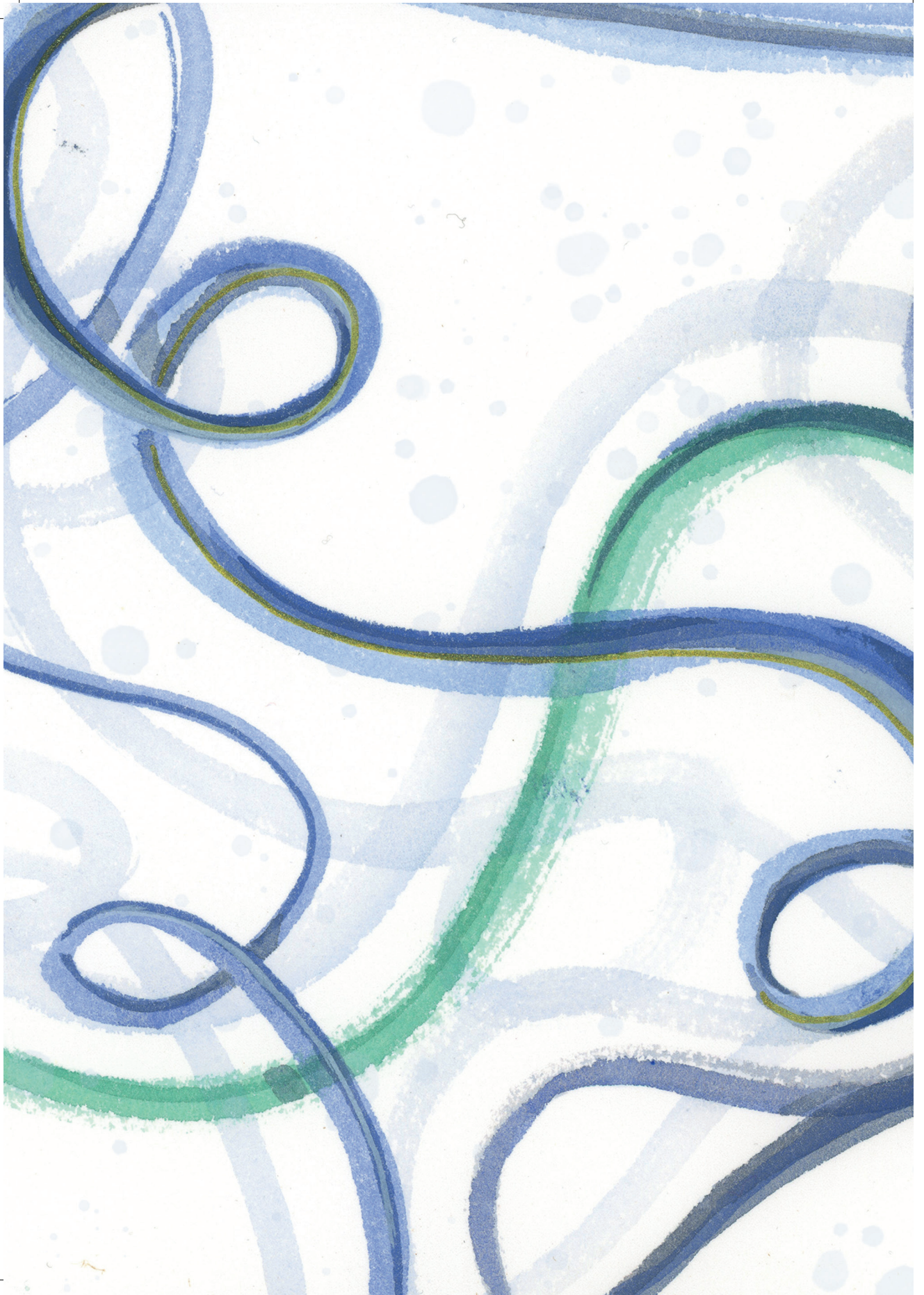
REFERENCES

1. Castillo M, Mukherji SK. MRI of enlarged dorsal ganglia, lumbar nerve roots, and cranial nerves in polyradiculoneuropathies. *Neuroradiology* 1996;38:516–520.
2. van Es HW, van den Berg LH, Franssen H, et al. Magnetic resonance imaging of the brachial plexus in patients with multifocal motor neuropathy. *Neurology* 1997;48:1218–1224.
3. Herraets IJT, Goedee HS, Telleman JA, et al. Nerve ultrasound for the diagnosis of chronic inflammatory neuropathy: a multicenter validation study. *Neurology* 2020;95:e1745–e1753.
4. van den Bergh PYK, Hadden RDM, Bouche P, et al. European Federation of Neurological Societies/Peripheral Nerve Society Guideline on management of chronic inflammatory demyelinating polyradiculoneuropathy: Report of a joint task force of the European Federation of Neurological Societies and the Peripher. *Eur. J. Neurol.* 2010;17:356–363.
5. Vlam L, Van Der Pol WL, Cats EA, et al. Multifocal motor neuropathy: Diagnosis, pathogenesis and treatment strategies. *Nat. Rev. Neurol.* 2012;8:48–58.
6. Jongbloed BA, Haakma W, Goedee HS, et al. Comparative study of peripheral nerve Mri and ultrasound in multifocal motor neuropathy and amyotrophic lateral sclerosis. *Muscle Nerve* 2016;54:1133–1135.
7. Goedee HS, Jongbloed BA, van Asseldonk J-TH, et al. A comparative study of brachial plexus sonography and magnetic resonance imaging in chronic inflammatory demyelinating neuropathy and multifocal motor neuropathy. *Eur. J. Neurol.* 2017;24:1307–1313.
8. Mandija S, Froeling M, van der Kolk A, et al. Large field-of-view high resolution 3D imaging of the thoracolumbar nerve roots inside the spinal canal. In: *ISMRM 2019 Abstracts*. 2019 p. 2883.
9. Van Schaik IN, Léger JM, Nobile-Orazio E, et al. European Federation of Neurological Societies/Peripheral Nerve Society Guideline on management of multifocal motor neuropathy. Report of a Joint Task Force of the European Federation of Neurological Societies and the Peripheral Nerve Society - First revis. *J Peripher Nerv Syst* 2010;15:295–301.
10. Brooks BR, Miller RG, Swash M, Munsat TL. El Escorial revisited: Revised criteria for the diagnosis of amyotrophic lateral sclerosis. *ALS Mot. neuron Disord.* 2000;1:293–299.
11. van Rosmalen MHJ, Goedee HS, van der Gijp A, et al. Quantitative assessment of brachial plexus MRI for the diagnosis of chronic inflammatory neuropathies. *J. Neurol.* 2020;268:978–988.
12. Koo TK, Li MY. A Guideline of Selecting and Reporting Intraclass Correlation Coefficients for Reliability Research. *J. Chiropr. Med.* 2016;15:155–163.
13. Kimura J. Principles and pitfalls of nerve conduction studies. *Ann. Neurol.* 1984;16:415–429.
14. Goedee H. High-resolution ultrasound in diagnosis of polyneuropathies. In: ISBN 9789462336841. 2017 p. 167–190.
15. Carvalho GA, Nikkhah G, Matthies C, et al. Diagnosis of root avulsions in traumatic brachial plexus injuries: Value of computerized tomography myelography and magnetic resonance imaging. *J. Neurosurg.* 1997;86:69–76.
16. Wade RG, Takwoingi Y, Wormald JCR, et al. Magnetic resonance imaging for detecting root avulsions in traumatic adult brachial plexus injuries: Protocol for a systematic review of diagnostic accuracy. *Syst. Rev.* 2018;7:4–9.
17. Wade RG, Takwoingi Y, Wormald JCR, et al. MRI for detecting root avulsions in traumatic adult brachial plexus injuries: A systematic review and meta-analysis of diagnostic accuracy. *Radiology* 2019;293:125–133.
18. Berciano J, Sedano MJ, Pelayo-Negro AL, et al. Proximal nerve lesions in early Guillain-Barré syndrome: implications for pathogenesis and



- disease classification. *J. Neurol.* 2017;264:221–236.
19. Byun WM, Park WK, Park BH, et al. Guillain-Barré syndrome: MR imaging findings of the spine in eight patients. *Radiology* 1998;208:137–141.
 20. Yikilmaz A, Doganay S, Gumus H, et al. Magnetic resonance imaging of childhood Guillain-Barré syndrome. *Child's Nerv. Syst.* 2010;26:1103–1108.
 21. Coskun A, Kumandas S, Pac A, et al. Childhood Guillain-Barré Syndrome: MR Imaging in Diagnosis and Follow-Up. *Acta radiol.* 2003;44:230–235.
 22. Mulkey SB, Glasier CM, El-Nabbout B, et al. Nerve root enhancement on spinal MRI in pediatric Guillain-Barré syndrome. *Pediatr. Neurol.* 2010;43:263–269.







Chapter 6

Quantitative MRI of the brachial plexus shows specific changes in nerve architecture in CIDP, MMN and motor neuron disease

Marieke H.J. van Rosmalen, H. Stephan Goedee, Rosina A. Derks, Fay-Lynn Asselman, Camiel Verhamme, Alberto de Luca, Jeroen Hendrikse, W. Ludo van der Pol*, Martijn Froeling*

* These authors contributed equally to the manuscript

European Journal of Neurology, 2021 Aug; 28, 2716 - 2726

ABSTRACT

Objective: The immunological pathophysiologies of chronic inflammatory demyelinating polyneuropathy (CIDP) and multifocal motor neuropathy (MMN) differ considerably, but neither has been elucidated completely. Quantitative magnetic resonance imaging (MRI) techniques as diffusion tensor imaging, T2 mapping, and fat fraction analysis may indicate *in vivo* pathophysiological changes in nerve architecture. Our study aims to systematically study nerve architecture of the brachial plexus in patients with CIDP, MMN, motor neuron disease (MND) and healthy controls using these quantitative MRI techniques.

Methods: We enrolled patients with CIDP (n = 47), MMN (n = 29), MND (n = 40) and healthy controls (n = 10). All patients underwent MRI of the brachial plexus and we obtained diffusion parameters, T2 relaxation times and fat fraction using an automated processing pipeline. We compared these parameters between groups using a univariate general linear model.

Results: Fractional anisotropy was lower in patients with CIDP compared to healthy controls ($p < 0.001$), patients with MND ($p = 0.010$) and MMN ($p < 0.001$). Radial diffusivity was higher in patients with CIDP compared to healthy controls ($p = 0.015$) and patients with MND ($p = 0.001$) and MMN ($p < 0.001$). T2 relaxation time was elevated in patients with CIDP compared to patients with MND ($p = 0.023$). Fat fraction was lower in patients with CIDP and MMN compared to patients with MND (both $p < 0.001$).

Conclusion: Our results show that quantitative MRI parameters differ between CIDP, MMN and MND, which may reflect differences in underlying pathophysiological mechanisms.

INTRODUCTION

Inflammation of peripheral nerves is the underlying disease mechanism that causes muscle weakness and sensory deficits in chronic inflammatory polyneuropathies, including multifocal motor neuropathy (MMN) and chronic inflammatory demyelinating polyneuropathy (CIDP). MMN is characterized by asymmetric weakness without sensory deficits that dominates in the arms, while CIDP may cause pure motor, pure sensory, or mixed deficits that are most pronounced in the legs. Nerve conduction studies may show conduction blocks and nerve imaging studies have revealed multifocal thickening of nerves in both CIDP and MMN.^{1,2}

The immunological pathophysiologies of CIDP and MMN differ considerably, but have not been elucidated completely. Autopsy studies, sural nerve biopsy, immunostaining with patient sera *in vitro* and animal models have provided insight in underlying immunological mechanisms.³⁻⁹ There is an obvious need for additional tools to study the condition of peripheral nerves *in vivo* to further dissect the underlying pathophysiological mechanisms. Quantitative magnetic resonance imaging (MRI) may bridge this gap: diffusion tensor imaging (DTI) and measurements of T2 relaxation times and fat fraction may indicate specific pathophysiological changes in the myelin sheath and axon in patients with CIDP and MMN.

DTI is an MRI technique that provides quantitative parameters as fractional anisotropy (FA), mean diffusivity (MD), axial diffusivity (AD) and radial diffusivity (RD). These parameters give insight in the microstructural integrity of (nervous) tissue and seem to correlate with histological findings.¹⁰⁻¹³ Previous DTI studies evaluated peripheral nerves such as the tibial, sciatic and median nerve of patients with CIDP or MMN and healthy controls.¹⁴⁻¹⁹ The brachial plexus was analyzed in a recent exploratory pilot study in a small cohort of patients and showed different FA values between patients with CIDP and MMN.²⁰ Studies using other quantitative MRI techniques, e.g. T2 mapping or fat fraction analysis, documented an increase in T2 relaxation time in the brachial and lumbosacral plexus and in the tibial nerve in small cohorts of patients with CIDP.²¹⁻²³ Complete and systematic studies of the brachial plexus are lacking.

We therefore performed a detailed and systematic quantitative MRI study in a large cohort of patients with CIDP, MMN, motor neuron disease (MND) and healthy controls, to compare diffusion parameters, T2 relaxation times and fat fraction of the brachial plexus. The aim of this study was to interpret these results in light of underlying pathophysiological mechanisms of CIDP and MMN.



METHODS

Study design

We performed a cross-sectional study in patients with CIDP, MMN, MND and healthy controls. We performed quantitative MRI in all patients and used an automated processing pipeline to obtain parameters on microstructural integrity. We compared these parameters between groups and explored correlations with clinical data.

Participants and clinical data

Consecutive patients with CIDP, MMN and MND were included at the outpatient clinic of the University Medical Center Utrecht (UMCU). Alle prevalent and incident patients with an established diagnosis of CIDP or MMN (definite, probable, possible), according to the predefined consensus criteria of the European Federation of Neurological Societies/Peripheral Nerve Society, were eligible for inclusion.^{2,24,25} Patients with MND (i.e. amyotrophic lateral sclerosis (ALS) or progressive muscular atrophy (PMA)), according to the Brooks criteria, were enrolled as disease controls.²⁶ Healthy controls were included if they had no history of neuromuscular disorders, neuropathy, nerve root injuries or other cervical spine disorders. We excluded patients aged < 18 years, patients with atypical forms of CIDP (e.g. Lewis Sumner Syndrome) and patients with MND that had a bulbar onset of symptoms to minimize heterogeneity in these groups, and participants who met one of the routine contraindications for MRI.

We documented demographic and clinical data from all patients, including muscle strength expressed as a Medical Research Council (MRC) sum score. We tested the following 12 muscle groups on both sides: finger flexion, finger extension, finger abduction, wrist flexion, wrist extension, elbow flexion, elbow extension, shoulder abduction, hip flexion, knee flexion, knee extension and foot dorsiflexion. We calculated MRC sum scores of these 24 measurements, ranging from 0 to 120 (normal). The medical ethical committee of the UMCU approved this study (18-349/NL 62866.041.17). This study conforms with the World Medical Association Declaration of Helsinki. Written informed consent was obtained from all study participants.

Equipment and MRI protocol

All participants underwent an MRI scan of the brachial plexus bilaterally in supine position on a 3.0 Tesla MRI scanner (Philips Healthcare, Best, the Netherlands) using a 24-channel head-neck coil. We performed DTI in a transversal slice orientation to obtain diffusion parameters, T2 mapping in a coronal slice orientation to obtain T2 relaxation times and T1 Dixon in a transverse slice orientation to obtain fat fraction. As an anatomical reference we used a 3D turbo spin-echo (TSE) spectral presaturation with inversion recovery (SPIR) sequence in a coronal slice orientation. The acquisition parameters are shown in **Table 6.1**. We performed a data quality check after enrollment of 43 participants that showed a higher-than-expected frequency (> 5%) of insufficient data due to low

signal to noise ratios (SNR). Therefore, we performed DTI twice in all the following participants to improve data quality. These two acquisitions were combined in a later stage during data processing. We exclude scans with low quality, for example due to movement or the presence of artifacts, from further processing.

Table 6.1 MRI parameters

Parameter	DTI	T2 mapping	T1 DIXON	3D TSE
Acquisition	2D SE-EPI	2D TSE	3D FFE	3D TSE
Field of view	240*180*150 mm ³	240*180*52.5 mm ³	288*288-200.25 mm ³	336*336*170 mm ³
Matrix size	96*71	96*96	192*192	224*223
Slice thickness	2.5 mm	2.5 mm	-	-
Voxel size	2.5*2.5*2.5 mm ³	2.5*2.5*2.5 mm ³	0.75*0.75*0.75 mm ³	0.75*0.75*1 mm ³
Echo time	60 ms	7.6 ms	1.186 ms	206 ms
Number of echoes	-	17	3	-
Repetition time	8595 ms	3242 ms	5615 ms	2200 ms
Flip angle	-	-	16°	-
Turbo spin echo factor	-	-	-	76
Sensitivity encoding factor	2.5	2.3	2 (AP); 1 (FH)	3 (RL); 1.5 (AP)
Fat suppression	SPAIR	-	-	SPIR
Gradient directions	37	-	-	-
b values (s/mm ²)	0, 50, 100, 150, 300, 400, 600	-	-	-
Acquisition time	05:43 minutes	04:45 minutes	01:56 minutes	03:59 minutes

Abbreviations: DTI = diffusion tensor imaging; TSE = turbo spin echo; SPAIR = spectral attenuated inversion recovery; SPIR = spectral presaturation with inversion recovery; SE EPI = spin echo-echo planar imaging; FFE = fast field echo; mm = millimeter; ms = milliseconds; AP = anterior/posterior; FH = foot/head; RL = right/left.

Data processing

DTI

We processed all DTI data semi-automatically, using a two-step custom-build processing pipeline based on the diffusion toolbox ExploreDTI which allows visualization of the spinal nerve roots, segmented tract analysis and extraction of diffusion parameters.²⁷ An overview of the pipeline is shown in **Figure 6.1**.

Before processing, we resampled the 3D TSE SPIR to a 2x2x2 mm³ isotropic resolution. Subsequently, we manually drew a rough mask of the brachial plexus area using ITK SNAP (10 minutes per data set).²⁸ These masks were drawn in the resampled 3D TSE SPIR and in the diffusion-weighted image to guide the registration and fiber tract selection (**Figure 6.1B**). The first automated part of the



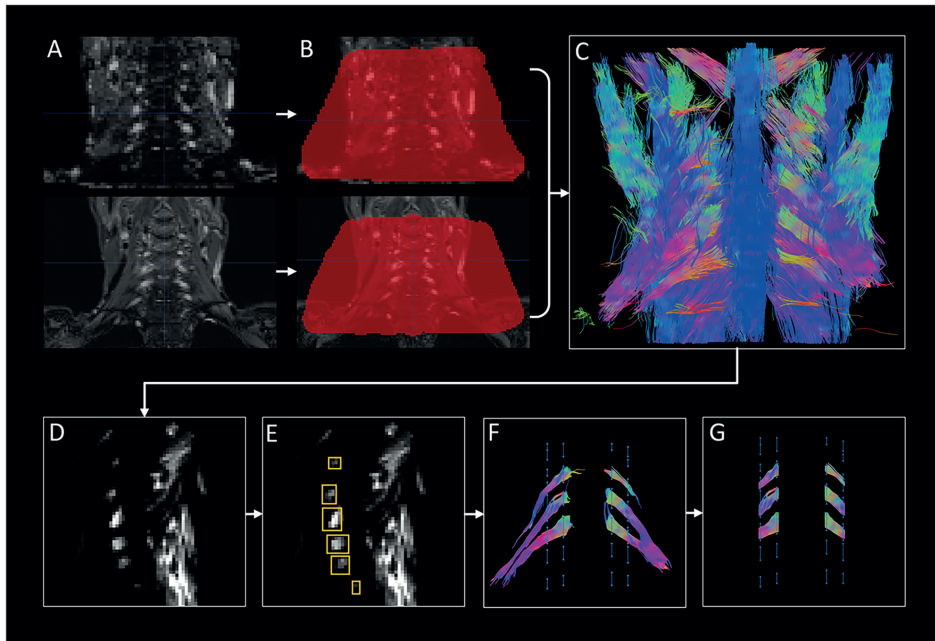
processing pipeline comprised data denoising, affine registration to correct for subject motion and eddy currents, b-spline registration to correct for echo-planar imaging distortions, tensor estimation using an iterative weighted linear least squares algorithm and whole volume fiber tractography (seed point resolution $1 \times 1 \times 1 \text{ mm}^3$, step size 1 mm, seed FA threshold 0.15, FA track range 0.1-0.8, fiber length range 20-200 mm, angle threshold 15° per step; **Figure 6.1C**). This first automated processing step required approximately 35 minutes per data set to complete.

Next, we manually defined slices with starting and ending points of tracts. Starting points were located next to the ganglion of nerve root C5, C6 and C7, ending points were located 5 slices further in the distal direction (5 minutes per data set). This aided a second algorithm to find all tract locations of the nerves using a tract density map (**Figure 6.1D**) and specifies the appropriate region of interests (ROI's) for nerve segmentation (**Figure 6.1E**). To pair ROI's in the proximal starting and distal ending slices, the algorithm performs a connectivity analysis for all defined ROI's. Every pair of ROIs with high connectivity is then defined as tract bundles which results in a reconstruction of the nerve roots (**Figure 1F**). Subsequently, the nerve root segments were constructed, using the predefined starting and ending slice (**Figure 6.1G**). These nerve root segments were used to standardize the site of extraction of diffusion parameters (FA, MD, AD, RD), i.e. next to the ganglion over a distance of 1 cm. This second automated part of the pipeline required approximately 5 minutes per data set to complete.

Finally, we visually identified and labeled the selected tracts as the left and right nerve roots of C5, C6, or C7 (5 minutes per data set). If necessary, manual ROI's were placed to optimize the result of the automated data processing (5 minutes per data set). When no tracts were found, nor with the algorithm, nor manually, the data set was excluded from further analysis. Finally, diffusion parameters per fiber tract were calculated using tract-based analysis.

T2 mapping and T1 DIXON

Dixon fat fraction maps were calculated using the water and fat image reconstructions of the vendor software. The data obtained with T2 mapping was processed using an extended phase graph fitting approach considering inhomogeneous B_1 .^{29,30} This method accounts for different T2 relaxation times for the water and fat component with the T2 of the fat component fixed to a value calibrated on the subcutaneous fat. Quantitative values of the T2 mapping and T1 DIXON were obtained using the same tract-based analysis used for DTI data. Data underwent registration to the same anatomical space (3D TSE SPIR image) as the DTI data. We obtained T2 relaxation time in milliseconds (ms) and fat fraction in percentages.

Figure 6.1 Overview of processing pipeline

A diffusion-weighted image and a resampled 3D TSE SPIR are obtained (A, upper and lower image respectively). After manually drawn masks of the brachial plexus area (B) the automatic processing pipeline results in whole volume fiber tractography (C). Nerve locations are found in a tract density map (D) which specifies region of interests (E). A connectivity analysis results in reconstruction of nerve roots (F) and subsequently in nerve root segments from which diffusion parameters are derived (G).

Statistical analysis

For statistical analysis we used IBM SPSS Statistics (Version 25, Armonk, New York, United States). To compare patient characteristics, we used one-way analysis of variance (ANOVA) for numerical data and a Chi-squared test for categorical data. We compared diffusion parameters, T2 relaxation times, and fat fraction per side (i.e. right/left) using a paired sample *t* test and corrected for multiple testing using the Bonferroni method. To analyze diffusion parameters, T2 relaxation times, and fat fraction between groups we used an univariate general linear model with the MRI parameters as the dependent variable and the study group as a fixed factor. Tukey HSD was used to correct for multiple testing. A *p* value < 0.05 was considered significant. We analyzed diffusion parameters, T2 relaxation times, and fat fraction of all nerve roots together and per nerve root (i.e. C5, C6, C7) separately. Correlations between the quantitative parameters and clinical data were analyzed using the Pearson correlation coefficient *r*. We considered $r \leq 0.35$ as a weak correlation, 0.36 – 0.70 as moderate, 0.70 – 0.89 as high and ≥ 0.90 as a very high correlation.³¹



RESULTS

Participants and clinical data

We enrolled 137 participants based on the in- and exclusion criteria. We had to exclude 11 more patients: 2 patients (1.5%) because of claustrophobia during scanning, 2 patients (1.5%) because of a changed diagnosis after inclusion, 1 patient (0.7%) due to movement artifacts that led to low data quality and an additional 6 patients (4.4%; CIDP = 3, MMN = 1, controls = 2) after processing and tract segmentation due to insufficient data quality. We used data from 126 study participants for further analysis (CIDP = 47, MMN = 29, MND = 40 (ALS = 19, PMA = 21), healthy controls = 10). The patient characteristics are summarized in **Table 6.2**. Patients with MMN were younger than patients with CIDP and PMA ($p < 0.001$). Other characteristics did not differ significantly between groups.

Table 6.2 Patient characteristics

Parameter	Inflammatory neuropathy		Motor neuron disease		Healthy controls	<i>p</i> value
	<i>CIDP</i>	<i>MMN</i>	<i>ALS</i>	<i>PMA</i>		
Number of participants	47	29	19	21	10	
Age, years (SD)	64.0 (9.6)	53.7 (11.2)	60.4 (12.3)	65.2 (10.4)	57.4 (7.3)	<0.001*
Male (%)	39 (83.0%)	27 (93.1%)	12 (63.2%)	18 (85.7%)	7 (70%)	0.088
Disease duration, months (SD)	34.5 (67.1)	65.1 (82.3)	30.8 (24.3)	57.5 (45.4)	-	0.100
MRC sum score (SD)	111.9 (10.1)	113.8 (4.6)	110.6 (7.9)	107.5 (11.2)	-	0.119

*Age differs significantly between patients with MMN and patients with CIDP, and between patients with MMN and patients with PMA. Age, disease duration and MRC sum score are mean. Abbreviations: CIDP = chronic inflammatory demyelinating polyneuropathy; MMN = multifocal motor neuropathy; ALS = amyotrophic lateral sclerosis; PMA = progressive muscular atrophy; SD = standard deviation; MRC = Medical Research Council.

Semi-automated data processing

After automated processing, we identified 92.9% of all nerve roots (93.3%, 98.4% and 86.9% for C5, C6 and C7 respectively), which increased to 96.0% of C5 nerve roots, 99.6% of C6 nerve roots and 95.6% of C7 after additional manual adjustments.

Quantitative MRI parameters

Diffusion parameters, T2 relaxation times and fat fraction did not differ between right and left side of the nerve roots, except for FA in nerve root C7 ($p < 0.001$). This only significant finding did not influence our data and we therefore decided to combine right and left sides in further analysis.

The same applies to patients with ALS and PMA. There were no significant differences in characteristics between patients with ALS and PMA (p values ranged from 0.075 – 0.999). We therefore present these data as one group of patients (MND) in further analysis.

Diffusion parameters

The means of all quantitative parameters are summarized in **Table 6.3** and visualized in **Figure 6.2**. We found a lower mean FA in patients with CIDP (0.27 (standard deviation (SD) 0.05)) compared to healthy controls (0.30 (SD 0.05); $p < 0.001$), patients with MND (0.28 (SD 0.04); $p = 0.010$) and MMN (0.30 (SD 0.06); $p < 0.001$). FA in patients with MMN and healthy controls was higher compared to patients with MND ($p = 0.002$ and $p = 0.038$, respectively).

We found a higher mean MD in patients with CIDP (1.40×10^{-3} mm²/s (SD 0.20)) compared to patients with MND (1.35×10^{-3} mm²/s (SD 0.20); $p = 0.008$) and MMN (1.35×10^{-3} mm²/s (SD 0.23); $p = 0.027$).

Also, the mean RD was higher in patients with CIDP (1.20×10^{-3} mm²/s (SD 0.19)) compared to healthy controls (1.12 (SD 0.17); $p = 0.015$), patients with MND (1.14×10^{-3} mm²/s (SD 0.16); $p = 0.001$) and MMN (1.13×10^{-3} mm²/s (SD 0.20); $p < 0.001$). We did not find any significant differences in AD between groups.

T2 relaxation time and fat fraction

We found a longer mean T2 relaxation time in patients with CIDP (42.37 ms (SD 5.36)) compared to patients with MND (41.02 ms (SD 4.81); $p = 0.023$). The fat fraction was lower in patients with CIDP (40.09% (SD 9.61); $p < 0.001$) and MMN (39.44% (SD 9.07); $p < 0.001$) compared to patients with MND (43.62% (9.74)).

Correlation with clinical data

For all four study groups (CIDP, MMN, MND, and healthy controls) we only found weak correlations between the MRI metrics, i.e. diffusion parameters, T2 relaxation time and fat fraction, and the clinical covariates, i.e. age, MRC sum score and disease duration (**Figure 6.3**).

For the correlation with age, r ranged from -0.19 – 0.14 for patients with CIDP, -0.35 – 0.31 for patients with MMN, -0.20 – 0.34 for patients with MND, and -0.18 – 0.24 for healthy controls. For MRC sum score, r ranged from -0.23 – 0.10 for patients with CIDP, -0.08 – 0.24 for patients with MMN, and -0.13 – 0.20 for patients with MND. For disease duration, r ranged from -0.24 – 0.25 for patients with CIDP; -0.21 – 0.23 for patients with MMN, and 0.02 – 0.23 for patients with MND.



Table 6.3 Quantitative MRI parameters per study group and per nerve root.

Nerve root	CIDP	MMN	MND	Healthy
FA				
All	0.27 (0.05)	0.30 (0.06)	0.28 (0.04)	0.30 (0.05)
C5	0.26 (0.05)	0.29 (0.05)	0.27 (0.04)	0.29 (0.04)
C6	0.27 (0.05)	0.29 (0.06)	0.28 (0.04)	0.31 (0.05)
C7	0.27 (0.05)	0.30 (0.06)	0.28 (0.05)	0.28 (0.05)
MD (x 10⁻³ mm²/s)				
All	1.40 (0.20)	1.35 (0.23)	1.35 (0.20)	1.34 (0.17)
C5	1.41 (0.21)	1.35 (0.22)	1.35 (0.19)	1.30 (0.21)
C6	1.39 (0.17)	1.35 (0.24)	1.32 (0.16)	1.33 (0.13)
C7	1.41 (0.23)	1.35 (0.22)	1.36 (0.23)	1.39 (0.16)
AD (x 10⁻³ mm²/s)				
All	1.81 (0.24)	1.79 (0.30)	1.77 (0.28)	1.78 (0.20)
C5	1.81 (0.27)	1.79 (0.30)	1.77 (0.31)	1.72 (0.24)
C6	1.80 (0.19)	1.78 (0.31)	1.74 (0.21)	1.80 (0.15)
C7	1.82 (0.27)	1.79 (0.29)	1.80 (0.32)	1.82 (0.19)
RD (x 10⁻³ mm²/s)				
All	1.20 (0.19)	1.13 (0.20)	1.14 (0.16)	1.12 (0.17)
C5	1.20 (0.19)	1.13 (0.20)	1.14 (0.15)	1.08 (0.19)
C6	1.19 (0.17)	1.13 (0.22)	1.11 (0.15)	1.10 (0.14)
C7	1.21 (0.21)	1.12 (0.20)	1.15 (0.19)	1.17 (0.16)
T2 relaxation time (ms)				
All	42.37 (5.36)	41.12 (5.18)	41.02 (4.81)	41.32 (6.72)
C5	41.97 (5.29)	40.54 (5.43)	40.47 (4.59)	41.00 (8.81)
C6	42.85 (4.65)	41.86 (5.35)	41.78 (4.63)	42.06 (5.10)
C7	42.27 (6.14)	40.90 (4.75)	40.75 (5.16)	40.90 (6.15)
Fat fraction (%)				
All	40.09 (9.61)	39.44 (9.07)	43.62 (9.74)	40.55 (10.33)
C5	38.51 (8.39)	37.23 (8.29)	42.56 (8.46)	38.16 (10.68)
C6	38.54 (8.97)	37.55 (8.75)	42.09 (9.02)	39.62 (9.52)
C7	43.53 (10.71)	43.37 (8.90)	46.35 (11.16)	43.87 (10.62)

Mean diffusion parameters, T2 relaxation time and fat fraction with standard deviation per study group and per nerve root with calculated *p* values. *p* value 1 = CIDP vs. MND; *p* value 2 = MMN vs. MND; *p* value 3 = CIDP vs. MMN; *p* value 4 = healthy controls vs. CIDP; *p* value 5 = healthy controls vs. MMN; *p* value 6 = healthy controls vs. MND. Significant differences are marked with an asterisk (*).

<i>p</i> 1 CIDP vs. MND	<i>p</i> 2 MMN vs. MND	<i>p</i> 3 CIDP vs. MMN	<i>p</i> 4 Healthy vs. CIDP	<i>p</i> 5 Healthy vs. MMN	<i>p</i> 6 Healthy vs. MND
0.010*	0.002*	<0.001*	<0.001*	0.999	0.038*
0.563	0.016*	<0.001*	0.035*	0.997	0.237
0.135	0.780	0.018*	0.002*	0.383	0.099
0.234	0.074	<0.001*	0.315	0.655	0.958
0.008*	0.999	0.027*	0.137	0.996	0.998
0.361	0.999	0.363	0.164	0.802	0.719
0.060	0.837	0.481	0.589	0.993	0.991
0.477	0.977	0.294	0.963	0.898	0.972
0.224	0.817	0.833	0.849	0.996	0.982
0.766	0.976	0.971	0.574	0.799	0.906
0.256	0.711	0.938	1.000	0.991	0.727
0.922	0.999	0.966	1.000	0.989	0.978
0.001*	0.970	<0.001*	0.015*	0.996	0.949
0.174	0.933	0.069	0.054	0.841	0.578
0.026*	0.918	0.225	0.205	0.922	0.997
0.216	0.871	0.049*	0.853	0.786	0.973
0.023*	0.998	0.072	0.626	0.996	0.986
0.279	1.000	0.413	0.923	0.992	0.986
0.482	1.000	0.613	0.943	0.999	0.997
0.319	0.999	0.471	0.826	1.000	1.000
<0.001*	<0.001*	0.904	0.991	0.908	0.266
0.014*	0.004*	0.823	0.999	0.984	0.292
0.051	0.020*	0.911	0.975	0.865	0.777
0.335	0.368	1.000	0.999	0.998	0.848

Abbreviations: CIDP = chronic inflammatory demyelinating polyneuropathy; MMN = multifocal motor neuropathy; MND = motor neuron disease; FA = fractional anisotropy; MD = mean diffusivity; AD = axial diffusivity; RD = radial diffusivity; ms = milliseconds.

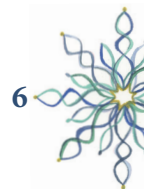
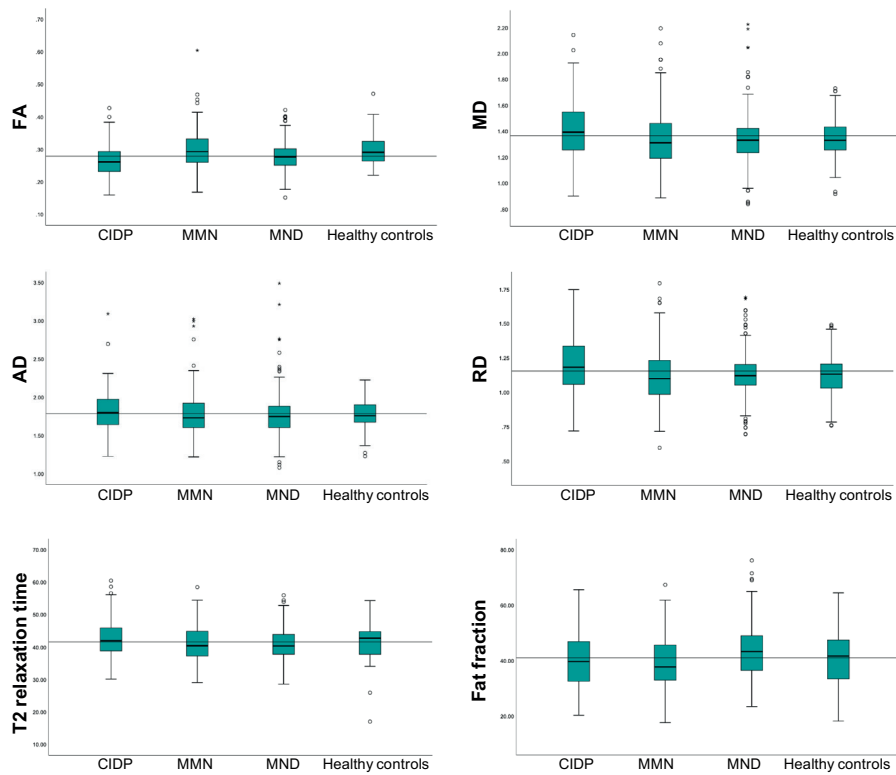
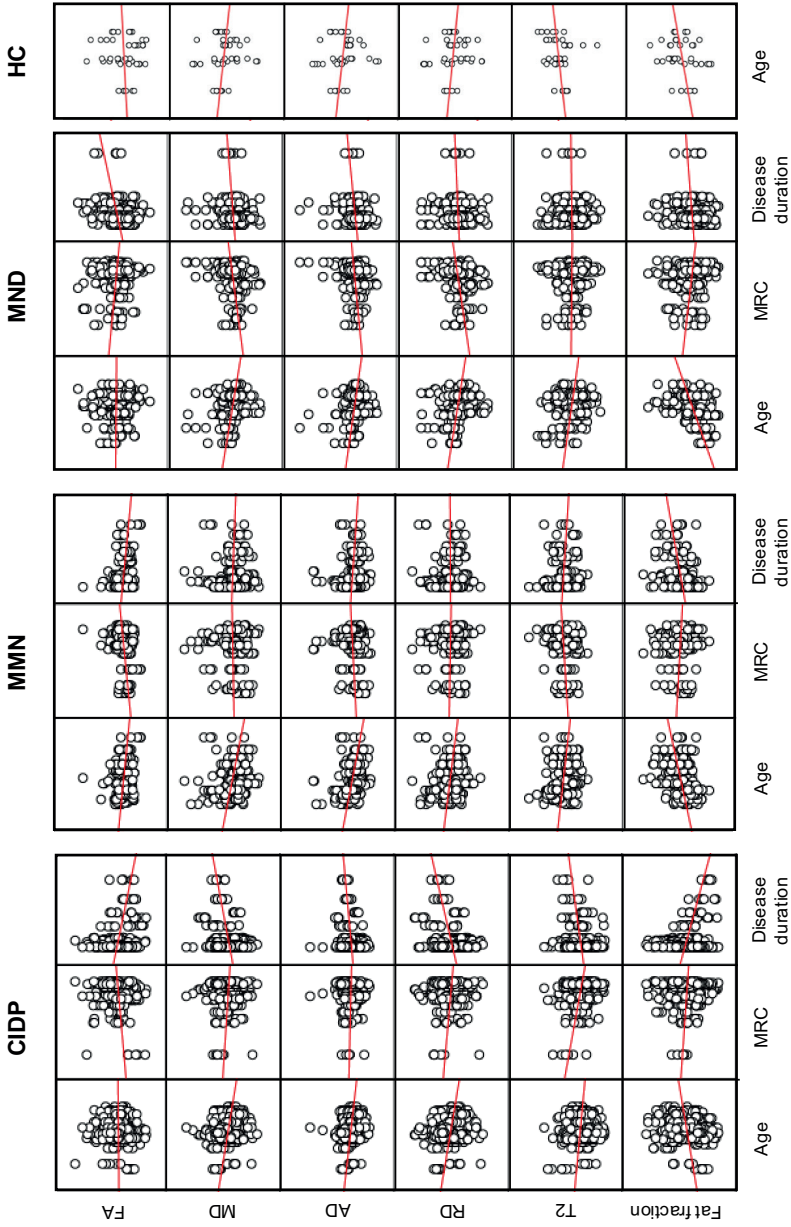


Figure 6.2. Boxplots of quantitative parameter per study group

Boxplots of diffusion parameters, T2 relaxation times and fat fraction with grand mean are shown. MD, AD and RD values are $\times 10^{-3} \text{ mm}^2/\text{s}$, T2 relaxation time is in milliseconds and fat fraction is a percentage. Abbreviations: FA = fractional anisotropy; MD = mean diffusivity; AD = axial diffusivity; RD = radial diffusivity; mm = millimeters; s = seconds; CIDP = chronic inflammatory demyelinating polyneuropathy; MMN = multifocal motor neuropathy; MND = motor neuron disease.

Figure 6.3. Correlation matrix of quantitative parameters with clinical data per study group



Correlation matrix of the MRI metrics FA, MD, AD, RD, T2 and fat fraction (y axis) with the clinical covariates age, MRC sum score and disease duration (x axis), shown per study group. Abbreviations: CIDP = chronic inflammatory demyelinating polyneuropathy; MMN = multifocal motor neuropathy; MND = motor neuron disease; HC = healthy controls; FA = Fractional anisotropy; MD = mean diffusivity; AD = axial diffusivity; RD = radial diffusivity; MRC = Medical research council.



DISCUSSION

With this study, we show that quantitative MRI techniques reveal differences in the brachial plexus between patients with CIDP, MMN, MND and healthy controls. CIDP is characterized by lower FA and higher RD than MMN, MND and healthy controls, whilst MMN is characterized by higher FA values than CIDP and MND. Patients with MMN and healthy controls did not differ. These differences between CIDP and MMN are the most remarkable and important finding as they emphasize important differences in the underlying pathophysiologies.

This is the first comparative quantitative MRI study in a relatively large cohort of patients with CIDP and MMN. Diffusion parameters obtained from the sciatic, tibial, median, ulnar and radial nerves were previously reported in smaller cohorts.^{14–17,19} The absolute differences of the measured parameters are around 2% between study groups, which indicates that differences are probably only found in larger groups. However, the finding of a decreased FA and an increased RD in our study patients with CIDP is in agreement with previous findings, indicating that this DTI profile is characteristic for CIDP and can be found throughout the peripheral nervous system.^{14–17,19} Experimental animal studies showed that increased RD may correspond with loss of myelin integrity.^{10–12} The combination of decreased FA and increased RD has also been reported in patients with Guillain-Barré syndrome (GBS) and demyelinating types of Charcot-Marie-Tooth (CMT), which corroborates that this reflects the disturbance of myelin integrity in peripheral nerves caused by inflammation.^{32–35} The longer T2 relaxation times and lower fat fraction in the CIDP cohort compared to the MND cohort indicate the presence of free water, which may also be due to inflammation, and have also been reported at the lumbosacral plexus.^{21,22,36} Although decreased FA in combination with increased RD is a robust finding in patients with CIDP, absolute diffusion values differ between proximal and distal nerve sites.^{14–17,19} This is probably explained by the proximal to distal decrease in the diameter of fascicles with a corresponding increase in the density of the perifascicular connective tissue.³⁷ In the well-organized tissues of the distal peripheral nerves, water molecule movement is more restricted in specific directions, which results in larger isotropic diffusion and a higher FA. The FA values of the brachial plexus in our study were lower than in previous studies of distal peripheral nerves in arms and legs, which is in line with this hypothesis.^{14–17,19}

FA and MD are summary measures from eigenvalues. Changes in FA and MD are therefore driven by changes in AD or RD. In CIDP, the increase in RD seems to drive the changes in FA and MD. RD indicates less hindrance of diffusion for water perpendicular to the nervous tissue. This can be the result of various cellular mechanisms, such as demyelination or a disturbance of the cytoskeleton caused by a loss of neurofilaments and microtubules. We think that our findings may reflect demyelination rather than a disturbance of the cytoskeleton as histological studies reported myelin detachment and myelin loss without damage to axons induced by macrophages around the

(inter)nodal regions in patients with CIDP.^{3-5,38-41} The mechanism of paranodal myelin detachment is present in some patients with CIDP, as described in earlier electrophysiological studies.⁴²⁻⁴⁴ Taken together, the changes in FA, MD and RD in our CIDP group most likely reflect the loss of myelin.

The absence of increased RD values in patients with MMN indicates that the underlying pathophysiological mechanism is different from that in CIDP and that demyelination is probably not the dominant pathophysiological process. Patients with MMN seem to have comparable quantitative MRI parameters as healthy controls. Scarce histological reports describe normal myelin sheets.⁶⁻⁸ Electrophysiological studies may support the idea of changed axon structure with largely intact myelin sheets.⁴⁴ However, it is rather remarkable that such different DTI profiles are found between patients with MMN and CIDP while diagnostic tools used in clinical practice, such as nerve conduction studies, nerve ultrasound and qualitative MRI of the brachial plexus may show similar abnormalities, e.g. conduction blocks and thickening of the nerves. The differences in DTI profiles indicate that these abnormalities are more likely to present common endpoints of different pathophysiological mechanisms rather than comparable etiologies.

In a previous study we found lower AD in the median and ulnar nerves in the forearm of patients with MMN compared to healthy controls and patients with ALS.¹⁸ It is assumed that AD correlates with axonal loss, e.g. due to axonal swelling due to the breakdown or change in the permeability of the axolemma, which is an important feature of MMN.^{11,45,46} We did not detect differences in AD between groups at the brachial plexus in this study, which can be explained by the fact that longer axons and distal parts of axons are more susceptible to injury than short and proximal parts of axons. Consequently, AD may remain relatively unchanged in the proximal spinal nerve roots of the brachial plexus. In the previous study we did not find a significant difference in FA between patients with MMN and ALS, although absolute values of FA were higher in patients with MMN.¹⁸ We found a significantly higher FA in patients with MMN compared to patients with MND in this study, which can be explained by the larger sample size and higher statistical power in the current study.

Correlations between clinical data and quantitative MRI parameters were weak. We refrained from studying correlations of nerve conduction studies and imaging results since the measurement sites did not match. More in general, imaging and electrophysiological studies may reveal different pathophysiological dimensions. Previous studies found that imaging results did not correlate with nerve conduction study results in cohorts of patients with inflammatory neuropathies.⁴⁷⁻⁵¹

A limitation of our study is the effect of partial volume, which may lead to an underestimation of diffusion parameters and fat fraction, and varying SNR which may lead to higher FA and lower RD in case of lower SNRs.⁵² However, the influence of partial volume effects and different SNR values were probably small as our results in DTI analysis, T2 mapping and fat fraction analysis are consistent with each other, and scans were performed in random order with the same software



versions. Another limitation might be the registration step in the processing pipeline. Due to an imperfect registration some tracts were not or incompletely found, particularly in nerve root C7 due to strong susceptibility artifacts caused by the lungs. Our healthy control group is small but we think the number of healthy controls is sufficient as standard deviations of the means of the quantitative MRI parameters were small and comparable to the other three study groups, indicating low levels of variation between individuals. Moreover, the diffusion parameters that we observed were similar to those previously reported in literature.⁵³ We analyzed relatively short segments of the brachial plexus, since analysis of longer tracts resulted in a significant dropout of data due to poor data quality. We therefore decided to only analyze the first centimeter next to the ganglion in order to maximize the number of datasets. Although we could not include the more distal parts of the brachial plexus, the advantage of this approach is a well-powered study that provides information on a large patient population derived with an automated pipeline without subjective bias.

In conclusion, our study gives insight into the nerve architecture of the brachial plexus in a relatively large cohort of patients with CIDP, MMN, MND and healthy controls. Our study shows that diffusion parameters differ between CIDP and MMN, which may reflect differences in the underlying pathophysiological mechanisms. Future studies should combine assessments of the brachial plexus and distal nerves and assess correlations between quantitative MRI parameters in roots, fascicles and peripheral nerves and specific clinical deficits. They should also address whether changes occur in disease course or after treatment.

REFERENCES

- Allen JA, Lewis RA. CIDP diagnostic pitfalls and perception of treatment benefit. *Neurology* 2015;85:498–504.
- Vlam L, Van Der Pol WL, Cats EA, et al. Multifocal motor neuropathy: Diagnosis, pathogenesis and treatment strategies. *Nat. Rev. Neurol.* 2012;8:48–58.
- Matthews WB, Howell DA, Hughes RC. Relapsing corticosteroid-dependent polyneuritis. *J. Neurol. Neurosurg. Psychiatry* 1970;33:330–337.
- Torvik A, Lundar T. A case of chronic demyelinating polyneuropathy resembling the Guillan-Barré Syndrome. *J. Neurol. Sci.* 1977;32:45–52.
- Matsuda M, Ikeda SI, Sakurai S, et al. Hypertrophic neuritis due to chronic inflammatory demyelinating polyradiculoneuropathy (CIDP): A postmortem pathological study. *Muscle and Nerve* 1996;19:163–169.
- Krarpur C, Stewart JD, Sumne AJ, et al. A syndrome of asymmetric limb weakness with motor conduction block. *Neurology* 1990;40:118–127.
- Adams D, Kuntzer T, Steck AJ, et al. Motor conduction block and high titres of anti-GM1 ganglioside antibodies: Pathological evidence of a motor neuropathy in a patient with lower motor neuron syndrome. *J. Neurol. Neurosurg. Psychiatry* 1993;56:982–987.
- Veugelers B, Theys P, Lammens M, et al. Pathological findings in a patient with amyotrophic lateral sclerosis and multifocal motor neuropathy with conduction block. *J. Neurol. Sci.* 1996;136:64–70.
- Harschnitz O, van den Berg LH, Johansen LE, et al. Autoantibody pathogenicity in a multifocal motor neuropathy induced pluripotent stem cell-derived model. *Ann. Neurol.* 2016;80:71–88.
- Song SK, Sun SW, Ramsbottom MJ, et al. Demyelination revealed through MRI as increased radial (but unchanged axial) diffusion of water. *Neuroimage* 2002;17:1429–1436.
- Song SK, Sun SW, Ju WK, et al. Diffusion tensor imaging detects and differentiates axon and myelin degeneration in mouse optic nerve after retinal ischemia. *Neuroimage* 2003;20:1714–1722.
- Morisaki S, Kawai Y, Umeda M, et al. In vivo assessment of peripheral nerve regeneration by diffusion tensor imaging. *J. Magn. Reson. Imaging* 2011;33:535–542.
- Jeon T, Fung MM, Koch KM, et al. Peripheral nerve diffusion tensor imaging: Overview, pitfalls, and future directions. *J. Magn. Reson. Imaging* 2018;47:1171–1189.
- Kakuda T, Fukuda H, Tanitame K, et al. Diffusion tensor imaging of peripheral nerve in patients with chronic inflammatory demyelinating polyradiculoneuropathy: A feasibility study. *Neuroradiology* 2011;53:955–960.
- Mathys C, Aissa J, Zu Hörste GM, et al. Peripheral Neuropathy: Assessment of Proximal Nerve Integrity By Diffusion Tensor Imaging. *Muscle Nerve* 2013;48:889–896.
- Markvardsen LH, Vaeggemose M, Ringgaard S, Andersen H. Diffusion tensor imaging can be used to detect lesions in peripheral nerves in patients with chronic inflammatory demyelinating polyneuropathy treated with subcutaneous immunoglobulin. *Neuroradiology* 2016;58:745–752.
- Kronlage M, Pitarokoili K, Schwarz D, et al. Diffusion Tensor Imaging in Chronic Inflammatory Demyelinating Polyneuropathy: Diagnostic Accuracy and Correlation with Electrophysiology. *Invest. Radiol.* 2017;52:701–707.
- Haakma W, Jongbloed BA, Froeling M, et al. MRI shows thickening and altered diffusion in the median and ulnar nerves in multifocal motor neuropathy. *Eur. Radiol.* 2017;27:2216–2224.
- Lichtenstein T, Sprenger A, Weiss K, et al. MRI biomarkers of proximal nerve injury in CIDP. *Ann. Clin. Transl. Neurol.* 2018;5:19–28.
- Oudeman J, Eftimov F, Strijkers GJ, et al.



- Diagnostic accuracy of MRI and ultrasound in chronic immune-mediated neuropathies. *Neurology* 2020;94:e62–e74.
21. Hiwatashi A, Togao O, Yamashita K, et al. Lumbar plexus in patients with chronic inflammatory demyelinating polyradiculoneuropathy: evaluation with simultaneous T2 mapping and neurography method with SHINKEI. *Br. J. Radiol.* 2018;91:20180501.
 22. Hiwatashi A, Togao O, Yamashita K, et al. Simultaneous MR neurography and apparent T2 mapping in brachial plexus: Evaluation of patients with chronic inflammatory demyelinating polyradiculoneuropathy. *Magn. Reson. Imaging* 2018;55:112–117.
 23. Felisaz PF, Poli A, Vitale R, et al. MR microneurography and quantitative T2 and DP measurements of the distal tibial nerve in CIDP. *J. Neurol. Sci.* 2019;400:15–20.
 24. van den Bergh PYK, Hadden RDM, Bouche P, et al. European Federation of Neurological Societies/Peripheral Nerve Society Guideline on management of chronic inflammatory demyelinating polyradiculoneuropathy: Report of a joint task force of the European Federation of Neurological Societies and the Peripher. *Eur. J. Neurol.* 2010;17:356–363.
 25. Van Schaik IN, Léger JM, Nobile-Orazio E, et al. European Federation of Neurological Societies/Peripheral Nerve Society Guideline on management of multifocal motor neuropathy. Report of a Joint Task Force of the European Federation of Neurological Societies and the Peripheral Nerve Society - First revis. *J Peripher Nerv Syst* 2010;15:295–301.
 26. Brooks BR, Miller RG, Swash M, Munsat TL. El Escorial revisited: Revised criteria for the diagnosis of amyotrophic lateral sclerosis. *ALS Mot. neuron Disord.* 2000;1:293–299.
 27. Leemans A, Jeurissen B, Sijbers J, Jones DK. ExploreDTI: a graphical toolbox for processing, analyzing, and visualizing diffusion MR data. *Proc. Int. Soc. Magn. Reson. Med.* 2009;17:3537.
 28. Yushkevich PA, Piven J, Hazlett HC, et al. User-guided 3D active contour segmentation of anatomical structures: Significantly improved efficiency and reliability. *Neuroimage* 2006;31:1116–1128.
 29. Marty B, Baudin PY, Reyngoudt H, et al. Simultaneous muscle water T2 and fat fraction mapping using transverse relaxometry with stimulated echo compensation. *NMR Biomed.* 2016;29:431–443.
 30. Keene KR, Beenakker JWM, Hooijmans MT, et al. T2 relaxation-time mapping in healthy and diseased skeletal muscle using extended phase graph algorithms. *Magn. Reson. Med.* 2020;84:2656–2670.
 31. Taylor R. Interpretation of the Correlation Coefficient: a Basic Review. *J. Diagnostic Med. Sonogr.* 1990;1:35–39.
 32. Cao J, He B, Wang S, et al. Diffusion Tensor Imaging of Tibial and Common Peroneal Nerves in Patients With Guillain–Barre Syndrome: A Feasibility Study. *J. Magn. Reson. Imaging* 2019;49:1356–1364.
 33. Vaeggemose M, Vaeth S, Pham M, et al. Magnetic resonance neurography and diffusion tensor imaging of the peripheral nerves in patients with Charcot-Marie-Tooth Type 1A. *Muscle and Nerve* 2017;56:78–84.
 34. Kim HS, Yoon YC, Choi B-O, et al. Diffusion tensor imaging of the sciatic nerve in Charcot-Marie-Tooth disease type I patients: a prospective case-control study. *Eur. Radiol.* 2019;1–12.
 35. Chhabra A, Carrino JA, Farahani SJ, et al. Whole-body MR neurography: Prospective feasibility study in polyneuropathy and Charcot-Marie-Tooth disease. *J. Magn. Reson. Imaging* 2016;44:1513–1521.
 36. McRobbie DW, Moore EA, Graves MJ. *MRI from picture to proton*. 2nd ed. Cambridge University Press, Cambridge; 2017.
 37. Bonnel F. Microscopic anatomy of the adult human brachial plexus: An anatomical and histological basis for microsurgery. *Microsurgery* 1984;5:107–117.
 38. Auer RN, Bell RB, Lee MA. Neuropathy with Onion Bulb Formations and Pure Motor Manifestations. *Can. J. Neurol. Sci. / J. Can.*

- des Sci. Neurol. 1989;16:194–197.
39. Oh SJ, Claussen G, Odabasi Z, Palmer CP. Multifocal demyelinating motor neuropathy: pathologic evidence of ‘inflammatory demyelinating polyradiculoneuropathy’. *Neurology* 1995;45:1828–1832.
 40. Sasaki M, Ohara S, Oide T, et al. An autopsy case of chronic inflammatory demyelinating polyradiculoneuropathy with respiratory failure. *Muscle and Nerve* 2004;30:382–387.
 41. Koike H, Nishi R, Ikeda S, et al. Ultrastructural mechanisms of macrophage-induced demyelination in CIDP. *Neurology* 2018;91:1051–1060.
 42. Franssen H, Straver DCG. Pathophysiology of immune-mediated demyelinating neuropathies-part I: Neuroscience. *Muscle Nerve* 2013;48:851–864.
 43. Franssen H, Straver DCG. Pathophysiology of immune-mediated demyelinating neuropathies-Part II: Neurology. *Muscle and Nerve* 2014;49:4–20.
 44. Garg N, Park SB, Howells J, et al. Conduction block in immune-mediated neuropathy: paranodopathy versus axonopathy. *Eur. J. Neurol.* 2019;26:1121–1129.
 45. Yan Aung W, Mar S, Benzinger TL. DTI as biomarker in axonal and myelin damage. *Imaging Med.* 2013;5:427–440.
 46. Van Asseldonk JTH, Van Den Berg LH, Kalmijn S, et al. Axon loss is an important determinant of weakness in multifocal motor neuropathy. *J. Neurol. Neurosurg. Psychiatry* 2006;77:743–747.
 47. Goedee H. High-resolution ultrasound in diagnosis of polyneuropathies. In: ISBN 9789462336841. 2017 p. 167–190.
 48. Kerasnoudis A, Pitarokoili K, Behrendt V, et al. Correlation of Nerve Ultrasound, Electrophysiological and Clinical Findings in Chronic Inflammatory Demyelinating Polyneuropathy. *J. Neuroimaging* 2015;25:207–216.
 49. Kerasnoudis A, Weitalla D, Gold R, et al. Multifocal motor neuropathy: correlation of nerve ultrasound, electrophysiological, and clinical finding. *J. Peripher. Nerv. Syst.* 2014;347:129–136.
 50. Rajabally YA, Morlese J, Kathuria D, Khan A. Median nerve ultrasonography in distinguishing neuropathy sub-types: A pilot study. *Acta Neurol. Scand.* 2012;125:254–259.
 51. Beekman R, Van Den Berg LH, Franssen H, et al. Ultrasonography shows extensive nerve enlargements in multifocal motor neuropathy. *Neurology* 2005;65:305–307.
 52. Vos SB, Jones DK, Viergever MA, Leemans A. Partial volume effect as a hidden covariate in DTI analyses. *Neuroimage* 2011;55:1566–1576.
 53. Oudeman J, Verhamme C, Engbersen MP, et al. Diffusion tensor MRI of the healthy brachial plexus. *PLoS One* 2018;13:1–15.







Chapter 7

Quantitative MRI of the brachial plexus in CIDP and MMN: a longitudinal cohort study

Marieke H.J. van Rosmalen, H. Stephan Goedee, Ruben P.A. van Eijk, Jeroen Hendrikse, Martijn Froeling*, W. Ludo van der Pol*

* These authors contributed equally to the manuscript

Submitted

ABSTRACT

Objective: Chronic inflammatory demyelinating polyneuropathy (CIDP) and multifocal motor neuropathy (MMN) respond to immunomodulatory treatment. Management of treatment may be challenging as treatment response varies between patients and predictive biomarkers for treatment response or disease course are lacking. Quantitative magnetic resonance imaging (MRI) techniques are potential biomarkers for disease course and treatment response. Therefore, we performed a longitudinal quantitative MRI study in patients with CIDP and MMN and evaluated their quantitative parameters over time.

Methods: We enrolled patients with CIDP ($n = 23$) and MMN ($n = 7$). All patients underwent MRI of the brachial plexus twice with a one-year interval. We obtained diffusion parameters, T2 relaxation times and fat fraction. We compared MRI parameters between baseline and follow-up scans using a linear mixed model and studied correlations with clinical parameters (e.g. treatment status and treatment response).

Results: In patients with CIDP, mean diffusivity, axial diffusivity and radial diffusivity decreased while fat fraction increased over time ($p = 0.012, 0.018, 0.015$ and 0.045 respectively). In MMN we found no significant differences between timepoints. We found no significant correlations between clinical parameters and quantitative MRI parameters in both patient groups.

Discussion: This study shows that quantitative MRI parameters change over time in patients with CIDP, but not with MMN. We found no significant correlations between the changes in quantitative MRI parameters and available clinical data. Quantitative MRI techniques evaluated in this study are unlikely to serve as a biomarker to predict prognosis or to monitor treatment response.

INTRODUCTION

Chronic inflammatory demyelinating polyneuropathy (CIDP) and multifocal motor neuropathy (MMN) are both rare chronic inflammatory neuropathies that respond to treatment with immunomodulation. Treatment may improve motor (MMN and CIDP) and sensory deficits (CIDP only).^{1,2} However, treatment response varies between patients and some patients may worsen over time despite treatment.³ Biomarkers that predict course of disease and correlate with treatment response are currently lacking which complicates management of these neuropathies. Early electrophysiological studies showed that axonal damage correlates with weakness and a functional impairment, but not with response to treatment or unfavorable disease course.⁴⁻⁶ Nerve ultrasound studies in patients with CIDP initially suggested that changes of nerve size and echotexture could correlate with clinical disease activity,⁷ but this has not been corroborated in other studies.⁸

Quantitative magnetic resonance imaging (MRI) techniques, including diffusion tensor imaging (DTI), T2 mapping and fat fraction analysis, can provide quantitative information on microstructural integrity of (nervous) tissue.⁹⁻¹² Longitudinal DTI studies of the brain have shown differences in diffusion parameters over time in patients with primary brain tumors, Alzheimer's disease and Parkinson's disease.¹³⁻¹⁹ Cross-sectional DTI, T2 mapping and fat fraction analysis studies of the brachial plexus and peripheral nerves in patients with CIDP and MMN showed differences between patients and controls, but follow-up studies have not been published.²⁰⁻²⁵ Therefore, we performed a longitudinal study in newly diagnosed patients with CIDP and MMN who did not use treatment at baseline.

METHODS

Study design

We performed a longitudinal study in a cohort of patients with CIDP and MMN. All patients started immunomodulatory treatment after enrollment (i.e. were treatment naive at baseline). We obtained quantitative MRI parameters of the brachial plexus at baseline and after approximately one-year. We compared quantitative MRI parameters between timepoints and studied correlations with clinical data.

Patients and clinical data

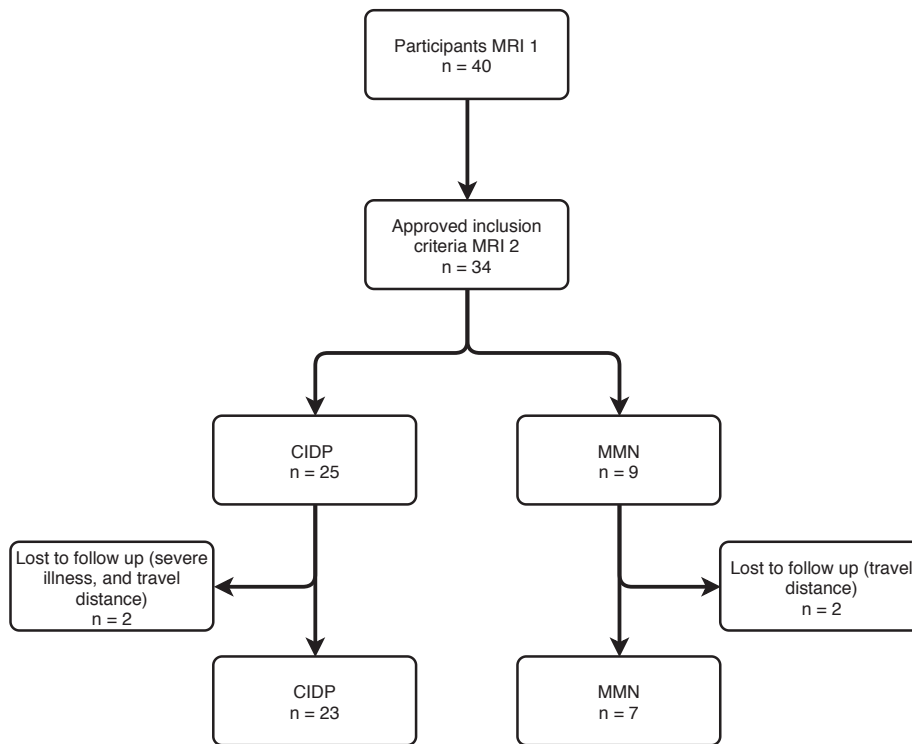
All patients participated in a previous DTI study and had a diagnosis of CIDP or MMN according to consensus criteria (definite, probable, possible).^{26,27} They were treatment naive at the time of the first research MRI²⁵. We excluded patients who did not start treatment between the first (t_0) and the second MRI (t_1) and patients who met one of the routine contraindications to MRI (**Figure 7.1**).



7

We obtained clinical data from electronic patients records, including age; disease duration, defined as months from diagnosis until t_0 ; MRI interval, defined as time in months between t_0 and t_1 ; treatment status (including type of treatment, receiving high dose therapy as start of treatment and need for maintenance therapy); treatment response as documented by the treating physician; and time since last maintenance treatment in days. The Medical Ethical Committee of the University Medical Center Utrecht approved this study. Written informed consent was obtained from all study participants.

Figure 7.1 Flow chart of patient selection procedure



Abbreviations: MRI = magnetic resonance imaging; CIDP = chronic inflammatory demyelinating polyneuropathy; MMN = multifocal motor neuropathy

Equipment and MRI protocol

All participants underwent an MRI scan of the brachial plexus at baseline and approximately one year later. We used a 3.0 Tesla MRI scanner (Philips Healthcare, Best, the Netherlands) with a 24-channel head neck coil. Patients were positioned in supine position. We used acquisition parameters as described in a previous study (**Table 7.1**).²⁵ In short, we performed a DTI sequence, T2 mapping and T1 Dixon. We used a 3D turbo spin-echo spectral presaturation with inversion recovery as an anatomical reference.

Table 7.1 MRI parameters

Parameter	DTI	T2 mapping	T1 DIXON	3D TSE
Acquisition	2D SE-EPI	2D TSE	3D FFE	3D TSE
Field of view	240*180*150 mm ³	240*180*52.5 mm ³	288*288-200.25 mm ³	336*336*170 mm ³
Matrix size	96*71	96*96	192*192	224*223
Slice thickness	2.5 mm	2.5 mm	-	-
Voxel size	2.5*2.5*2.5 mm ³	2.5*2.5*2.5 mm ³	0.75*0.75*0.75 mm ³	0.75*0.75*1 mm ³
Echo time	60 ms	7.6 ms	1.186 ms	206 ms
Number of echoes	-	17	3	-
Repetition time	8595 ms	3242 ms	5615 ms	2200 ms
Flip angle	-	-	16°	-
Turbo spin echo factor	-	-	-	76
Sensitivity encoding factor	2.5	2.3	2 (AP); 1 (FH)	3 (RL); 1.5 (AP)
Fat suppression	SPAIR	-	-	SPIR
Gradient directions	37	-	-	-
b values (s/mm ²)	0, 50, 100, 150, 300, 400, 600	-	-	-
Acquisition time	05:43 minutes	04:45 minutes	01:56 minutes	03:59 minutes

Abbreviations: DTI = diffusion tensor imaging; TSE = turbo spin echo; SPAIR = spectral attenuated inversion recovery; SPIR = spectral presaturation with inversion recovery; SE EPI = spin echo-echo planar imaging; FFE = fast field echo; mm = millimeter; ms = milliseconds; AP = anterior/posterior; FH = foot/head; RL = right/left.

Data processing

We processed MRI data semi-automatically using a two-step custom-build processing pipeline, as described in detail previously.²⁵ In short, the processing pipeline provided whole volume fiber tractography of the brachial plexus and reconstruction of cervical nerve roots C5, C6 and C7. This allowed us to extract diffusion parameters (i.e. fractional anisotropy (FA), mean diffusivity (MD), axial diffusivity (AD), and radial diffusivity (RD)), T2 relaxation times and fat fraction from a standardized site, i.e. over a 1 cm segment next to the ganglion.

Statistical analysis

We used IBM SPSS Statistics (Version 26, Armonk, New York, United States) for statistical analysis. To compare patient characteristics, we used an independent samples *t* test. The mean difference over time for the quantitative parameters (i.e. diffusion parameters, T2 relaxation times and fat fraction) was estimated between t_0 and t_1 . We used a linear mixed model to correct for the multiple paired measurements per subject and calculated the mean difference with 95% confidence intervals and *p* values. A *p* value < 0.05 was considered significant. Correlations between the quantitative parameters and clinical data were analyzed using an independent samples *t* test for categorical data and using the Pearson correlation coefficient *r* for continuous data. We considered $r \leq 0.35$ as a weak correlation, 0.36 – 0.70 as moderate, 0.70 – 0.89 as high and ≥ 0.90 as a very high correlation.²⁸



RESULTS

Patients and clinical data

We included 30 patients: 23 with CIDP and 7 with MMN. Patient characteristics are summarized in **Table 7.2**. Patients with MMN were younger than patients with CIDP and disease controls ($p < 0.001$). Other characteristics did not differ significantly.

Table 7.2 Patient characteristics

Parameter	CIDP	MMN	<i>p</i>
Number of subjects	23	7	-
Age, years (SD)	64.7 (6.3)	45.5 (4.9)	< 0.001
Male (%)	20 (87%)	6 (86%)	-
Disease duration, months (SD)	2.4 (3.0)	1.4 (1.7)	0.45
MRI interval, months (SD)	11.6 (4.8)	14.6 (6.3)	0.18
Duration since last maintenance treatment, days (SD)	16.6 (9.7)	14.9 (16.4)	0.76
Treatment details			
Received High Dose Therapy	23 (100%)	7 (100%)	
Positive treatment response (%)	16 (70%)	7 (100%)	
Requires maintenance treatment (%)	14 (61%)	7 (100%)	
<i>Immunoglobulins</i>	12	7	
<i>Dexamethasone</i>	2	0	

Disease duration = time in months between diagnosis and research MRI 1; MRI interval = time in months between research MRI 1 and research MRI 2; Duration since last maintenance treatment = time between last treatment and research MRI 2. Age, disease duration, MRI interval and duration since last treatment are mean (SD). Abbreviations: CIDP = chronic inflammatory demyelinating polyneuropathy; MMN = multifocal motor neuropathy; p = p value; SD = standard deviation.

Feasibility of data processing

Automated processing identified 87.2% of all nerve roots (88%, 95% and 78% for C5, C6 and C7 respectively). With additional manual adjustments a total of 95% of all C5 nerve roots, 100% of C6 nerve roots and 95% of C7 could be identified.

Quantitative MRI parameters

Mean differences of the quantitative MRI parameters between t_0 and t_1 can be found in **Table 7.3**. MD, AD and RD decreased and fat fraction increased over time in patients with CIDP ($p = 0.012$, 0.018 , 0.015 , and 0.045 respectively), but not in patients with MMN. **Figure 7.2** shows the changes of the quantitative MRI parameters between t_0 and t_1 for each patient.

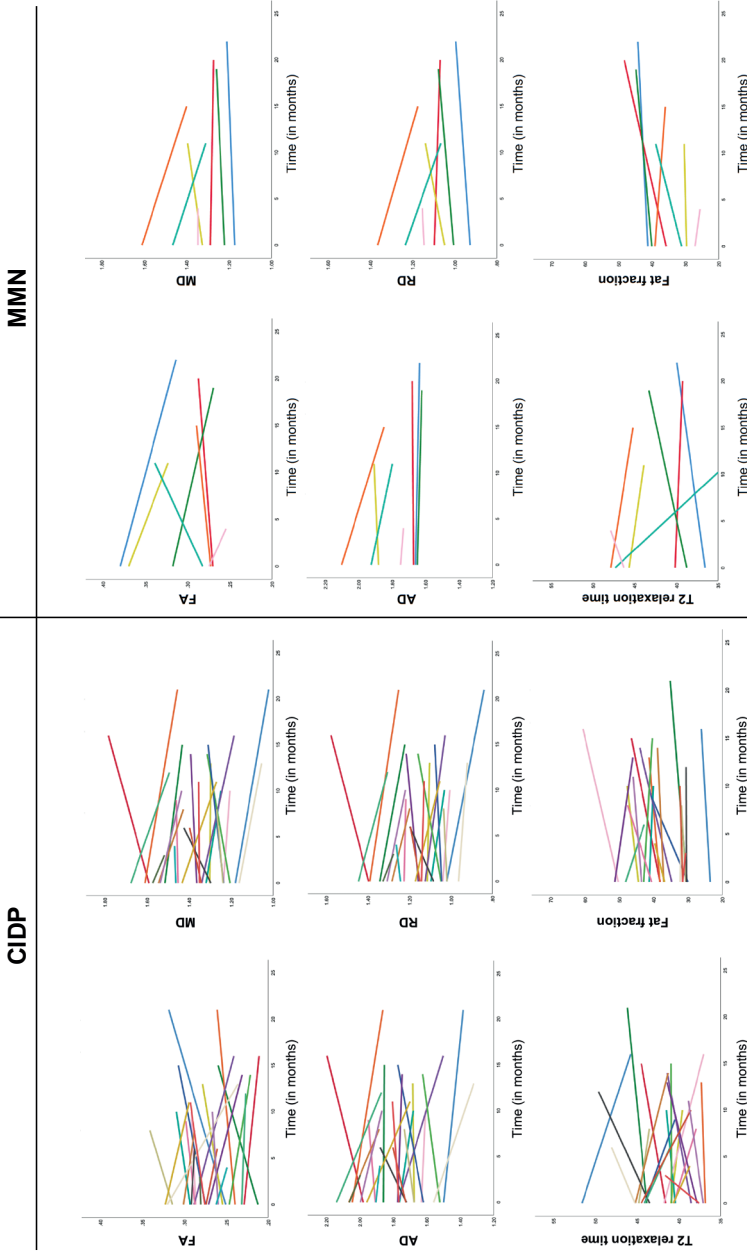
Table 7.3 Mean differences of MRI parameters between the first and second research MRI

Parameter	Nerve root	CIDP (n = 23)			MMN (n = 7)		
		Mean dif	95% CI	p	Mean dif	95% CI	p
FA	All	-0.005	-0.019 – 0.010	0.544	-0.019	-0.068 – 0.029	0.368
	C5	-0.003	-0.024 – 0.019	0.788	-0.045	-0.139 – 0.048	0.280
	C6	-0.002	-0.021 – 0.018	0.863	-0.015	-0.071 – 0.042	0.550
	C7	-0.010	-0.032 – 0.011	0.318	0.002	-0.030 – 0.034	0.907
MD (x 10 ⁻³ mm ² /s)	All	-0.054	-0.095 – -0.014	0.012	-0.064	-0.168 – 0.040	0.184
	C5	-0.080	-0.155 – -0.004	0.040	-0.123	-0.378 – 0.133	0.285
	C6	-0.010	-0.056 – 0.037	0.666	-0.001	-0.173 – 0.172	0.991
	C7	-0.078	-0.164 – 0.009	0.076	-0.068	-0.131 – -0.005	0.037
AD (x 10 ⁻³ mm ² /s)	All	-0.072	-0.129 – -0.014	0.018	-0.098	-0.199 – 0.003	0.057
	C5	-0.100	-0.205 – 0.005	0.063	-0.206	-0.550 – 0.139	0.195
	C6	-0.015	-0.084 – 0.055	0.669	-0.003	-0.180 – 0.174	0.968
	C7	-0.108	-0.213 – 0.004	0.042	-0.085	-0.163 – -0.007	0.035
RD (x 10 ⁻³ mm ² /s)	All	-0.045	-0.081 – -0.010	0.015	-0.047	-0.150 – 0.056	0.310
	C5	-0.069	-0.132 – -0.006	0.034	-0.081	-0.300 – 0.138	0.400
	C6	-0.007	-0.047 – 0.032	0.705	0.000	-0.172 – 0.173	0.998
	C7	-0.064	-0.141 – 0.018	0.123	-0.059	-0.128 – 0.009	0.083
T2 relaxation time (ms)	All	-0.379	-0.212 – 1.172	0.552	-1.398	-6.789 – 4.235	0.591
	C5	-0.781	-2.697 – 1.140	0.407	1.327	-5.404 – 9.539	0.522
	C6	-0.280	-2.535 – 1.975	0.798	-2.012	-8.992 – 4.969	0.507
	C7	-0.057	-2.423 – 2.154	0.903	-3.315	-8.106 – 1.475	0.141
Fat fraction (%)	All	2.307	0.050 – 4.463	0.045	3.184	-1.854 – 8.218	0.174
	C5	2.412	0.166 – 4.657	0.036	5.068	-4.108 – 14.412	0.223
	C6	2.777	-0.510 – 6.063	0.093	1.180	-3.868 – 6.227	0.622
	C7	1.647	-1.606 – 4.893	0.299	3.440	-4.074 – 10.954	0.341

Mean differences of diffusion parameters, T2 relaxation time and fat fraction between research MRI 1 and research MRI 2, with 95% confidence intervals and *p* values, visualized for patients with CIDP and MMN separately. Abbreviations: CIDP = chronic inflammatory demyelinating polyneuropathy; MMN = multifocal motor neuropathy; Mean dif = mean difference; CI = confidence interval; FA = fractional anisotropy; MD = mean diffusivity; AD = axial diffusivity; RD = radial diffusivity; ms = milliseconds.

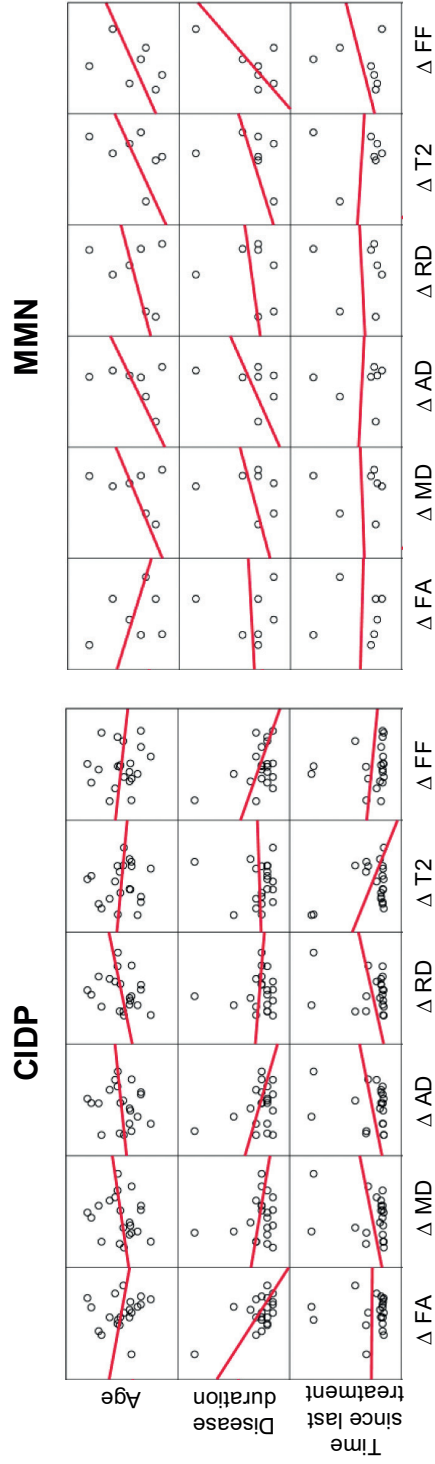


Figure 7.2 Course of quantitative parameters over time



Plots of FA, MD, AD, RD, T2 relaxation time (in milliseconds) and fat fraction (in percentage) over time (months) for patients with CIDP (left panels) and MMN (right panels). Every colored line reflects one patient and the course of its quantitative parameter between the first (t_0) and second (t_1) MRI. MD, AD and RD values are $\times 10^{-3} \text{ mm}^2/\text{s}$. Abbreviations: CIDP = chronic inflammatory demyelinating polyneuropathy; MMN = multifocal motor neuropathy; fractional anisotropy = FA; MD = mean diffusivity; AD = axial diffusivity; RD = radial diffusivity.

Figure 7.3 Correlation matrix of quantitative parameters with clinical data per study group



Correlation matrix of the MRI metrics Δ FA, Δ MD, Δ AD, Δ RD, Δ T2 and Δ FF with the clinical covariates age, disease duration and time since last treatment, showed for patients with CIDP (left) and patients with MMN (right). Patients with CIDP had a moderate inverse correlation between Δ FA and disease duration ($r = -0.50, p = 0.02$). Abbreviations: FA = fractional anisotropy; MD = mean diffusivity; AD = axial diffusivity; RD = radial diffusivity; T2 = T2 relaxation time; FF = fat fraction.



Table 7.4 Outcomes of correlation analysis between quantitative MRI parameters and clinical data

Clinical parameter		CIDP (n = 23)					
		ΔFA	ΔMD	ΔAD	ΔRD	$\Delta T2 (ms)$	$\Delta FF (%)$
Categorical variables							
Sex (male/female)							
	Mean D	0.01	0.00	0.04	-0.01	0.04	1.42
	<i>p</i>	0.53	0.98	0.67	0.91	0.99	0.64
Receiving maintenance treatment (no/yes)							
	Mean D	-0.01	0.06	0.08	0.05	0.94	-0.96
	<i>p</i>	0.52	0.16	0.20	0.17	0.56	0.66
Treatment response (poor/good)							
	Mean D	-0.01	0.06	0.07	0.05	2.16	-3.27
	<i>p</i>	0.48	0.24	0.31	0.22	0.21	0.15
Continuous variables							
Age							
	<i>r</i>	-0.25	0.19	0.10	0.24	-0.11	-0.14
	<i>p</i>	0.26	0.39	0.66	0.26	0.64	0.56
Disease duration							
	<i>r</i>	-0.50	-0.21	-0.33	-0.09	0.04	-0.41
	<i>p</i>	0.02*	0.34	0.12	0.67	0.87	0.07
Time since last treatment							
	<i>r</i>	-0.04	0.23	0.21	0.22	-0.37	-0.09
	<i>p</i>	0.85	0.30	0.33	0.31	0.10	0.69

Different clinical parameters are compared within patients with CIDP and MMN. For each quantitative MRI parameter mean differences and *p* values are calculated per categorical variable, and Pearson's correlation coefficient (*r*) with accompanying *p* values are calculated per continuous variable. All patients with MMN received maintenance treatment and had a good treatment response so these variables could not be compared within patients (cells with minus sign).

MMN (n = 7)

ΔFA	ΔMD	ΔAD	ΔRD	$\Delta T2$ (ms)	ΔFF (%)
0.06	-0.08	-0.04	-0.10	-5.49	0.53
0.22	0.53	0.74	0.46	0.44	0.94
-	-	-	-	-	-
-	-	-	-	-	-
-	-	-	-	-	-
-	-	-	-	-	-
-0.30	0.34	0.37	0.32	0.42	0.37
0.51	0.45	0.42	0.49	0.35	0.41
0.05	0.21	0.32	0.16	0.27	0.68
0.91	0.65	0.48	0.74	0.56	0.09
-0.03	0.03	0.04	0.06	-0.06	0.22
0.96	0.95	0.93	0.90	0.90	0.64

None of the quantitative parameters had a significant correlation with the clinical data, except for ΔFA and disease duration in patients with CIDP. Abbreviations: CIDP = chronic inflammatory demyelinating polyneuropathy; MMN = multifocal motor neuropathy; FA = fractional anisotropy; MD = mean diffusivity; AD = axial diffusivity; RD = radial diffusivity; T2 = T2 relaxation time; ms = milliseconds; FF = fat fraction; Mean D = mean difference; $p = p$ value; $r =$ Pearson's correlation coefficient; * = correlation is significant. MD, AD and RD values are $\times 10^{-3}$ mm²/s.



Correlation with clinical data

We found a moderate inverse correlation between the difference in FA between baseline and one-year follow-up (Δ FA) and disease duration in patients with CIDP ($r = -0.50, p = 0.02$; **Figure 7.3**). Correlations between the other quantitative parameters and continuous clinical variables (age, disease duration or time since last treatment) were poor and/or not significant. Sex, maintenance treatment and treatment response did not correlate with quantitative MRI parameters in patients with CIDP (**Table 7.4**). We did not find any significant correlations between the quantitative MRI parameters and the continuous clinical variables in patients with MMN (**Table 7.4**). Sex did not influence the differences in quantitative parameters over time.

DISCUSSION

This study shows that MD, AD, RD and fat fraction change over time in patients with CIDP, but not with MMN. We did not establish relevant correlations between the changes in quantitative MRI parameters and clinical data. Quantitative MRI techniques evaluated in this study, i.e. DTI, T2 mapping and fat fraction analysis, are therefore unsuited as biomarkers to predict prognosis or to monitor treatment response.

DTI is a promising imaging technique for central and possibly peripheral neurological disorders. Previous longitudinal studies in patients with primary brain tumors and neurodegenerative disorders suggested a potential of quantitative MRI parameters as biomarkers^{13–18}. Experimental models of sciatic nerve injury in rats ($n = 62$) suggested that differences in FA correlated with nerve regeneration²⁹. Particularly relevant for our study is one cross-sectional DTI study in patients with CIDP ($n = 14$) that showed a correlation between FA in the sciatic and tibial nerves and severity of the neuropathy evaluated with the Neuropathy Impairment Score (NIS)³⁰. The NIS is a composite score of weakness of the muscles innervated by the cranial nerves and proximal and distal muscles of the arms and legs, presence or absence of tendon reflexes and sensory function³¹. We did not use NIS in our patients, since it is probably less informative for disease status in MMN. However, we did not find an association with quantitative MRI of the brachial plexus and weakness (MRC sum scores) of the arms and legs or any other clinical data.

We previously found differences in quantitative MRI parameters between CIDP and MMN²⁵. This suggests important differences in (the dynamics of) microstructural integrity of nervous tissue between these disorders. The quantitative MRI parameters changed longitudinally in CIDP, but not in MMN. It is not likely that these changes in CIDP can be attributed to treatment. First, all quantitative MRI parameters did shift towards values found in healthy controls, except for AD. Second, we did not find a correlation between quantitative MRI data and treatment response. The differences in longitudinal data between patients with CIDP and MMN are therefore more likely to

reflect other processes, for example differences in nerve changes that are part of the natural history of CIDP. Explorative studies of other techniques for biomarker potential, such as nerve conduction and nerve ultrasound, also failed to show changes after the start of immunomodulatory treatment^{4,6,8}. This may suggest that effective treatment induces changes in nerves at other levels than those captured by imaging or conduction.

Quantitative MRI correlates with histological findings⁹⁻¹¹. RD indicates hindrance of diffusion for water perpendicular to the nervous tissue. An increased RD indicates an increased possibility of water diffusion and can be the result of demyelination or disturbance of the cytoskeleton⁹⁻¹¹. The observed RD decreases could thus reflect remyelination following demyelination in CIDP that has been described in histological studies³²⁻³⁴. AD reflects the degree of diffusion along the axon and further decreases may correlate with swelling due to the breakdown or change in the permeability of the axolemma and axonal loss. The ongoing decrease of AD in CIDP might indicate progression of axonal loss. Fat fraction is an indicator for the presence of free water in (nervous) tissue and a decrease of fat fraction probably reflects active inflammation. The increase of fat fraction over time could be the result of remyelination or attenuation of inflammation.

This study obviously has limitations. Although the sample size is bigger than in previous studies, it remains small, in particular for MMN. More inclusions would obviously have led to a more powered study. Patient characteristics nevertheless showed that the group of patients with MMN was clinically homogeneous and the sample size is in line with the exploratory character of this study. More information could have been obtained with a longer follow-up time, but treatment effects already occur in the course of weeks. We only evaluated the brachial plexus, but this is a site where abnormalities are often found, as shown by previous nerve ultrasound and qualitative MRI studies^{35,36}.

Based on this first longitudinal study on the prognostic value of quantitative MRI parameters in CIDP and MMN, we conclude that DTI, T2 mapping and fat fraction capture changes in the course of CIDP, but that their value as a prognostic instrument is probably low.

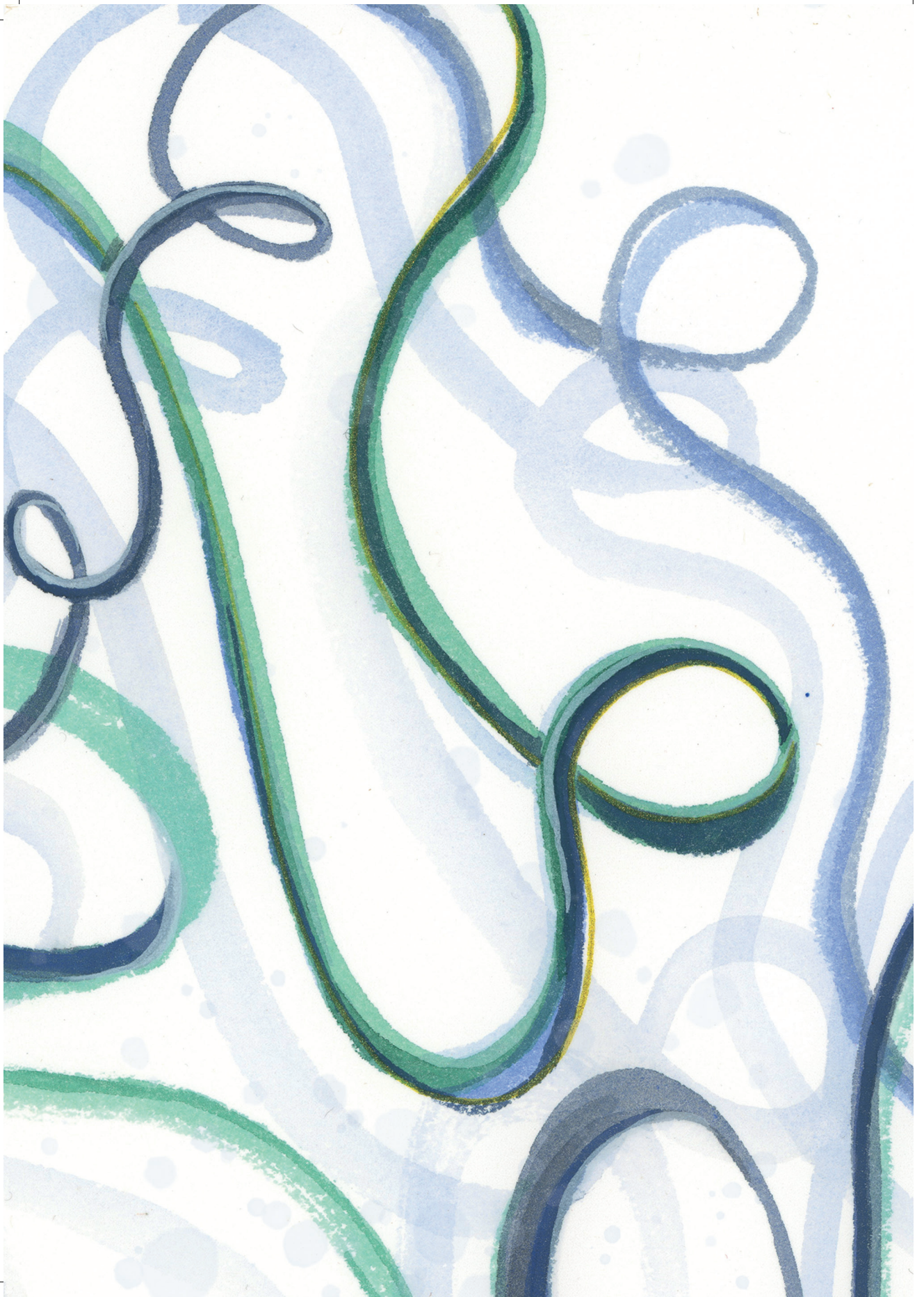


REFERENCES

1. Oaklander A, Lunn M, Hughes R, et al. Treatments for chronic inflammatory demyelinating polyradiculoneuropathy (CIDP): An overview of systematic reviews. *Cochrane Database Syst. Rev.* 2017;13:1–33.
2. van Schaik I, van den Berg L, de Haan R, Vermeulen M. Intravenous immunoglobulin for multifocal motor neuropathy. *Cochrane Database Syst. Rev.* 2005;2:920–921.
3. Herraets I, van Rosmalen MH, Bos J, et al. Clinical outcomes in multifocal motor neuropathy: A combined cross-sectional and follow-up study. *Neurology* 2020;95:e1979–e1987.
4. Van Asseldonk JTH, Van den Berg LH, Van den Berg-Vos RM, et al. Demyelination and axonal loss in multifocal motor neuropathy: Distribution and relation to weakness. *Brain* 2003;126:186–198.
5. Vucic S, Black K, Baldassari LE, et al. Long-term effects of intravenous immunoglobulin in CIDP. *Clin. Neurophysiol.* 2007;118:1980–1984.
6. Iijima M, Yamamoto M, Hirayama M, et al. Clinical and electrophysiologic correlates of IVIg responsiveness in CIDP. *Neurology* 2005;64:1471–1475.
7. Zaidman CM, Pestronk A. Nerve Size in CIDP Varies with Disease Activity and Therapy Response Over Time: A Retrospective Ultrasound Study. *Muscle Nerve* 2014;50:733–738.
8. Telleman J, Herraets I, Goedee H, et al. Prognostic value of nerve ultrasound: a prospective multicenter study on the natural history of polyneuropathy. *Eur. J. Neurol.* 2021;28:2327–2338.
9. Song SK, Sun SW, Ramsbottom MJ, et al. Dysmyelination revealed through MRI as increased radial (but unchanged axial) diffusion of water. *Neuroimage* 2002;17:1429–1436.
10. Song SK, Sun SW, Ju WK, et al. Diffusion tensor imaging detects and differentiates axon and myelin degeneration in mouse optic nerve after retinal ischemia. *Neuroimage* 2003;20:1714–1722.
11. Morisaki S, Kawai Y, Umeda M, et al. In vivo assessment of peripheral nerve regeneration by diffusion tensor imaging. *J. Magn. Reson. Imaging* 2011;33:535–542.
12. Jeon T, Fung MM, Koch KM, et al. Peripheral nerve diffusion tensor imaging: Overview, pitfalls, and future directions. *J. Magn. Reson. Imaging* 2018;47:1171–1189.
13. Nowranghi M, Lyketsos C, Leoutsakos J-M, et al. Longitudinal, region-specific course of diffusion tensor imaging measures in mild cognitive impairment and Alzheimer’s disease. *Bone* 2013;9:519–528.
14. Kitamura S, Kiuchi K, Taoka T, et al. Longitudinal white matter changes in Alzheimer’s disease: A tractography-based analysis study. *Brain Res.* 2013;1515:12–18.
15. Genc S, Steward CE, Malpas CB, et al. Short-term white matter alterations in Alzheimer’s disease characterized by diffusion tensor imaging. *J. Magn. Reson. Imaging* 2016;43:627–634.
16. Mayo CD, Mazerolle EL, Ritchie L, et al. Longitudinal changes in microstructural white matter metrics in Alzheimer’s disease. *NeuroImage Clin.* 2017;13:330–338.
17. Sampedro F, Martínez-Horta S, Marín-Lahoz J, et al. Longitudinal intracortical diffusivity changes in de-novo Parkinson’s disease: A promising imaging biomarker. *Park. Relat. Disord.* 2019;68:22–25.
18. Tringale K, Nguyen T, Bahrami N, et al. Identifying early diffusion imaging biomarkers of regional white matter injury as indicators of executive function decline following brain radiotherapy: A prospective clinical trial in primary brain tumor patients. *Radiother Oncol* 2019;132:27–33.
19. van der Burgh HK, Westeneng HJ, Walhout R, et al. Multimodal longitudinal study of structural

- brain involvement in amyotrophic lateral sclerosis. *Neurology* 2020;94:e2592–e2604.
20. Oudemans J, Eftimov F, Strijkers GJ, et al. Diagnostic accuracy of MRI and ultrasound in chronic immune-mediated neuropathies. *Neurology* 2020;94:e62–e74.
 21. Haakma W, Jongbloed BA, Froeling M, et al. MRI shows thickening and altered diffusion in the median and ulnar nerves in multifocal motor neuropathy. *Eur. Radiol.* 2017;27:2216–2224.
 22. Hiwatashi A, Togao O, Yamashita K, et al. Lumbar plexus in patients with chronic inflammatory demyelinating polyradiculoneuropathy: evaluation with simultaneous T2 mapping and neurography method with SHINKEI. *Br. J. Radiol.* 2018;91:20180501.
 23. Hiwatashi A, Togao O, Yamashita K, et al. Simultaneous MR neurography and apparent T2 mapping in brachial plexus: Evaluation of patients with chronic inflammatory demyelinating polyradiculoneuropathy. *Magn. Reson. Imaging* 2018;55:112–117.
 24. Felisaz PF, Poli A, Vitale R, et al. MR microneurography and quantitative T2 and DP measurements of the distal tibial nerve in CIDP. *J. Neurol. Sci.* 2019;400:15–20.
 25. van Rosmalen M, Goedee H, Derks R, et al. Quantitative MRI of the brachial plexus shows specific changes in nerve architecture in chronic inflammatory demyelinating polyneuropathy, multifocal motor neuropathy and motor neuron disease. *Eur. J. Neurol.* 2021;28:2716–2726.
 26. van den Bergh PYK, Hadden RDM, Bouche P, et al. European Federation of Neurological Societies/Peripheral Nerve Society Guideline on management of chronic inflammatory demyelinating polyradiculoneuropathy: Report of a joint task force of the European Federation of Neurological Societies and the Peripher. *Eur. J. Neurol.* 2010;17:356–363.
 27. Van Schaik IN, Léger JM, Nobile-Orazio E, et al. European Federation of Neurological Societies/Peripheral Nerve Society Guideline on management of multifocal motor neuropathy. Report of a Joint Task Force of the European Federation of Neurological Societies and the Peripheral Nerve Society - First revis. *J Peripher Nerv Syst* 2010;15:295–301.
 28. Taylor R. Interpretation of the Correlation Coefficient: a Basic Review. *J. Diagnostic Med. Sonogr.* 1990;1:35–39.
 29. Farinas AF, Esteve IVM, Pollins AC, et al. Diffusion Magnetic Resonance Imaging Predicts Peripheral Nerve Recovery in a Rat Sciatic Nerve Injury Model. *Plast. Reconstr. Surg.* 2020;145:949–956.
 30. Markvardsen LH, Vaeggemose M, Ringgaard S, Andersen H. Diffusion tensor imaging can be used to detect lesions in peripheral nerves in patients with chronic inflammatory demyelinating polyneuropathy treated with subcutaneous immunoglobulin. *Neuroradiology* 2016;58:745–752.
 31. Dyck PJ, Boes CJ, Mulder D, et al. History of standard scoring, notation, and summation of neuromuscular signs. A current survey and recommendation. *J. Peripher. Nerv. Syst.* 2005;10:158–173.
 32. Auer RN, Bell RB, Lee MA. Neuropathy with Onion Bulb Formations and Pure Motor Manifestations. *Can. J. Neurol. Sci. / J. Can. des Sci. Neurol.* 1989;16:194–197.
 33. Matsuda M, Ikeda SI, Sakurai S, et al. Hypertrophic neuritis due to chronic inflammatory demyelinating polyradiculoneuropathy (CIDP): A postmortem pathological study. *Muscle and Nerve* 1996;19:163–169.
 34. Sasaki M, Ohara S, Oide T, et al. An autopsy case of chronic inflammatory demyelinating polyradiculoneuropathy with respiratory failure. *Muscle and Nerve* 2004;30:382–387.
 35. Goedee HS, Van Der Pol WL, Van Asseldonk JTH, et al. Diagnostic value of sonography in treatment-naive chronic inflammatory neuropathies. *Neurology* 2017;88:143–151.
 36. van Rosmalen MHJ, Goedee HS, van der Gijp A, et al. Quantitative assessment of brachial plexus MRI for the diagnosis of chronic inflammatory neuropathies. *J. Neurol.* 2020;268:978–988.





Chapter 8

General discussion



GENERAL DISCUSSION

This thesis focuses on the different clinical and imaging characteristics of chronic inflammatory neuropathies. Diagnostic, pathophysiological and prognostic characteristics are evaluated by clinical and magnetic resonance imaging (MRI) studies in chronic inflammatory demyelinating polyneuropathy (CIDP) and multifocal motor neuropathy (MMN). This chapter discusses the main findings of this thesis, puts these findings into perspective of the current literature and provides recommendations for clinical practice.

Disease hetero- and homogeneity

Clinical presentation, treatment options and prognosis differ between patients with CIDP and MMN. CIDP has a very heterogeneous presentation. Typical CIDP (approximately 50-70% of patients with CIDP) is characterized by slowly progressive symmetric proximal and distal weakness and sensory deficits with absent reflexes in the extremities.^{1,2} Symptoms are present in all extremities, but are most pronounced in the legs.² Variants of CIDP include focal CIDP (< 5% of patients with CIDP), distal CIDP (7-15%), multifocal CIDP (also known as Lewis-Sumner syndrome, MADSAM or MIDN, 4-15%), motor CIDP (4-9%) and sensory CIDP (4-35%).³⁻⁵ Diagnosis of CIDP can be challenging as its atypical variants may be difficult to recognize. This might result in underdiagnosis which is undesirable as CIDP responds to treatment with immunoglobulins, corticosteroids or plasmapheresis.⁶ Early treatment can improve muscle strength or sensory symptoms, and prevents progression of symptoms and permanent axonal damage. Immunoglobulins are probably the most effective treatment option (76-82% responsiveness), followed by corticosteroids (59-70% responsiveness) and plasmapheresis (58-67% responsiveness).^{7,8} Patients with CIDP can improve using a second treatment option if the first treatment was ineffective, as shown by a multi-center study in treatment-naïve patients with CIDP.⁸ Prognosis of CIDP is as heterogeneous as its clinical presentation. Previous longitudinal studies on disease course of CIDP report that approximately 25% of patients with CIDP experience remission after treatment that allows discontinuation of treatment.⁷ Partial remission occurs in 60% of patients: in half of these patients treatment can be discontinued, the other half requires maintenance treatment.⁷ In approximately 10% of patients symptoms remain severe after five years of treatment.^{7,9} Predictors for complete remission are a subacute onset, symmetry of symptoms and absence of muscle atrophy. Nerve conduction abnormalities in the distal segments are predictors for complete remission or good response to initial therapy.⁷

MMN has a more homogeneous presentation than CIDP. MMN is usually characterized by slowly progressive, asymmetric weakness without sensory deficits that dominates in the arm but weakness may also be present in the distal leg.¹⁰ Important clinical mimics of MMN are motor neuron disease (MND), such as amyotrophic lateral sclerosis (ALS) or progressive muscular atrophy (PMA), and segmental spinal muscular atrophy. MMN mimics the early stages of these disorders, in particular MND, and differentiation can be challenging. However, differentiation is important as the prognosis



and treatment options of MMN and MND differ considerably. Patients with MMN have a normal life expectancy while median survival time in patients with MND, in particular ALS, is 3-5 years.¹¹ Furthermore, MMN responds to treatment with immunoglobulins while there are no symptomatic or curative treatment options for MND.¹² It is important to note that treatment options between MMN and CIDP differ. MMN does not respond to treatment with corticosteroids or plasmapheresis and symptoms may even deteriorate following the start of corticosteroids. Differentiation between MMN and (the atypical variants of) CIDP is therefore also important.

An early start of treatment with immunoglobulins in MMN slows progression of symptoms although treatment cannot always prevent the development of permanent axonal damage.^{12,13} Unlike CIDP, a lot is unknown on the other factors that influence disease progression and prognosis in MMN. Therefore, we performed a combined cross-sectional and longitudinal study in **chapter 2** to explore the natural history of patients with MMN and to define predictive factors for disease progression and prognosis. This study confirms that, in the large majority of patients, MMN is a progressive disorder, despite the fact that 87% of the patients were treated with immunoglobulins. This finding corroborates with findings in earlier smaller studies on natural history in patients with MMN (n = 11 – 46).¹³⁻¹⁵ We found that predictors of a progressive disease course (i.e. a larger decrease of the Medical Research Council (MRC) sum score over time) were (1) the absence of at least one reflex at baseline and (2) more weakness (i.e. a lower MRC sum score) at baseline. We also found that more severe weakness was influenced by a longer disease duration before treatment and the presence of serum anti-GM1 antibodies, which is similar to findings of previous studies.¹⁶⁻¹⁸ These findings indicate that it is crucial to reduce the time to diagnosis and start treatment as early as possible in order to prevent more severe weakness and disease progression. Improvement of the diagnostic value of the currently available diagnostic tools, such as MRI, could help to reduce the time to diagnosis.

Diagnosis

The next part of this thesis focuses on diagnosis of CIDP and MMN. Several sets of different diagnostic consensus criteria have been developed for CIDP and MMN, which underlines the difficulty of diagnosing these chronic inflammatory neuropathies. The diagnostic criteria for CIDP and MMN consist of a combination of a characteristic clinical presentation and specific features on nerve conduction studies (NCS).

The criteria of the European Federation of Neurological Societies/Peripheral Nerve Society (EFNS/PNS) seem to be the most accurate and widely used set of criteria for CIDP.¹⁹ This was established by a study that compared 15 diagnostic criteria sets for CIDP. They found that the criteria of the EFNS/PNS had the highest sensitivity (73%) and specificity (91%).²⁰ Another study exclusively focused on comparison of three sets of electrodiagnostic criteria for CIDP and also found highest sensitivity (81%) and specificity (79-96%) for the EFNS/PNS criteria.²¹ Therefore, we based our evaluation

and recommendations in this chapter on these criteria for CIDP. For MMN, such comparative studies of sets of diagnostic criteria do not exist and we will use the Utrecht criteria for further evaluation as these criteria also predict treatment response to immunoglobulins.^{10,22–24}

The challenge of diagnosing CIDP or MMN relies mainly on the fact that the diagnostic tools used in both sets of criteria have their limitations in current clinical practice. In both sets of criteria abnormalities on NCS are the key feature of diagnosis of CIDP and MMN. However, NCS does not always show the required specific electrophysiological features. Signs of demyelination could be easily missed as the NCS protocols are extensive and require specific expertise. If NCS does not fulfill the electrodiagnostic criteria, diagnosis remains uncertain. This led in the nineties to the search for additional tools that support diagnosis of CIDP or MMN. Early studies on magnetic resonance imaging (MRI) of the cauda equina and the nerve roots of the lumbosacral and brachial plexus showed thickening, a hyperintense signal on T2-weighted imaging and enhancement of the nerve roots after infusion with gadolinium.^{25–29} This led to the inclusion MRI as a supportive criterion in current guidelines for diagnosis of CIDP and MMN. Unfortunately, the diagnostic value of MRI has not been studied in detail previously. MRI is qualitatively assessed by (neuro)radiologists which is potentially a major limitation in current clinical practice. **Table 8.1** summarizes the diagnostic criteria for CIDP and MMN and their limitations.

Qualitative assessments of brachial (or lumbosacral) plexus MRI are subjective and large systemic studies that report objective cut-off values of nerve size are lacking. This may lead to large interrater variations as the reliability of the current assessment method has not been systematically studied. In **chapter 3** we therefore performed a study that evaluated interrater reliability of the current qualitative assessment approach of brachial plexus MRI. We found that raters agreed in only 52% of all brachial plexus images, with a Cohen's kappa indicating minimal agreement and a poor reliability (0.30, 95% confidence interval 0.14–0.46). Difficulties in assessing the brachial plexus were mostly related to distinguishing more subtle cases of nerve thickening. One other study evaluated qualitative assessment of brachial plexus MRI in a small cohort of patients with CIDP ($n = 13$) and MMN ($n = 10$) using a 4-point scale for nerve thickening.³⁰ They also found a poor interrater reliability evaluated with the interclass correlation coefficient ($ICC = 0.47$), which corroborates our findings. A qualitative assessment as currently used in clinical practice is, based on these results, not very helpful. Another approach is needed if we want to improve reproducibility and reliability of assessment. Quantification of nerve thickness represents an obvious strategy as earlier nerve ultrasound studies showed excellent test characteristics for the detection of CIDP and MMN.^{31,32} In **chapter 4** we therefore developed a quantitative measurement method for MRI and calculated its diagnostic value. We measured nerve root sizes at standardized measurement sites (i.e. next to the ganglion and 1 cm distal from this point) in nerve root C5–C7. We found an acceptable reliability (intrarater $ICC = 0.55–0.87$; interrater $ICC = 0.65–0.90$) and diagnostic value (area under the curve $0.78–0.81$). Three other studies explored the feasibility of a quantitative assessment of MRI in patients with CIDP (but



not MMN).³³⁻³⁵ Two of these studies measured nerve root sizes *in* the ganglion in patients with CIDP (n = 14 in both studies) and healthy controls (n = 10 and n = 9 respectively).^{33,34} They obtained a cut-off value of 5.0 mm for nerve root C6-C8 and 6.5 mm for C5-T1 respectively. The ganglion often appears larger on MRI and measurements *in* the ganglion may therefore overestimate nerve root thickness. The latter study also measured nerve thickness at random, not predefined, sites distal from the ganglion (C5-T1), and reported a cut-off value of 4.0 mm with an area under the curve of 0.76.³⁴ We found a comparable area under the curve for measurements of nerve root size, although comparison is difficult as measurement sites were not standardized in the latter study.³⁴ Interrater reliability was higher (0.95) compared to our study but method and analysis of interrater reliability are not well-explained in the paper. For example, it is unknown if raters scored the scans at the same time or with a time interval and whether exact measurement sites were known prior to assessment. Also, details are missing on reliability per nerve root, as they calculated reliability for all nerve roots together which further complicates comparison with our data. The third study measured nerve root diameter in the ganglion and did not find any differences between patients with CIDP (n = 15) and disease controls, most of them with cervical spondylosis (n = 19).³⁵ A major limitation in all three studies is sample size which hampers interpretation and translation of the results in clinical practice. Also, the control groups are less relevant for clinical practice in all three studies.

Our study in **chapter 4** included a relatively large sample of patients with CIDP and MND (n = 81). We included disease controls (i.e. patients with a clinical phenotype that mimics CIDP or MMN) instead of healthy controls as we tried to represent clinical practice as much as possible. This resulted in the inclusion of a homogeneous group of patients with MND with a lower motor neuron syndrome at onset of symptoms. As earlier described, differentiation with this patient group is of great importance as patients with MND have a much less favorable prognosis and have no symptomatic or curative options for treatment compared to patients with CIDP and MMN.³⁶ Patients with MND mimic patients with MMN, but also 11% of patients with a clinical suspicion of CIDP are initially diagnosed with MND.³⁷ The majority of patients with CIDP present with slowly progressive motor deficits (approximately 90%).⁹ The homogeneity of our control group facilitates the translation to clinical practice, especially to neuromuscular centers that focus on diagnosis of MND. Inclusion of a more varied control group, e.g. inclusion of patients with axonal neuropathies, hereditary demyelinating polyneuropathies and paraproteinemic polyneuropathies may further improve the representativity of our results. However, the hereditary demyelinating polyneuropathies and paraproteinemic polyneuropathies are a heterogeneous group of neuropathies and could also be differentiated from CIDP and MMN through their characteristic clinical phenotypes and laboratory findings. MRI is normally not needed as part of the diagnostic work-up of these neuropathies. The prevalence of hereditary demyelinating polyneuropathies is approximately 16-30/100.000 citizens and diagnosis is based on characteristic clinical features as pes cavus and a symmetric distal motor neuropathy with pronounced atrophy of lower leg muscles, combined with a positive family history or confirmative genetic defect.³⁸⁻⁴¹ Diagnosis of paraproteinemic polyneuropathies relies on the

identification of the monoclonal gammopathy, and presence of a possible underlying hematologic disorder (e.g. antibodies to myelin associated glycoprotein, Waldenström's macroglobulinemia or amyloidosis).⁴² These clinical and laboratory features will often guide a clinician to the right diagnosis without the use of nerve imaging techniques. Optimization of MRI for these neuropathies may therefore be less relevant for clinical practice. Patients with axonal neuropathies normally do not have thickened nerve roots on nerve ultrasound or MRI.^{31,32} The results of our study may therefore be representative to the group of axonal neuropathies as well.

Another important result of our study is that combinations of measurements of nerve root size are probably more useful than a fixed cut-off. The inflammatory changes in the cervical nerve roots are not always homogeneous, but often have a patchy distribution. Variable cut-off values are therefore preferred over fixed cut-off values. We further found that 6 bilateral measurements close to the ganglion of root C5, C6 and C7 in coronal plane were easy to implement in routine practice (3 minutes per subject) and resulted in optimal test characteristics with high specificity levels (95%). We implemented these results in a practical risk chart that predicts the chance of having an inflammatory neuropathy (**Figure 4.3**). Sensitivity levels of quantitative assessment of brachial plexus MRI were lower (approximately 27%) than those reported in qualitative studies (approximately 51%).^{34,35} This may be explained by a degree of inclusion bias in earlier studies, as shown by another recent prospective cohort study that reported a relatively low sensitivity (36%) of qualitative brachial and lumbosacral plexus MRI in patients with suspected CIDP.⁴³ Validation of our results in a future prospective study would further establish that a quantitative assessment is preferred over a qualitative assessment of brachial plexus MRI.

Our study in **chapter 4** primary focused on thickness and did not evaluate T2 signal of the nerve roots. As earlier described, an increase of signal intensity of nerve roots on T2-weighted imaging is, combined with nerve root thickening, one of the abnormalities that can be found on (brachial) plexus MRI in CIDP and MMN.^{25,44} Tissues appear bright on T2-weighted images when they have a long T2 relaxation time and therefore retain more signal, e.g. water. Hyperintense nerve roots indicate that there is an increase of the amount of water, for example due to oedema caused by an inflammatory reaction. Previous qualitative MRI studies of the brachial plexus reported that these T2 hyperintensities occur in 58-74% of patients with CIDP and 33-43% of patients with MMN.^{30,45} Although T2 hyperintensity also occurs without the presence of nerve root thickening, most patients (70% of the patients with CIDP and 82% of the patients with MMN) have T2 hyperintensities accompanied by thickening of the cervical nerve roots.⁴⁵



Table 8.1 Diagnostic criteria for CIDP and MMN with their limitations

	CIDP
Clinical criteria	<p><u>Typical</u></p> <p>1. Chronic (> 2 months), progressive, symmetric, proximal and distal weakness and sensory dysfunction of all extremities</p> <p>2. Absent or reduced tendon reflexes in all extremities</p> <p><u>Variants</u></p> <p>1. Predominantly focal, distal, multifocal, pure motor or pure sensory neuropathy</p> <p>2. Tendon reflexes may be normal in the unaffected limb</p>
Electrodiagnostic criteria	<p><u>Definite</u> (at least one of the following): (a) motor distal latency prolongation \geq 50% above ULN in 2 nerves; (b) reduction of motor conduction velocity \geq 30% below LLN; (c) prolongation of F-wave latency \geq 30% above ULN in 2 nerves; (d) absence of F-waves in 2 nerves + \geq 1 other demyelinating parameter; (e) partial motor conduction block, i.e. \geq 50% amplitude reduction of the CMAP; (f) abnormal temporal dispersion in \geq 2 nerves; (g) distal CMAP duration increase in \geq 1 nerve + \geq 1 other demyelinating parameter in \geq 1 other nerve.</p> <p><u>Probable</u>: \geq 30% amplitude reduction of the CMAP in 2 nerves, or in 1 nerve + \geq 1 other demyelinating parameter in \geq 1 other nerve</p> <p><u>Possible</u>: as in 'definite' but in only one nerve</p>
Supportive criteria	
<i>Laboratory findings</i>	Elevated CSF protein (CIDP); CSF protein < 1 g/L and elevated anti-GM1 antibodies (MMN)
<i>Treatment response</i>	Objective clinical improvement following immunomodulatory treatment
<i>MRI</i>	Nerve root thickening, increased signal intensity on T2-weighted images and/or enhancement with gadolinium of the cauda equina, lumbosacral or brachial plexus
<i>NCS</i>	Abnormal sensory electrophysiology in \geq 1 nerve (CIDP only)
<i>Nerve biopsy</i>	Evidence of demyelination and/or remyelination (CIDP only)
Diagnostic categories	
<i>Definite</i>	Typical or atypical clinical presentation (1 and 2) + definite NCS; or probable CIDP + \geq 1 supportive criterion; or possible CIDP + \geq 2 supportive criteria
<i>Probable</i>	Typical or atypical clinical presentation (1 and 2) + probable NCS; or possible CIDP + \geq 1 supportive criterion
<i>Possible</i>	Typical or atypical clinical presentation (1 and 2) + possible NCS

Summary of the EFNS/PNS diagnostic criteria for CIDP¹⁹ and the Utrecht criteria for MMN²⁴ with current limitations. Abbreviations: CIDP = chronic inflammatory demyelinating polyneuropathy; MMN = multifocal motor neuropathy; ULN = upper limit of normal values; LLN = lower limit of normal values; CMAP = compound muscle action potential; CSF = cerebrospinal fluid.

MMN	Limitations
<p>Slowly progressive, asymmetric, predominantly distal weakness without sensory dysfunction. Decreased or absent tendon reflexes in affected limb; predominant upper limb involvement; age of onset 20-65 years; no bulbar signs, upper motor neuron features, other neuropathies or myopathies.</p>	<p>Atypical variants of CIDP may be difficult to recognize, differentiation of MMN and early stages of ALS may be difficult</p>
<p><u>Definite motor conduction block</u>: CMAP area reduction $\geq 50\%$ over a long segment, or a CMAP amplitude reduction of $\geq 30\%$ over a short distance.</p>	<p>Extensive protocol that is not always completely performed; protocol requires specific expertise (signs of demyelination could be easily missed); protocol costs a lot of time; NCS are often burdensome to patients</p>
<p><u>Probable motor conduction block</u>: CMAP amplitude reduction of $\geq 30\%$ over a long segment.</p>	
<p><u>Slowing of conduction compatible with demyelination</u>: motor conduction velocity $< 75\%$ of LLN; distal motor latency or shortest F-wave latency $> 130\%$ of ULN or absence of F-waves.</p>	
<p>Normal sensory conduction in arm segments with conduction block. Normal SNAP amplitudes.</p>	
	<p>Expensive, risk of adverse events, no clear definition (or biomarker) of treatment response Qualitative assessment without cut-off values for nerve size</p>
	<p>Invasive procedure, sample bias</p>
<p>Fulfills all clinical criteria + CSF protein < 1 g/L + definite NCS and normal sensory conduction Fulfills part of clinical criteria + CSF protein < 1 g/L + probable NCS and normal sensory conduction Fulfills part of clinical criteria + elevated anti GM1-bodies <i>or</i> abnormal MRI results <i>or</i> slowing of conduction and normal sensory conduction</p>	



T2 hyperintensity and thickening of nerve roots are both important key abnormalities on brachial plexus MRI. However, nerve thickening is easily quantitatively measured, while T2 hyperintensity is not. This is mainly explained by the challenges to develop and perform a method to quantify T2 hyperintensity. The intensity in a T2-weighted image, i.e. how white the signal appears, depends on several factors such as differences between sequence parameters and MRI machines. Already small variations in the MRI scan protocol may lead to large changes in T2 signal intensities. Therefore, measurements of signal intensity on qualitative MRI are difficult to reproduce and validate in other centers. Some studies did measure signal intensity by determining a nerve-to muscle contrast-to-noise ratio.³⁵ Although interrater reliability was acceptable in this study, reproducibility remains a problem due to technical limitations. A more reproducible method would be objective quantification of T2 relaxation times by T2 mapping. T2 mapping is an innovative quantitative MRI technique and produces objective measures for the T2 relaxation time in milliseconds of a structure of interest (**chapter 1**). The diagnostic value of T2 mapping has been widely studied in cardiac tissue but is unknown in the peripheral nerves.⁴⁶⁻⁴⁸ To obtain quantitative T2 measures of the peripheral nerves some post-processing steps are required which could be a possible limitation for implementation in clinical practice. This limitation will be discussed later in this chapter (see paragraph '*Implementation of quantitative MRI in clinical practice*').

MRI and nerve ultrasound

Nerve ultrasound is a relatively new tool in diagnosis of chronic inflammatory neuropathies and may show nerve thickening of the nerve roots of the brachial plexus and the peripheral nerves. Nerve ultrasound is a dynamic tool and has a (theoretically) large field-of-view so that the nerves in the arms and, to a lesser extent, legs are easily evaluated in one examination. Furthermore, nerve ultrasound is a relatively cheap diagnostic tool. Because of the characteristics and advantages of nerve ultrasound, recent studies favor a more prominent role for nerve ultrasound in the new diagnostic guidelines for CIDP and MMN.^{31,32,49} Nerve conduction studies (NCS) and nerve ultrasound seem to be compatible techniques as NCS has a high specificity (97%) and nerve ultrasound has a high sensitivity (94%).⁴⁹ Diagnostic strategies in which both techniques (i.e. NCS and nerve ultrasound) are combined are preferred over replacement of one technique by the other. In these diagnostic strategies nerve ultrasound could be used as a screening tool for CIDP or MMN and treatment could be started after a positive test result, which reduces the number of unnecessary NCS by 56%.⁴⁹ If nerve ultrasound does not show nerve (root) thickening, NCS should be performed. However, nerve ultrasound is not widely implemented in clinical practice, particularly not in non-academic centers, although exact numbers are lacking. Moreover, the use of nerve ultrasound requires a specific expertise that is not always available.

Nerve ultrasound and MRI differ in many ways. Nerve ultrasound is able to measure nerve root thickness of the brachial plexus and peripheral nerves in one examination, while MRI has a smaller field-of-view and, particularly due to time limitations, only one body structure can be imaged in one examination. MRI, on the other hand, can provide information on T2 signal intensity and enhancement

of nerve roots after infusion with gadolinium while ultrasound only informs on nerve thickness. MRI images tissues in three directions (coronal, sagittal and transversal), and these directions can even be combined in a 3D image, while ultrasound is a 2D imaging technique. MRI is more versatile than ultrasound and has a lot of modalities that are still un- or less-explored. These modalities might be of interest for use in scientific research or clinical practice in the future, for example to study other characteristics than thickening of damaged or injured nerves. Currently explored imaging techniques only show one-dimensional morphological changes (i.e. thickening of damaged or injured nerves and nerve roots) in CIDP and MMN. Other morphological changes still remain at the sub-imaging level.

Comparative studies between nerve ultrasound and MRI in patients with CIDP or MMN have been performed but are scarce. One study compared nerve (root) measurements using nerve ultrasound and MRI in patients with CIDP ($n = 18$) and measured cross-sectional areas of the median, ulnar and radial nerve, and the brachial plexus. They found a positive correlation between nerve ultrasound and MRI measurements in the peripheral nerves ($r = 0.72 - 0.74, p = 0.002 - 0.003$), but not in the brachial plexus.⁵⁰ Another study compared cross-sectional areas of the median and ulnar nerve on nerve ultrasound and MRI in patients with MMN ($n = 10$) and ALS ($n = 10$) and also found a positive correlation ($r = 0.60, p < 0.001$).⁵¹ This study also showed that both nerve ultrasound and MRI were able to differentiate MMN from ALS.

Nerve ultrasound has some advantages over MRI as it is a better tolerated, less-expensive and less time-consuming tool, especially when multiple limbs are imaged. MRI, on the other hand, is widely available. Based on the above mentioned studies ultrasound and qualitative MRI *of the peripheral nerves* have comparable characteristics. However, the added diagnostic value of measurements *of the brachial plexus* remains unknown as the CIDP study did not show a correlation between nerve ultrasound and MRI of the brachial plexus, and the MMN study did not image the brachial plexus, while MRI of the brachial plexus is part of the diagnostic criteria of both CIDP and MMN (**Table 8.1**).^{50,51} We therefore evaluated the added diagnostic value of MRI on nerve ultrasound in the last part of our study in **chapter 4**. We used the developed risk chart in **Figure 4.3** with its cut-off values to determine which patients had an abnormal MRI. We found that the majority of patients with abnormal ultrasound findings also had abnormal MRI findings, which corroborates with the comparative studies as earlier described in this paragraph.^{50,51} In some patients we found that nerve ultrasound showed thickening while MRI did not. This could be explained by the fact that also the peripheral nerves were imaged with nerve ultrasound while MRI only imaged the brachial plexus, i.e. that this was mainly due to the differences in field-of-view between nerve ultrasound and MRI. The added value of MRI was calculated in the subgroup of patients with CIDP and MMN that did not fulfill the electrodiagnostic criteria for CIDP or MMN and who had no abnormalities on nerve ultrasound. In patients with CIDP we found that 5/50 (10%) patients had an abnormal MRI result, while NCS did not fulfill the electrodiagnostic criteria for CIDP and nerve ultrasound did not show abnormalities. These 5 patients all responded to immunomodulatory treatment. Only one patient with MMN did

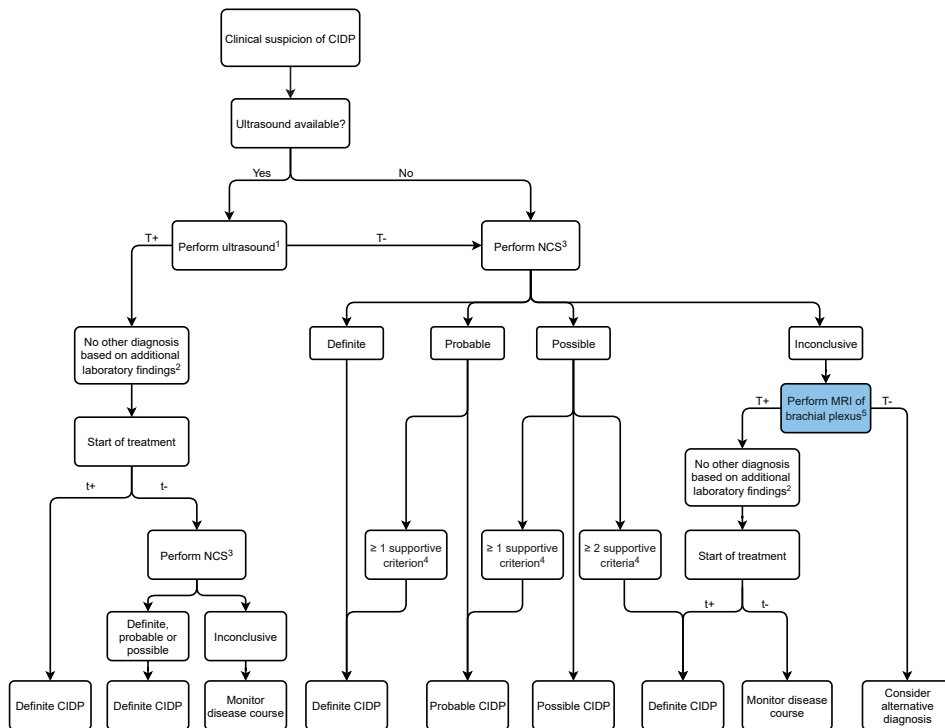


not fulfill the electrodiagnostic criteria for MMN. This patient did not have abnormalities on nerve ultrasound, neither on MRI. Diagnosis in this patient was based on clinical presentation combined with elevated liquor protein and treatment response. We concluded that MRI was of added diagnostic value even in the context of extensive NCS and nerve ultrasound in CIDP, but not in MMN.

Recommendations for clinical practice

All the above results combined, I would recommend to avoid a qualitative assessment of brachial plexus MRI. Quantitative assessment is reliable and relatively easy to implement in routine practice. Combinations of different measurements are preferred over fixed cut-off points in a quantitative assessment of brachial plexus MRI. Results of brachial plexus MRI could be interpreted using our risk chart (**chapter 4, Figure 4.3**). Secondly, MRI should only be performed when clinical suspicion remains high despite a normal nerve ultrasound or NCS that does not fulfill the electrodiagnostic criteria in patients with CIDP (but not MMN). If, based on our risk chart, MRI shows abnormalities compatible with CIDP, other possible diagnoses should be excluded with additional laboratory examination. Next, immunomodulatory treatment could be started as trial. It is important that symptoms and treatment response are monitored over time. This strategy prevents that treatment is withheld from patients and might help the clinician with further differentiation in diagnosis.

These recommendations for CIDP are summarized in a flow chart (**Figure 8.1**) that integrates the results of recent nerve ultrasound and MRI studies in the current EFNS/PNS criteria for CIDP.¹⁹ For MMN, MRI could still be a supportive criterion in the diagnostic criteria of MMN, especially when nerve ultrasound is not available (**Figure 8.2**). Finally, it is important to increase the availability of nerve ultrasound in (non-academic) medical centers. Based on previous studies, nerve ultrasound should be used as a screening tool before NCS is performed. Nerve ultrasound examination should consist of assessment of the median nerve in the forearms and upper arms and of C5 nerve root of the brachial plexus and should be considered abnormal when ≥ 1 measurement site is enlarged.^{31,32} When nerve ultrasound is not available in a medical center, I would recommend to perform NCS when a patient is clinically suspected of CIDP or MMN and follow the current diagnostic criteria, with the exception that MRI should always be quantitatively assessed.

Figure 8.1 Proposal of revision of diagnostic criteria for CIDP

This flow chart summarizes results from recent diagnostic nerve ultrasound and MRI studies on diagnosis of CIDP and integrates them in the current diagnostic criteria of the EFNS/PNS.¹⁹ In the blue rectangle the position of MRI of the brachial plexus based on our study in **chapter 4** of this thesis.

¹ Examination of the median nerve in the forearms (> 10 mm²), upper arms (> 13 mm²) and C5 nerve root (> 8 mm²). Abnormal when ≥ 1 measurement site is enlarged.

² Additional laboratory examination consists of determination of protein in cerebrospinal fluid and exclusion of other (metabolic) causes of neuropathy (e.g. diabetes, hypothyroidism, liver or renal insufficiency, vitamin deficiencies).

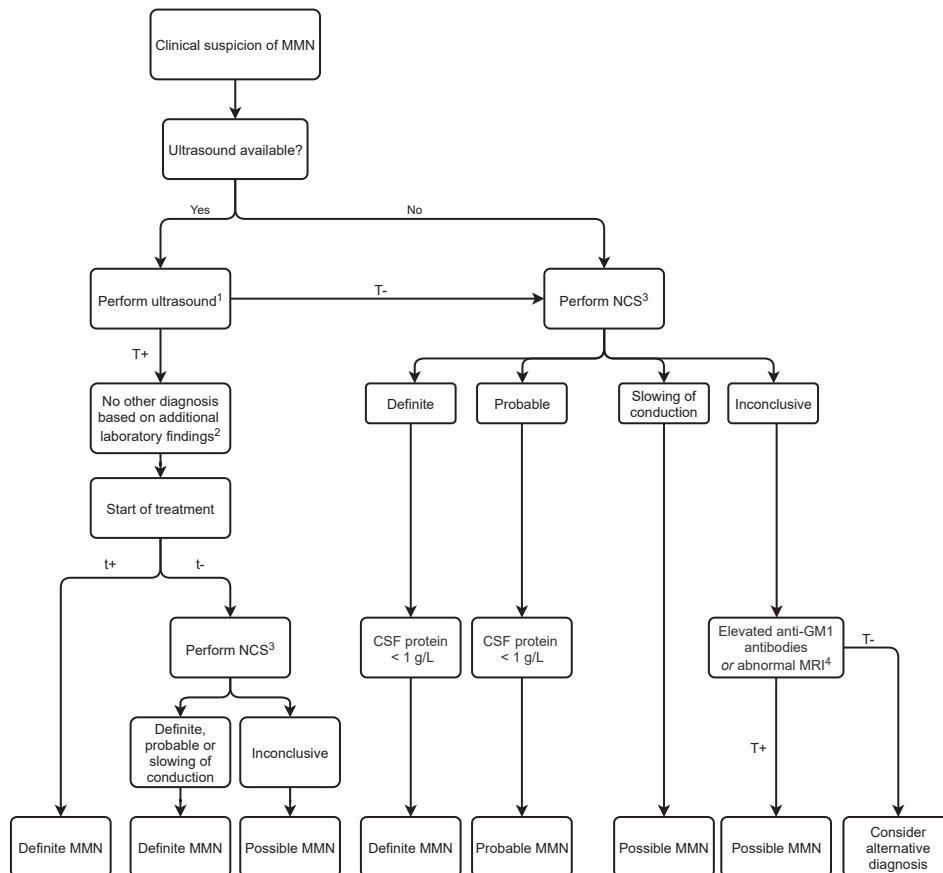
³ Results of NCS should be interpreted according to the electrodiagnostic criteria of the EFNS/PNS guideline.¹⁹

⁴ Supportive criteria of CIDP can be found in **Table 8.1**. MRI should be quantitatively assessed.

⁵ Results of MRI examination should be quantitatively assessed and interpreted using the risk chart in **chapter 4, Figure 4.3**.

Abbreviations: CIDP = chronic inflammatory demyelinating polyneuropathy; NCS = nerve conduction studies; MRI = magnetic resonance imaging; T+ = positive result of test; T- = negative result of test; t+ = good treatment response; t- = no treatment response.



Figure 8.2 Proposal of revision of diagnostic criteria for MMN

This flow chart summarizes results from recent diagnostic nerve ultrasound and MRI studies on diagnosis of MMN and integrates them in the current diagnostic Utrecht criteria.²⁴

¹ Examination of the median nerve in the forearms (> 10 mm²), upper arms (> 13 mm²) and C5 nerve root (> 8 mm²). Abnormal when ≥ 1 measurement site is enlarged.

² Additional laboratory examination consists of determination of protein in cerebrospinal fluid, serum anti-GM1 antibodies and exclusion of other (metabolic) causes of neuropathy (e.g. diabetes, hypothyroidism, liver or renal insufficiency, vitamin deficiencies).

³ Results of NCS should be interpreted according to the Utrecht electrodiagnostic criteria.²⁴

⁴ Supportive criteria of MMN can be found in **Table 8.1**. MRI should be quantitatively assessed.

⁵ Results of MRI examination should be quantitatively assessed and interpreted using the risk chart in **chapter 4, Figure 4.3**

Abbreviations: MMN = multifocal motor neuropathy; NCS = nerve conduction studies; CSF = cerebrospinal fluid; MRI = magnetic resonance imaging; T+ = positive result of test; T- = negative result of test; t+ = good treatment response; t- = no treatment response.

Pathophysiology

The second part of this thesis focuses on the feasibility of advanced qualitative and quantitative MRI to study pathophysiology of CIDP and MMN.

Qualitative MRI of the intraspinal roots

Until now, the majority of studies on nerve imaging in chronic inflammatory neuropathies focused on the peripheral nerves and the brachial or lumbosacral plexus.^{25,32,52} Previous studies showed thickening in both CIDP and MMN that suggest that (inflammatory) abnormalities are sometimes more widespread than results from NCS seem to indicate.^{10,19,25,26,32} Thickening of the peripheral nerves and brachial plexus did not correlate with phenotype or clinical characteristics.⁴⁵ Recently developed advanced MRI techniques allow assessment of the morphology of the intraspinal roots (i.e. motor ventral roots and sensory dorsal roots) and provide a new opportunity to assess the most proximal nerve roots and to correlate morphological with functional changes.⁵³ In **chapter 5** we performed a hypothesis generating study to explore whether the cervical intraspinal nerve roots were affected in CIDP and MMN by measuring intraspinal nerve root size. This study showed that the morphology of the intraspinal nerve roots change in CIDP and MMN and that the ventral or dorsal root location of these changes corresponds with the nature of neurological deficits. The heterogeneity of the clinical presentation of CIDP as earlier described is reflected in the abnormalities of the intraspinal roots as well. The pattern of the thickening of the intraspinal nerve reflects the various clinical phenotypes of CIDP. Dorsal intraspinal roots (i.e. sensory roots) were thicker in patients with a pure sensory or ataxic phenotype (i.e. pure sensory CIDP) compared to patients with a sensorimotor CIDP ($p = 0.001$) and patients with MND ($p = 0.006$). Patients with pure motor CIDP had thicker ventral intraspinal roots (i.e. motor roots) compared to patients with a sensorimotor phenotype ($p = 0.018$). MMN has a more homogenous presentation and we found that only the ventral roots were thicker in MMN compared to patients with MND ($p = 0.002$) and patients with CIDP with a sensorimotor phenotype ($p = 0.018$). These findings for the first time show that anatomical abnormalities correspond with clinical deficits in chronic inflammatory neuropathies. Previous MRI studies of the intraspinal roots have been performed in patients with Guillain-Barré syndrome ($n = 24$) and showed enhancement in the spinal roots after infusion with gadolinium with a preferential involvement of the ventral spinal roots in patients with pure motor Guillain-Barré syndrome. This study also showed enhancement of the ventral and dorsal spinal roots in patients with a sensorimotor phenotype. Our study extends these results to chronic inflammatory neuropathies in a large sample of patients.⁵⁴⁻⁵⁸

MRI of the intraspinal nerve roots allows us to truly study the most proximal parts of the peripheral nervous system. Although NCS techniques can be used to gather information regarding the most proximal parts of the peripheral nerve roots by using F-waves, this technique does not localize the exact site of injury. Furthermore, previous NCS studies did not show a clear relation between nerve function and nerve morphology.⁵⁹⁻⁶¹



The results of our study indicate that motor and sensory nerves can be specific targets for pathophysiological processes in inflammatory neuropathies. We think that a widespread thickening of the peripheral nerves is likely to be caused by specific isolated changes in motor or sensory nerves in CIDP and MMN. This first study on MRI of the intraspinal roots contributes to our understanding of the pathophysiology of CIDP and MMN.

Quantitative MRI of the brachial plexus

MRI is a versatile tool and with adjustments of the acquisition parameters quantitative MRI data can be obtained. Innovative MRI techniques, such as diffusion tensor imaging (DTI), T2 mapping and fat fraction analysis, provide quantitative parameters (**chapter 1**). These parameters are assumed to give information on microstructural integrity of (nervous) tissue and could contribute to our understanding of pathophysiology, for example by correlating these quantitative MRI parameters to histological findings. The basic principle is summarized in **chapter 1, Figure 1.3**. Correlations of diffusion parameters with histology are mainly based on small experimental mice studies.^{62,63} One study compared diffusion parameters (i.e. fractional anisotropy (FA), radial diffusivity (RD) and axial diffusivity (AD)) between shiverer mice (mouse model with myelin defects, n = 7) and control mice.⁶³ Histology of white matter tracts in the brain, the optic nerve and the trigeminal nerve of the shiverer mice showed a lack of myelin sheaths and DTI of these tissues showed a lower FA and a higher RD compared to the control mice, while AD did not differ. Another study evaluated RD, AD and histology of the optic nerve on four points in time in Swiss Webster mice (normal laboratory mice, n = 11) with and without retinal ischemia.⁶² AD was lower in the injured nerve after three days of ischemia and remained low, while RD remained stable and started to increase after one week. Mice were sacrificed in subgroups to correlate diffusion parameters to histology at different time points. Histological analysis after three days and seven days showed axonal loss, while myelin sheets remained intact after three days but were affected after seven days. The corresponding decrease of AD after three days and increase of RD after seven days suggests that AD correlates with axonal loss and RD with demyelination. These findings were corroborated by a comparable DTI study.⁶⁴ It is a clear limitation that only a few studies are at the base of our assumption that AD and RD correlate with axonal loss and demyelination, respectively. It seems obvious that these diffusion parameters may not only reflect axonal loss and demyelination. For example, RD reflects the degree of diffusion of water perpendicular on tissue and an increase of RD might therefore also be the result of the breakdown of the axolemma or a change in its permeability, loss of neurofilaments and microtubules, axonal swelling or an increase of the extracellular space. Changes in diffusion parameters should therefore always be carefully interpreted in the pathophysiological context of the disease.

Interpretation of changes in fat fraction and T2 relaxation times in the peripheral nerves are mainly based on our (limited) knowledge of the histological structure of the peripheral nerves and MRI physics. Interpretation of fat fraction is based on the histological fact that the peripheral nerves are surrounded by myelin. Myelin contains a high content of lipids, and the formation of the myelin sheath requires high levels of fatty acid and lipid synthesis, together with the uptake of extracellular fatty acids.⁶⁵ A decrease of the fat fraction in peripheral nerves may therefore reflect demyelination or another process that could decrease fat fraction, such as the increase of water surrounding the nerves, for example due to oedema. An increased T2 relaxation time indicates, based on MRI physics, an increase of the amount of water, for example due to oedema caused by an inflammatory reaction. However, just as interpretation of changes in diffusion parameters, these correlations between histology and changes in fat fraction and T2 relaxation time should be carefully interpreted. **Table 8.2** summarizes the (assumed) correlations between quantitative MRI parameters and histology.

Table 8.2 Possible correlations of quantitative MRI parameters and histological changes

Quantitative MRI parameter	Definition ¹	Assumed histological correlation
FA	Measures degree of anisotropy of water molecules	Tissue injury, nonspecific
MD	Summary measure of AD and RD	Tissue injury, nonspecific
AD	Degree of diffusion of water along the main axis	When decreased: axonal loss
RD	Degree of diffusion of water perpendicular on tissue	When increased: demyelination, breakdown or change in permeability of axolemma, loss of neurofilaments and microtubules, axonal swelling, increase extracellular space.
T2 relaxation time	Constant of the fitted exponential decay curve of signal intensity and different echo times	When increased: oedema
Fat fraction	Percentage of fat of the total signal on an MR image	When decreased: demyelination, oedema

Abbreviations: MRI = magnetic resonance imaging; FA = fractional anisotropy; MD = mean diffusivity; RD = radial diffusivity; AD = axial diffusivity.

¹ For an extensive explanation see **chapter 1** of this thesis.

Despite the limitations described in the previous paragraph, quantitative MRI techniques can be explored to study the condition of the peripheral nerves *in vivo* in patients with chronic inflammatory neuropathies. A few studies already showed differences in diffusion tensor parameters and T2 relaxation times in smaller cohorts of patients with CIDP, MMN and



healthy controls (n = 10 – 18).^{30,66–73} As large and systematic studies are currently lacking, we performed a relatively large cross-sectional study in **chapter 6** and evaluated quantitative MRI techniques (i.e. DTI, T2 mapping and fat fraction analysis) in patients with CIDP, MMN, MND and healthy controls. We found that CIDP is characterized by a lower FA and a higher RD than MMN, MND and healthy controls. Fat fraction was decreased and T2 relaxation times were increased in patients with CIDP. In the light of the earlier assumptions on diffusion parameters and histology, we think that the increase of RD and the decrease of fat fraction most likely reflects demyelination in our patients with CIDP. Myelin detachment and myelin loss induced by macrophages around the (inter)nodal regions have been reported in several studies on biopsies in CIDP.^{74–80} We explain the increased T2 relaxation as a result of oedema surrounding the nerves, caused by an inflammatory reaction.

RD values differed between patients with MMN and patients with CIDP, but not between patients with MMN, MND and healthy controls. This is one of our most remarkable findings as it emphasizes important differences in the underlying pathophysiologies of CIDP and MMN. We think that demyelination is probably not the dominant pathophysiological process in MMN and this is supported by scarce histological reports and electrophysiological studies that report a changed axon structure but largely intact myelin sheets.^{81–84} Also, observational studies have noted that most patients with MMN suffer from cold paresis, a feature that is not compatible with demyelination.⁸⁵ The similarities in abnormalities across diagnostic NCS, nerve ultrasound and qualitative MRI in clinical practice are therefore remarkable as well. These similar abnormalities are more likely to present common endpoints of different pathophysiological mechanisms rather than comparable etiologies, although this should be established in comparative studies that evaluate both histology and DTI.

Future studies on quantitative MRI and histology

The major limitation in the interpretation of the results of quantitative MRI studies is a lack of knowledge of the exact correlation between quantitative MRI parameters and histological changes. There are no human studies available, mostly due to the obvious ethical concerns. The ultimate, albeit theoretical, study should, in my opinion, include nerve biopsies in patients with CIDP, MMN and healthy controls, for example of nerve sites that showed conduction blocks on NCS, combined with MRI DTI, T2 mapping and fat fraction analysis of these sites. Nerve biopsy is an invasive procedure and could result in persistent nerve damage and loss of nerve function and is therefore not feasible. An alternative could be a post-mortem study in patients with CIDP or MMN but inclusion rate would probably be low and results could reflect mostly end stage disease. A better alternative is therefore the use of animal models such as experimental autoimmune neuritis (EAN) or equivalents, which is used to model Guillain-Barré syndrome and CIDP and can be induced in rats, mice, rabbits and guinea pigs.⁸⁶ Animals start to develop ataxia and weakness 2 weeks after immunization with peripheral nerve myelin proteins or other constituents. Quantitative MRI and NCS should be performed under anesthesia at baseline, after 1 week, 2 weeks and after full development of symptoms and its

parameters should be compared over time. A subgroup of the animals should be sacrificed at the same time points to correlate histological findings. This method may induce sample bias but it seems to be the best alternative available. An animal model for MMN does not exist but the rabbit model for acute motor axonal neuropathy is elicited by GM1 antibodies.⁸⁷ This triggers complement activation and can potentially disrupt the node of Ranvier, paranodal junctions and presynaptic terminals, in a similar way to that induced by antiganglioside IgG antibodies.^{87,88} Histological changes can already be seen one week after injection.⁸⁹ Quantitative MRI, NCS and histological analysis should be performed at baseline, after 4 days, 1-2 weeks, and after full development of symptoms. Future studies in these for CIDP and MMN representative animal models could give us better insights in the correlation between quantitative MRI and histology and consequently in underlying pathophysiological mechanisms.

Implementation of quantitative MRI in clinical practice

Besides its pathophysiological utilities, quantitative MRI can differentiate CIDP from MMN. Quantitative MRI shows differences in its parameters between patients with CIDP and MMN although these neuropathies show similar abnormalities on diagnostic NCS, nerve ultrasound and MRI. Quantitative MRI could be explored as a diagnostic instrument to differentiate focal or asymmetric CIDP from MMN. However, some practical challenges regarding the processing of quantitative MRI data have to be overcome if we want to implement this technique in clinical practice. Processing of quantitative MRI data occurs after acquisition of the data. These processing steps can be performed manually or automated. To minimize subjective bias, the use of an automated pipeline that processes all the data the same way is preferable. We described a custom-build automated processing pipeline in **chapter 6** that processes one data set in approximately 60 minutes and requires some technical background and training for proper use. Duration of the pipeline and user-friendliness should be improved if we finally want to implement quantitative MRI in clinical practice. A close cooperation between technical scientists and medical professionals is the key to the solution.

Prognosis

The last part of this thesis explores the role of MRI as a potential tool for prognosis, e.g. to monitor disease course and treatment effects, in patients with CIDP and MMN. In current clinical practice, challenges in management of chronic inflammatory neuropathies concern dosing (frequencies) of immunoglobulins and monitoring of treatment response. These challenges mainly rely on the fact that objective markers that predict disease course and treatment response are lacking. As advanced MRI techniques, such as DTI, can provide quantitative parameters on nerve architecture, these techniques are of interest to serve as biomarkers. Longitudinal quantitative MRI studies in patients with CIDP and MMN are currently lacking. We therefore evaluated quantitative MRI of the brachial plexus in patients with CIDP and MMN in an exploratory longitudinal study, which is described in **chapter 7**. We used the data collected in **chapter 6** as our baseline data and compared these data with data of quantitative MRI (i.e. diffusion parameters, T2 relaxation times and fat fraction) after one-year follow-up. We found that mean diffusivity, AD, RD



and fat fraction changed over time in patients with CIDP, but not in MMN. Unfortunately, we could not establish high correlations between these alterations and clinical data (i.e. age, disease duration, time since last treatment, sex, receiving maintenance treatment and treatment response). Despite the lack of clinical correlations, we established that the quantitative MRI parameters after one-year follow-up differed between patients with CIDP and MMN, which is similar to the results we found in **chapter 6**. We concluded that the differences in longitudinal data between CIDP and MMN are probably based on nerve changes that are part of the natural history of CIDP, and for example cannot be attributed to treatment response as extensively explained in the discussion section of **chapter 7**.

Previous longitudinal quantitative MRI studies mainly focused on DTI of the brain and only one study correlated clinical outcome measures (i.e. a decline in executive function) to an increase of RD after radiation therapy in patients with a primary brain tumor ($n = 22$).⁹⁰ Only one study focused on the peripheral nervous system (i.e. sciatic nerve injury) but this study was performed in rats ($n = 63$) and only evaluated FA.⁹¹ The authors reported a correlation between an increase of FA and nerve regeneration. FA is a summary measure of AD and RD and changes in FA, without knowledge of changes in AD or RD, are unspecific. Although our study is one of the first longitudinal studies of the peripheral nervous system, the results indicate that DTI, T2 mapping and fat fraction analyses of the brachial plexus are unlikely to serve as a biomarker to predict prognosis or to monitor treatment response.

Future research into reliable and robust biomarkers for (early) treatment response and prognosis could focus on other tissues as target for imaging (e.g. muscle) or on other techniques than MRI, such as laboratory findings or electrophysiology. The use of other techniques is preferred as imaging of other tissues, such as the muscles or the peripheral nerves, has considerable limitations. Quantitative muscle MRI has been studied as a potential biomarker for neuromuscular diseases, such as Duchenne muscular dystrophy, Becker muscular dystrophy, limb-girdle muscular dystrophy and spinal muscular atrophy (SMA).⁹²⁻⁹⁵ However, these studies are performed in diseases that affect the large muscles of the arms and legs. In the majority of patients with CIDP and MMN symptoms are most pronounced in the smaller distal muscles of the hands and feet. Smaller structures may be less suited for imaging studies. This might lead to lower data quality, more artifacts and loss of data and this compromise feasibility for use as a biomarker. Imaging of the peripheral nerves is an alternative but these relatively thin structures might also lead to artifacts and loss of data.⁷⁰ Furthermore, to image the peripheral nerves in the arms with MRI a patient has to be positioned with the arms above the head, which is an uncomfortable position, particularly when scan duration is long. Also other imaging modalities, such as nerve ultrasound, failed to show correlations between nerve size and clinical disease activity or treatment response in a recent longitudinal study.⁹⁶

Laboratory findings or electrophysiology to monitor disease course might be more appropriate options to explore. For example, serum neurofilament light chain (sNfL) has been studied as a biomarker in various neurological disorders, such as multiple sclerosis, SMA and ALS.⁹⁷ sNfL is released into the cerebrospinal fluid and into the blood as a subunit of a cytoskeletal protein in case of neuroaxonal damage. Two exploratory studies have been performed on the prognostic value of sNfL in disease course of patients with CIDP and MMN. The first study included patients with various acquired polyneuropathies (n = 25, from which 12 patients with CIDP and 3 with MMN) and found increased levels of sNfL in patients with a polyneuropathy, correlating to disease activity measured with the overall neuropathy limitations scale.^{98,99} As this study included various polyneuropathies the results could not be translated to a prognostic value for CIDP and MMN. A recent study that included patients with CIDP (n = 80) and healthy controls correlated sNfL levels to NCS results and found a correlation between sNfL and axonal damage.¹⁰⁰ Unfortunately, not all patients in this study underwent NCS and the found correlation was not significant when corrected for age. They also found that patients with an active disease (i.e. patients who did not respond to treatment and patients who relapsed) had higher sNfL levels compared to patients with stable disease (i.e. patients who responded to treatment and patients who were successfully withdrawn) which is promising for future studies. Future studies could include more time points of serum collection, repeated NCS and neurological examination, and eventually the use of a validated scale for impairment such as the inflammatory Rasch-built overall disability scale.¹⁰¹

Another quantitative technique that might be of interest for monitoring disease course in CIDP and MMN is the compound muscle action potential (CMAP) scan. A CMAP scan plots the response size of motor units against stimulus intensity which results in a visual assessment of one entire muscle.¹⁰² A CMAP scan can be performed in the large muscles of the arms and legs as well as in the small muscles of the hands and feet. This makes this technique of interest for patients with CIDP and MMN. The CMAP scan is rarely used in electrodiagnosis in current clinical practice but is increasingly used in scientific research. For example, the CMAP scan has been explored in patients with ALS (n = 10) and PMA (n = 3) as a potential biomarker to monitor disease progression.¹⁰³ They correlated a CMAP scan-based progression score to motor unit number estimation, which provides an estimate of the number of functional motor units, and found a significant correlation. They concluded that the CMAP scan is able to quantify disease progression in muscles affected by MND, but unfortunately did not report correlations with clinical data. Recently, the first CMAP scan study results in patients with CIDP (n = 16) have been reported in a prospective study.¹⁰⁴ This study showed that some CMAP scan parameters of the abductor pollicis brevis (i.e. step number and step percentage) decreased after 6 months of treatment, which was negatively correlated to pinch power, handgrip strength and upper MRC sum scores. Future studies should validate these results and should include more CMAP scan examinations during treatment (e.g. before and after a dose of immunoglobulins).



Conclusions

This thesis aimed to explore the feasibility of qualitative and quantitative MRI in diagnosis, pathophysiology, and prognosis of CIDP and MMN. The value of qualitative brachial plexus MRI in diagnosis of CIDP and MMN can be improved by using a quantitative assessment method. Quantitative assessment is reliable and is able to identify patients who respond to treatment but who would have been missed by nerve conduction studies and nerve ultrasound. Advanced MRI techniques, such as qualitative MRI of the intraspinal roots, provide new information on morphological changes in the cervical intraspinal roots in CIDP and MMN that correspond with functional deficits. Relatively new quantitative MRI techniques, i.e. DTI, T2 mapping and fat fraction analysis, are able to dissect pathophysiology by showing important differences in diffusion parameters between CIDP and MMN. These quantitative MRI techniques have been explored as a biomarker to predict prognosis and treatment response as well but their value as a prognostic instrument is probably low.

REFERENCES

1. Eftimov F, Lucke IM, Querol LA, et al. Diagnostic challenges in chronic inflammatory demyelinating polyradiculoneuropathy. *Brain* 2020;143:3214–3224.
2. Viala K. Diagnosis of atypical forms of chronic inflammatory demyelinating polyradiculoneuropathy: a practical overview based on some case studies. *Int. J. Neurosci.* 2016;126:777–785.
3. Doneddu PE, Cocito D, Manganelli F, et al. Atypical CIDP: Diagnostic criteria, progression and treatment response. Data from the Italian CIDP Database. *J. Neurol. Neurosurg. Psychiatry* 2019;90:125–132.
4. Ikeda S, Koike H, Nishi R, et al. Clinicopathological characteristics of subtypes of chronic inflammatory demyelinating polyradiculoneuropathy. *J. Neurol. Neurosurg. Psychiatry* 2019;90:988–996.
5. Bunschoten C, Jacobs BC, Van den Bergh PYK, et al. Progress in diagnosis and treatment of chronic inflammatory demyelinating polyradiculoneuropathy. *Lancet Neurol.* 2019;18:784–794.
6. Oaklander A, Lunn M, Hughes R, et al. Treatments for chronic inflammatory demyelinating polyradiculoneuropathy (CIDP): An overview of systematic reviews. *Cochrane Database Syst. Rev.* 2017;13:1–33.
7. Kuwabara S, Misawa S, Mori M, et al. Long term prognosis of chronic inflammatory demyelinating polyneuropathy: A five year follow up of 38 cases. *J. Neurol. Neurosurg. Psychiatry* 2006;77:66–70.
8. Kuitwaard K, Hahn AF, Vermeulen M, et al. Intravenous immunoglobulin response in treatment-naïve chronic inflammatory demyelinating polyradiculoneuropathy. *J. Neurol. Neurosurg. Psychiatry* 2015;86:1331–1336.
9. Nobile-Orazio E. Chronic inflammatory demyelinating polyradiculoneuropathy and variants: where we are and where we should go. *J Peripher Nerv Syst* 2014;13:2–13.
10. Vlam L, Van Der Pol WL, Cats EA, et al. Multifocal motor neuropathy: Diagnosis, pathogenesis and treatment strategies. *Nat. Rev. Neurol.* 2012;8:48–58.
11. Westeneng HJ, Debray TPA, Visser AE, et al. Prognosis for patients with amyotrophic lateral sclerosis: development and validation of a personalised prediction model. *Lancet Neurol.* 2018;17:423–433.
12. van Schaik I, van den Berg L, de Haan R, Vermeulen M. Intravenous immunoglobulin for multifocal motor neuropathy. *Cochrane Database Syst. Rev.* 2005;2:920–921.
13. Van Den Berg-Vos RM, Franssen H, Wokke JHJ, Van Den Berg LH. Multifocal motor neuropathy: long-term clinical and electrophysiological assessment of intravenous immunoglobulin maintenance treatment. *Brain* 2002;125:1875–1886.
14. Van den Berg-Vos RM, Franssen H, Visser J, et al. Disease severity in multifocal motor neuropathy and its association with the response to immunoglobulin treatment. *J. Neurol.* 2002;249:330–336.
15. Taylor B V., Wright RA, Harper CM, Dyck PJ. Natural history of 46 patients with multifocal motor neuropathy with conduction block. *Muscle and Nerve* 2000;23:900–908.
16. Al-Zuhairy A, Sindrup SH, Andersen H, Jakobsen J. A population-based and cross-sectional study of the long-term prognosis in multifocal motor neuropathy. *J. Peripher. Nerv. Syst.* 2019;24:64–71.
17. Cats EA, Jacobs BC, Yuki N, et al. Multifocal motor neuropathy: Association of anti-GM1 IgM antibodies with clinical features. *Neurology* 2010;75:1961–1967.
18. Vlam L, Cats EA, Harschnitz O, et al. Complement activity is associated with disease severity in multifocal motor neuropathy. *Neurol. Neuroimmunol. NeuroInflammation* 2015;2:1–8.
19. van den Bergh PYK, Hadden RDM, Bouche P, et al. European Federation of Neurological Societies/Peripheral Nerve Society Guideline on management of chronic inflammatory



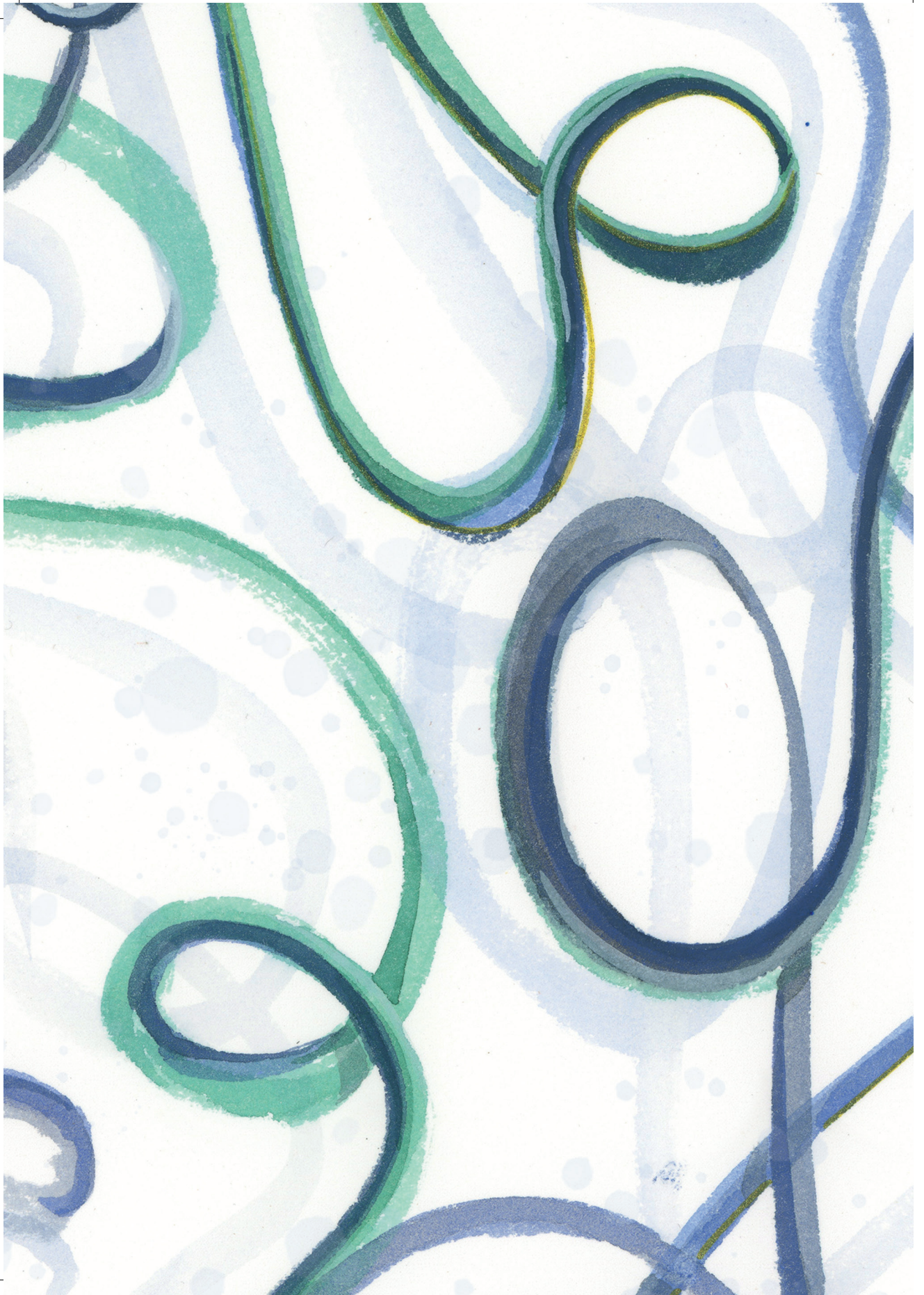
- demyelinating polyradiculoneuropathy: Report of a joint task force of the European Federation of Neurological Societies and the Peripher. Eur. J. Neurol. 2010;17:356–363.
20. Breiner A, Brannagan TH. Comparison of sensitivity and specificity among 15 criteria for chronic inflammatory demyelinating polyneuropathy. *Muscle and Nerve* 2014;50:40–46.
 21. Rajabally YA, Nicolas G, Piéret F, et al. Validity of diagnostic criteria for chronic inflammatory demyelinating polyneuropathy: A multicentre European study. *J. Neurol. Neurosurg. Psychiatry* 2009;80:1364–1368.
 22. Van Schaik IN, Léger JM, Nobile-Orazio E, et al. European Federation of Neurological Societies/Peripheral Nerve Society Guideline on management of multifocal motor neuropathy. Report of a Joint Task Force of the European Federation of Neurological Societies and the Peripheral Nerve Society - First revis. *J Peripher Nerv Syst* 2010;15:295–301.
 23. Olney RK, Lewis RA, Putnam TD, Campellone J V. Consensus criteria for the diagnosis of multifocal motor neuropathy. *Muscle and Nerve* 2003;27:117–121.
 24. Van Den Berg-Vos RM, Franssen H, Wokke JHJ, et al. Multifocal motor neuropathy: Diagnostic criteria that predict the response to immunoglobulin treatment. *Ann. Neurol.* 2000;48:919–926.
 25. van Es HW, van den Berg LH, Franssen H, et al. Magnetic resonance imaging of the brachial plexus in patients with multifocal motor neuropathy. *Neurology* 1997;48:1218–1224.
 26. Castillo M, Mukherji SK. MRI of enlarged dorsal ganglia, lumbar nerve roots, and cranial nerves in polyradiculoneuropathies. *Neuroradiology* 1996;38:516–520.
 27. Duggins AJ, Mcleod JG, Pollard JD, et al. Spinal root and plexus hypertrophy in chronic inflammatory demyelinating polyneuropathy. *Brain* 1999;1383–1390.
 28. Morgan GW, Barohn RJ, Bazan III C, et al. Nerve root enhancement with MRI in inflammatory demyelinating polyradiculoneuropathy. *Neurology* 1993;43:618–620.
 29. Eurelings M, Notermans NC, Franssen H, et al. MRI of the brachial plexus in polyneuropathy associated with monoclonal gammopathy. *Muscle and Nerve* 2001;24:1312–1318.
 30. Oudeman J, Eftimov F, Strijkers GJ, et al. Diagnostic accuracy of MRI and ultrasound in chronic immune-mediated neuropathies. *Neurology* 2020;94:e62–e74.
 31. Goedee HS, Van Der Pol WL, Van Asseldonk JTH, et al. Diagnostic value of sonography in treatment-naïve chronic inflammatory neuropathies. *Neurology* 2017;88:143–151.
 32. Herraets IJT, Goedee HS, Telleman JA, et al. Nerve ultrasound for the diagnosis of chronic inflammatory neuropathy: a multicenter validation study. *Neurology* 2020;95:e1745–e1753.
 33. Tazawa K-I, Matsuda M, Yoshida T, et al. Spinal Nerve Root Hypertrophy on MRI: Clinical Significance in the Diagnosis of Chronic Inflammatory Demyelinating Polyradiculoneuropathy. *Intern. Med.* 2008;47:2019–2024.
 34. Hiwatashi A, Togao O, Yamashita K, et al. Evaluation of chronic inflammatory demyelinating polyneuropathy: 3D nerve-sheath signal increased with inked rest-tissue rapid acquisition of relaxation enhancement imaging (3D SHINKEI). *Eur. J. Radiol.* 2017;27:447–453.
 35. Tanaka K, Mori N, Yokota Y, Suenaga T. MRI of the cervical nerve roots in the diagnosis of chronic inflammatory demyelinating polyradiculoneuropathy: a single-institution, retrospective case-control study. *BMJ Open* 2013;3:e003443.
 36. vanEsMA, Hardiman O, Chio A, et al. Amyotrophic lateral sclerosis. *Lancet* 2017;390:2084–2098.
 37. Allen JA, Lewis RA. CIDP diagnostic pitfalls and perception of treatment benefit. *Neurology* 2015;85:498–504.
 38. Combarros O, Calleja J, Polo JM, Berciano J. Prevalence of hereditary motor and sensory neuropathy in Cantabria. *Acta Neurol. Scand.* 1987;75:9–12.
 39. Theadom A, Roxburgh R, MacAulay E, et al. Prevalence of Charcot-Marie-Tooth disease across the lifespan: A population-based epidemiological

- study. *BMJ Open* 2019;9:e029240.
40. Müller KI, Ghelue M Van, Lund I, et al. The prevalence of hereditary neuromuscular disorders in Northern Norway. *Brain Behav.* 2021;11:e01948.
 41. Fridman V, Reilly MM. Inherited Neuropathies. *Semin. Neurol.* 2015;35:407–423.
 42. Rison RA, Beydoun SR. Paraproteinemic neuropathy: A practical review. *BMC Neurol.* 2016;16:1–14.
 43. Jomier F, Bousson V, Viala K, et al. Prospective study of the additional benefit of plexus MRI in the diagnosis of CIDP. *Eur. J. Neurol.* 2020;27:181–187.
 44. Briani C, Cacciavillani M, Lucchetta M, et al. MR neurography findings in axonal multifocal motor neuropathy. *J. Neurol.* 2013;260:2420–2422.
 45. Goedee HS, Jongbloed BA, van Asseldonk J-TH, et al. A comparative study of brachial plexus sonography and magnetic resonance imaging in chronic inflammatory demyelinating neuropathy and multifocal motor neuropathy. *Eur. J. Neurol.* 2017;24:1307–1313.
 46. Ferreira V, Piechnik S, Robson M, et al. Myocardial tissue characterization with magnetic resonance imaging. *J. Thorac. Imaging* 2014;29:147–154.
 47. Dekkers IA, Lamb HJ. Clinical application and technical considerations of T1 and T2(*) mapping in cardiac, liver, and renal imaging. *Br. J. Radiol.* 2018;91:1–13.
 48. Kim PK, Hong YJ, Im DJ, et al. Myocardial T1 and T2 mapping: Techniques and clinical applications. *Korean J. Radiol.* 2017;18:113–131.
 49. Herraets IJT, Goedee HS, Telleman JA, et al. Nerve ultrasound improves detection of treatment-responsive chronic inflammatory neuropathies. *Neurology* 2020;94:e1470–e1479.
 50. Pitarokoili K, Kronlage M, Bäumer P, et al. High-resolution nerve ultrasound and magnetic resonance neurography as complementary neuroimaging tools for chronic inflammatory demyelinating polyneuropathy. *Ther. Adv. Vaccines* 2018;11:1–11.
 51. Jongbloed BA, Haakma W, Goedee HS, et al. Comparative study of peripheral nerve MRI and ultrasound in multifocal motor neuropathy and amyotrophic lateral sclerosis. *Muscle Nerve* 2016;54:1133–1135.
 52. van Rosmalen MHJ, Goedee HS, van der Gijp A, et al. Quantitative assessment of brachial plexus MRI for the diagnosis of chronic inflammatory neuropathies. *J. Neurol.* 2020;268:978–988.
 53. Mandija S, Froeling M, van der Kolk A, et al. Large field-of-view high resolution 3D imaging of the thoracolumbar nerve roots inside the spinal canal. In: *ISMRM 2019 Abstracts*. 2019 p. 2883.
 54. Berciano J, Sedano MJ, Pelayo-Negro AL, et al. Proximal nerve lesions in early Guillain-Barré syndrome: implications for pathogenesis and disease classification. *J. Neurol.* 2017;264:221–236.
 55. Byun WM, Park WK, Park BH, et al. Guillain-Barré syndrome: MR imaging findings of the spine in eight patients. *Radiology* 1998;208:137–141.
 56. Yikilmaz A, Doganay S, Gumus H, et al. Magnetic resonance imaging of childhood Guillain-Barré syndrome. *Child's Nerv. Syst.* 2010;26:1103–1108.
 57. Coskun A, Kumandas S, Pac A, et al. Childhood Guillain-Barré Syndrome: MR Imaging in Diagnosis and Follow-Up. *Acta radiol.* 2003;44:230–235.
 58. Mulkey SB, Glasier CM, El-Nabbout B, et al. Nerve root enhancement on spinal MRI in pediatric Guillain-Barré syndrome. *Pediatr. Neurol.* 2010;43:263–269.
 59. Kimura J. Principles and pitfalls of nerve conduction studies. *Ann. Neurol.* 1984;16:415–429.
 60. Goedee H. High-resolution ultrasound in diagnosis of polyneuropathies. In: *ISBN 9789462336841*. 2017 p. 167–190.
 61. Pitarokoili K, Schlamann M, Kerasnoudis A, et al. Comparison of clinical, electrophysiological, sonographic and MRI features in CIDP. *J. Neurol. Sci.* 2015;357:198–203.
 62. Song SK, Sun SW, Ju WK, et al. Diffusion tensor imaging detects and differentiates axon and myelin degeneration in mouse optic nerve after retinal ischemia. *Neuroimage* 2003;20:1714–1722.
 63. Song SK, Sun SW, Ramsbottom MJ, et al. Dysmyelination revealed through MRI as



- increased radial (but unchanged axial) diffusion of water. *Neuroimage* 2002;17:1429–1436.
64. Morisaki S, Kawai Y, Umeda M, et al. In vivo assessment of peripheral nerve regeneration by diffusion tensor imaging. *J. Magn. Reson. Imaging* 2011;33:535–542.
65. Poitelon Y, Kopec AM, Belin S. Myelin Fat Facts: An Overview of Lipids and Fatty Acid Metabolism. *Cells* 2020;9:1–17.
66. Kakuda T, Fukuda H, Tanitame K, et al. Diffusion tensor imaging of peripheral nerve in patients with chronic inflammatory demyelinating polyradiculoneuropathy: A feasibility study. *Neuroradiology* 2011;53:955–960.
67. Mathys C, Aissa J, Zu Hörste GM, et al. Peripheral Neuropathy: Assessment of Proximal Nerve Integrity By Diffusion Tensor Imaging. *Muscle Nerve* 2013;48:889–896.
68. Markvardsen LH, Vaeggemose M, Ringgaard S, Andersen H. Diffusion tensor imaging can be used to detect lesions in peripheral nerves in patients with chronic inflammatory demyelinating polyneuropathy treated with subcutaneous immunoglobulin. *Neuroradiology* 2016;58:745–752.
69. Kronlage M, Pitarokoili K, Schwarz D, et al. Diffusion Tensor Imaging in Chronic Inflammatory Demyelinating Polyneuropathy: Diagnostic Accuracy and Correlation with Electrophysiology. *Invest. Radiol.* 2017;52:701–707.
70. Haakma W, Jongbloed BA, Froeling M, et al. MRI shows thickening and altered diffusion in the median and ulnar nerves in multifocal motor neuropathy. *Eur. Radiol.* 2017;27:2216–2224.
71. Lichtenstein T, Sprenger A, Weiss K, et al. MRI biomarkers of proximal nerve injury in CIDP. *Ann. Clin. Transl. Neurol.* 2018;5:19–28.
72. Hiwatashi A, Togao O, Yamashita K, et al. Simultaneous MR neurography and apparent T2 mapping in brachial plexus: Evaluation of patients with chronic inflammatory demyelinating polyradiculoneuropathy. *Magn. Reson. Imaging* 2018;55:112–117.
73. Hiwatashi A, Togao O, Yamashita K, et al. Lumbar plexus in patients with chronic inflammatory demyelinating polyradiculoneuropathy: evaluation with simultaneous T2 mapping and neurography method with SHINKEI. *Br. J. Radiol.* 2018;91:20180501.
74. Matthews WB, Howell DA, Hughes RC. Relapsing corticosteroid-dependent polyneuritis. *J. Neurol. Neurosurg. Psychiatry* 1970;33:330–337.
75. Torvik A, Lunder T. A case of chronic demyelinating polyneuropathy resembling the Guillan-Barré Syndrome. *J. Neurol. Sci.* 1977;32:45–52.
76. Matsuda M, Ikeda SI, Sakurai S, et al. Hypertrophic neuritis due to chronic inflammatory demyelinating polyradiculoneuropathy (CIDP): A postmortem pathological study. *Muscle and Nerve* 1996;19:163–169.
77. Auer RN, Bell RB, Lee MA. Neuropathy with Onion Bulb Formations and Pure Motor Manifestations. *Can. J. Neurol. Sci. / J. Can. des Sci. Neurol.* 1989;16:194–197.
78. Oh SJ, Claussen G, Odabasi Z, Palmer CP. Multifocal demyelinating motor neuropathy: pathologic evidence of ‘inflammatory demyelinating polyradiculoneuropathy’. *Neurology* 1995;45:1828–1832.
79. Sasaki M, Ohara S, Oide T, et al. An autopsy case of chronic inflammatory demyelinating polyradiculoneuropathy with respiratory failure. *Muscle and Nerve* 2004;30:382–387.
80. Koike H, Nishi R, Ikeda S, et al. Ultrastructural mechanisms of macrophage-induced demyelination in CIDP. *Neurology* 2018;91:1051–1060.
81. Krarup C, Stewart JD, Sumne AJ, et al. A syndrome of asymmetric limb weakness with motor conduction block. *Neurology* 1990;40:118–127.
82. Adams D, Kuntzer T, Steck AJ, et al. Motor conduction block and high titres of anti-GM1 ganglioside antibodies: Pathological evidence of a motor neuropathy in a patient with lower motor neuron syndrome. *J. Neurol. Neurosurg. Psychiatry* 1993;56:982–987.
83. Veugelers B, Theys P, Lammens M, et al. Pathological findings in a patient with amyotrophic lateral sclerosis and multifocal motor neuropathy with conduction block. *J. Neurol. Sci.* 1996;136:64–70.

84. Garg N, Park SB, Howells J, et al. Conduction block in immune-mediated neuropathy: paraneoplastic versus axonopathy. *Eur. J. Neurol.* 2019;26:1121–1129.
85. Straver DCG, Van Asseldonk JTH, Notermans NC, et al. Cold paresis in multifocal motor neuropathy. *J. Neurol.* 2011;258:212–217.
86. Soliven B. Animal models of autoimmune neuropathy. *ILAR J.* 2014;54:282–290.
87. Susuki K, Nishimoto Y, Yamada M, et al. Acute motor axonal neuropathy rabbit model: Immune attack on nerve root axons. *Ann. Neurol.* 2003;54:383–388.
88. Piepers S, Jansen MD, Cats EA, et al. IVIg inhibits classical pathway activity and anti-GM1 IgM-mediated complement deposition in MMN. *J. Neuroimmunol.* 2010;229:256–262.
89. Uncini A, Santoro M, Corbo M, et al. Conduction abnormalities induced by sera of patients with multifocal motor neuropathy and anti-GM1 antibodies. *Muscle Nerve* 1993;16:610–615.
90. Tringale K, Nguyen T, Bahrami N, et al. Identifying early diffusion imaging biomarkers of regional white matter injury as indicators of executive function decline following brain radiotherapy: A prospective clinical trial in primary brain tumor patients. *Radiother Oncol* 2019;132:27–33.
91. Farinas AF, Esteve IVM, Pollins AC, et al. Diffusion Magnetic Resonance Imaging Predicts Peripheral Nerve Recovery in a Rat Sciatic Nerve Injury Model. *Plast. Reconstr. Surg.* 2020;145:949–956.
92. Warman Chardon J, Straub V. The Role of Muscle Imaging in the Diagnosis and Assessment of Children with Genetic Muscle Disease. *Neuropediatrics* 2017;48:233–241.
93. Ponrartana S, Ramos-Platt L, Wren TAL, et al. Effectiveness of diffusion tensor imaging in assessing disease severity in Duchenne muscular dystrophy: preliminary study. *Pediatr. Radiol.* 2015;45:582–589.
94. Durmus H, Yilmaz R, Gulsen-Parman Y, et al. Muscle magnetic resonance imaging in spinal muscular atrophy type 3: Selective and progressive involvement. *Muscle and Nerve* 2017;55:651–656.
95. Otto L, Froeling M, van Eijk R, et al. Quantification of disease progression in spinal muscular atrophy with muscle MRI – a pilot study. *NMR Biomed.* 2021;in press
96. Telleman J, Herraets I, Goedee H, et al. Prognostic value of nerve ultrasound: a prospective multicenter study on the natural history of polyneuropathy. *Eur. J. Neurol.* 2021;in press
97. Khalil M, Teunissen CE, Otto M, et al. Neurofilaments as biomarkers in neurological disorders. *Nat. Rev. Neurol.* 2018;14:577–589.
98. Mariotto S, Farinazzo A, Magliozzi R, et al. Serum and cerebrospinal neurofilament light chain levels in patients with acquired peripheral neuropathies. *J. Peripher. Nerv. Syst.* 2018;23:174–177.
99. Graham RC, Hughes RAC. A modified peripheral neuropathy scale: The Overall Neuropathy Limitations Scale. *J. Neurol. Neurosurg. Psychiatry* 2006;77:973–976.
100. van Lieverloo GGA, Wieske L, Verhamme C, et al. Serum neurofilament light chain in chronic inflammatory demyelinating polyneuropathy. *J. Peripher. Nerv. Syst.* 2019;24:187–194.
101. Nes S Van, Vanhoutte E, van Doorn P, et al. Rasch-built Overall Disability Scale (R-ODS) for immune-mediated peripheral neuropathies. *Int. Classif.* 2011;76:337–345.
102. Blok JH, Ruitenbergh A, Maathuis EM, Visser GH. The electrophysiological muscle scan. *Muscle and Nerve* 2007;36:436–446.
103. Maathuis EM, Drenthen J, Van Doorn PA, et al. The CMAP scan as a tool to monitor disease progression in ALS and PMA. *Amyotroph. Lateral Scler. Front. Degener.* 2013;14:217–223.
104. Okhovat AA, Advani S, Moradi K, et al. Application of CMAP scan for the evaluation of patients with chronic inflammatory demyelinating polyneuropathy: a prospective study. *Clin. Neurophysiol.* 2021;online ahead of print.



Addendum

Nederlandse samenvatting

Review comité

Dankwoord

Publicatielijst

Curriculum Vitae



NEDERLANDSE SAMENVATTING

Het perifere zenuwstelsel verbindt de hersenen en het ruggenmerg met de spieren in ons lichaam. Via de perifere zenuwen wordt informatie van en naar de hersenen getransporteerd en zijn wij in staat om kracht te zetten en te bewegen, en om temperatuurverschillen, pijn en aanraking te voelen. Bij schade aan deze perifere zenuwen wordt er gesproken van een neuropathie (of van een polyneuropathie als meer dan 1 zenuw beschadigd is). Neuropathieën kunnen verschillende oorzaken hebben, zoals beschadiging van de zenuw door alcohol, medicatie, lever- of nierfalen, vitaminedeficiënties of een idiopathische oorzaak. Behandeling en beloop van de neuropathie kan erg variëren afhankelijk van de onderliggende oorzaak. Het is daarom belangrijk om de juiste oorzaak te vinden en zo de juiste diagnose te stellen. Bij het zoeken naar de juiste diagnose maakt de neuroloog gebruik van de klinische presentatie en het neurologisch onderzoek. Ook aanvullende onderzoekstechnieken, zoals bloedonderzoek, zenuwgeleidingsonderzoek en beeldvorming kunnen hierbij helpen. Het is belangrijk dat deze aanvullende onderzoekstechnieken betrouwbaar zijn en dat zij met ruim voldoende zekerheid de aan- of afwezigheid van de ziekte kunnen voorspellen, want alleen dan zijn ze bruikbaar in de klinische praktijk.

Chronische inflammatoire demyeliniserende polyneuropathie (CIDP) en multifocale motore neuropathie (MMN) zijn beide zeldzame polyneuropathieën met een inflammatoire oorzaak. Bij patiënten met “typische” CIDP is er sprake van een langzaam progressief, symmetrisch en distaal krachtsverlies, dat gepaard gaat met gevoelsstoornissen en de afwezigheid van de reflexen in alle extremiteiten. CIDP is echter een heterogeen ziektebeeld en bestaat uit typische CIDP en varianten hiervan. Het stellen van de diagnose ‘CIDP’ is daarom soms een uitdaging voor de neuroloog. Het stellen van de juiste diagnose is echter belangrijk omdat CIDP reageert op behandeling met immunoglobulinen, corticosteroiden of plasmaferese. De behandeling kan het krachtsverlies en de gevoelsstoornissen verbeteren en kan verdere progressie en onomkeerbare schade aan de zenuwen voorkomen.

MMN daarentegen is een homogener ziektebeeld en de klachten treden vooral asymmetrisch op en met name in de handen, maar soms ook in de voeten. Er is sprake van krachtsverlies zonder gevoelsstoornissen. De symptomen bij MMN kunnen erg lijken op de symptomen van amyotrofische laterale sclerose (ALS) of progressieve spinale musculaire atrofie (PSMA). Het is in de klinische praktijk belangrijk om onderscheid te maken tussen MMN en ALS en PSMA omdat de prognose en behandelopties erg verschillen. Voor ALS en PSMA bestaat op dit moment nog altijd geen symptomatische of curatieve behandeling, terwijl MMN, net als CIDP, op behandeling met immunoglobulinen reageert. MMN verslechtert op behandeling met corticosteroiden en het onderscheid met CIDP moet daarom ook altijd gemaakt worden.



Uit eerdere studies over CIDP is bekend dat er een aantal factoren zijn die een gunstig beloop van de ziekte en de prognose kunnen voorspellen, zoals een subacuut begin, symmetrie van de klachten en afwezigheid van spieratrofie. Er is weinig bekend over de factoren, anders dan het gebruik van immunoglobulinen, die van invloed zijn op de ziekteprogressie bij MMN. Hier is weinig onderzoek naar gedaan. Om hier beter inzicht in te krijgen is het ziektebeloop bij (met immunoglobulinen behandelde) patiënten met MMN bestudeerd in **hoofdstuk 2**. De resultaten van deze longitudinale studie laten zien dat MMN een progressieve aandoening is en dat de meeste patiënten, ondanks behandeling met immunoglobulinen, een langzame afname van de spierkracht ervaren. Factoren die van invloed zijn op deze afname van de spierkracht zijn afwezige reflexen ten tijde van het stellen van de diagnose, als ook het aanwezig zijn van reeds zeer uitgesproken zwakte op dat moment. Deze uitgesproken zwakte wordt weer beïnvloed door de aanwezigheid van anti-GM1 antilichamen in het bloed van de patiënt en door een langere ziekteduur tot aan start van therapie. Op basis van deze resultaten is het dus van cruciaal belang om de diagnose MMN tijdig te stellen zodat vlot gestart kan worden met de behandeling met immunoglobulinen.

Het stellen van de diagnose CIDP of MMN is in de huidige klinische praktijk gestoeld op een aantal criteria die de kernsymptomen omvatten van CIDP of MMN, tezamen met het vinden van specifieke afwijkingen bij zenuwgeleidingsonderzoek. Er bestaan in de huidige literatuur verschillende versies van deze diagnostische consensus criteria, wat aangeeft dat er weinig overeenstemming bestaat over hoe de diagnose CIDP of MMN gesteld zou moeten worden. Daarnaast hebben de diagnostische hulpmiddelen die gebruikt worden in de huidige diagnostische criteria hun beperkingen wat de toepassing van de criteria verder bemoeilijkt. Zenuwgeleidingsonderzoek kan bij patiënten met CIDP of MMN vertragingen laten zien in de zenuwgeleiding en de meest specifieke afwijkingen bestaan uit het vinden van blokkades in de zenuwgeleiding (*demyelinisatie*). Het vinden van deze vertragingen of blokkades is niet gemakkelijk en meestal is er veel ervaring en neurofysiologische expertise nodig om de afwijkingen te vinden. Dit maakt het zenuwgeleidingsonderzoek voor CIDP en MMN lastig en kan ervoor zorgen dat de afwijkingen worden gemist. Als het zenuwgeleidingsonderzoek geen of onvoldoende aanwijzingen toont voor demyelinisatie kunnen ondersteunende onderzoekstechnieken nodig zijn om de diagnose CIDP of MMN te stellen of juist te verwerpen. Deze ondersteunende onderzoekstechnieken bestaan uit bloedonderzoek en beeldvorming van de zenuwen. Beeldvorming van de zenuwen betreft doorgaans magnetic resonance imaging (MRI) maar in gespecialiseerde medische centra wordt tegenwoordig ook gebruik gemaakt van zenuwechografie. Op een MRI van het zenuwvlechtwerk in de nek, de *plexus brachialis*, kunnen verdikkingen worden gezien van de cervicale zenuwwortels (**Figuur 1.4A**). Daarnaast kan het signaal van de zenuwwortels ‘intenser’, ofwel witter, zijn op T2-gewogen opnamen (**Figuur 1.4B**) of kunnen de zenuwwortels aankleuren na toediening van gadolinium.

In de huidige klinische praktijk worden de MRI-scans van de plexus brachialis subjectief beoordeeld omdat er geen afkapwaarden bestaan voor abnormale zenuwdikte. Dit kan leiden tot grote variaties tussen beoordelaars en het beperkt de betrouwbaarheid van de uitslag van het onderzoek en

daarmee ook de diagnostische waarde. Systematische studies naar de betrouwbaarheid van de huidige beoordelingsmethode ontbreken en daarom is in **hoofdstuk 3** onderzocht hoe betrouwbaar de huidige (kwalitatieve) beoordelingsmethode is. Deze betrouwbaarheid is bepaald aan de hand van de inter-observer variabiliteit. Uit de studie blijkt dat de inter-observer variabiliteit hoog is, wat erop wijst dat er veel variatie is tussen beoordelaars. In slechts 52% van alle beoordeelde scans blijken de beoordelaars het eens te zijn. De resultaten van deze studie onderstrepen dat een meer objectieve en kwantitatieve beoordelingsmethode nodig is als we de diagnostische waarde van MRI voor CIDP en MMN willen verbeteren. In **hoofdstuk 4** is daarom een kwantitatieve beoordelingsmethode ontwikkeld voor het beoordelen van MRI van de plexus brachialis. De inter- en intra-observer variabiliteit en de diagnostische waarde van de beoordelingsmethode wordt onderzocht en tevens wordt de toegevoegde waarde van MRI bovenop zenuwgeleidingsonderzoek en zenuwechografie uitgezocht. De kwantitatieve beoordelingsmethode heeft een acceptabele betrouwbaarheid (intra-rater interclass correlation coefficient (ICC) 0.55 – 0.87; interrater ICC 0.65 – 0.90) en voldoende diagnostische waarde (area under the curve 0.78 – 0.81). Uit deze studie blijkt verder dat MRI van de plexus brachialis vooral van toegevoegde waarde is voor patiënten met CIDP die géén afwijkingen laten zien bij zenuwgeleidingsonderzoek of zenuwechografie maar wel een hoge klinische verdenking hebben. Bij 5 van de 50 (10%) patiënten is MRI toch nog afwijkend als gebruik gemaakt wordt van de in deze studie ontwikkelde kwantitatieve beoordelingsmethode. Deze patiënten laten bij behandeling een goede behandelrespons zien en zij zijn dus gebaat bij het maken van een MRI. Uit deze studie blijkt ook dat het minder nuttig is om nog een MRI te maken als zenuwgeleidingsonderzoek of zenuwechografie al een afwijkend resultaat laten zien. Zenuwgeleidingsonderzoek en zenuwechografie kunnen tezamen namelijk al met voldoende zekerheid de diagnose stellen of juist verwerpen. Voor patiënten met MMN geldt dat het maken van een MRI van beperkte toegevoegde waarde is. Bij een verdenking op MMN is het alleen nuttig om een MRI te maken als er geen zenuwechografie beschikbaar is in het ziekenhuis. Zenuwechografie is, zoals eerder genoemd, een relatief nieuwe onderzoekstechniek die vooral beschikbaar is in academische medische centra. In een aanzienlijk deel van de ziekenhuizen in Nederland (en daarbuiten) is zenuwechografie nog niet beschikbaar en kan het verrichten van een MRI wel van toegevoegde waarde zijn. In **Figuur 8.1** en **Figuur 8.2** worden aanbevelingen gedaan om de huidige diagnostische criteria voor respectievelijk CIDP en MMN te herzien op basis van de resultaten afkomstig uit de studies in **hoofdstuk 3** en **hoofdstuk 4**.

MRI wordt in de huidige klinische praktijk vooral ingezet als diagnostisch hulpmiddel. Echter is MRI een zeer veelzijdig beeldvormend instrument en kan het ook op andere manieren een bijdrage leveren aan de medische praktijk. Door het aanpassen van de instellingen van de MRI-scanner kan MRI bijvoorbeeld gebruikt worden om een beter inzicht te krijgen in onderliggende pathofysiologische mechanismen of als biomarker voor ziekteprogressie. Het tweede gedeelte van dit proefschrift besteedt aandacht aan deze toepassing van MRI middels het bestuderen van nieuwere en geavanceerde MRI-technieken.



Huidige studies over zenuwbeeldvorming bij CIDP en MMN hebben zich voornamelijk gericht op het in beeld brengen van de perifere zenuwen en de plexus brachialis of lumbosacralis. Over eventuele afwijkingen, zoals verdikkingen, in de meer proximale delen van de perifere zenuwen, de intraspinale zenuwwortels, is weinig bekend. In **hoofdstuk 5** wordt gebruik gemaakt van een relatief nieuw ontwikkelde MRI-sequentie om deze intraspinale zenuwwortels (i.e. de ventrale motore zenuwwortels en de dorsale sensibele zenuwwortels) af te beelden. Deze studie laat zien dat ook de intraspinale zenuwwortels verdikt kunnen zijn in vergelijking met gezonde controles ($p < 0.001$) en ziektecontroles (patiënten met ALS en PSMA; $p = 0.003$). In deze studie wordt ook gekeken naar verdikkingen binnen klinische fenotypes. Er wordt onderscheid gemaakt tussen patiënten met een puur motorische neuropathie (patiënten met MMN en motorische CIDP), een puur sensibele of atactische neuropathie (sensibele of atactische CIDP) en een sensomotorische neuropathie (sensomotorische CIDP). Uit de resultaten blijkt dat patiënten met een puur sensibele neuropathie verdikte dorsale zenuwwortels hebben, terwijl de patiënten met een puur motorische neuropathie verdikte ventrale zenuwwortels hebben. Deze studie laat voor het eerst zien dat er veranderingen zijn in de intraspinale zenuwwortels in patiënten met CIDP en MMN en dat de locatie van deze veranderingen overeenkomt met de neurologische klachten. Eerdere zenuwechografie- of zenuwgeleidingsonderzoekstudies zijn er nog niet in geslaagd om een dergelijke correlatie aan te tonen. De verdikkingen die gezien worden in de plexus brachialis of lumbosacralis en perifere zenuwen van de armen en benen zouden dus vooral veroorzaakt kunnen worden door geïsoleerde veranderingen in ofwel motorische ofwel sensorische zenuwen. Hiermee draagt deze studie bij aan een beter begrip van de pathofysiologie van CIDP en MMN.

Een andere geavanceerde MRI-techniek betreft kwantitatieve MRI. In de huidige klinische praktijk wordt er vooral gebruikt gemaakt van kwalitatieve MRI en is het product van een scansessie alleen een plaatje. MRI-technieken die kwantitatief van aard zijn produceren naast een (3D) plaatje ook een getal of parameter. Voorbeelden van kwantitatieve MRI-technieken zijn diffusion tensor imaging (DTI), T2 mapping en analyse van de vetfractie. DTI produceert verschillende parameters die iets zeggen over de mate en richting van de diffusie van watermoleculen langs rechte structuren, zoals de zenuwbanen. T2 mapping produceert een parameter die iets zegt over de T2 relaxatietijd. Analyse van de vetfractie produceert een percentage dat de hoeveelheid vet in een bepaalde structuur weergeeft. Op basis van eerdere studies wordt aangenomen dat deze kwantitatieve MRI-parameters kunnen correleren aan histologische bevindingen. Hiermee bieden deze MRI-technieken de mogelijkheid om *in vivo* de zenuwarchitectuur te bestuderen en dat kan weer gebruikt worden om de pathofysiologie te ontrafelen of om te dienen als biomarker voor ziekteprogressie. In CIDP en MMN zijn tot op heden enkele explorerende studies verricht in kleine groepen patiënten. Omdat grote en systematische studies ontbreken is in **hoofdstuk 6** een studie verricht in een grote groep patiënten met CIDP en MMN. De studie bestudeert welke kwantitatieve MRI-technieken verschillen kunnen aantonen tussen patiënten met CIDP en MMN. De plexus brachialis wordt hierbij in beeld gebracht met DTI en er wordt gebruik gemaakt van T2 mapping en analyse van de vetfractie van de

zenuwen. De opvallendste bevinding uit deze studie is dat er verschillen zijn in de diffusieparameters tussen patiënten met CIDP en MMN. Zo hebben patiënten met CIDP een hogere 'radial diffusivity' dan patiënten met MMN ($p < 0.001$), een diffusie parameter die lijkt te correleren met demyelinisatie. Dit kan erop wijzen dat het onderliggende pathofysiologische proces wezenlijk anders is bij patiënten met CIDP en MMN, terwijl zij wel dezelfde afwijkingen vertonen bij zenuwgeleidingsonderzoek, zenuwechografie en kwalitatieve MRI. De resultaten suggereren met name dat het pathofysiologische proces bij patiënten met MMN niet primair lijkt te berusten op demyelinisatie. Deze studie draagt bij aan een beter begrip van de onderliggende pathofysiologische processen in CIDP en MMN en geeft verdere richting aan toekomstig onderzoek naar mogelijke biomarkers voor ziekteprogressie en behandelrespons.

Het laatste gedeelte van dit proefschrift richt zich op kwantitatieve MRI en de toepassing hiervan voor gebruik als biomarker. Biomarkers kunnen onder andere gebruikt worden om het ziektebeloop te vervolgen en om behandelrespons te monitoren. Voor CIDP en MMN bestaan er op dit moment geen robuuste en betrouwbare biomarkers, terwijl dit voor de klinische praktijk wel nodig is gezien het ziektebeloop en de respons op behandeling van patiënt tot patiënt kan variëren. **Hoofdstuk 7** beschrijft daarom een longitudinale studie die onderzoekt of kwantitatieve MRI van de plexus brachialis geschikt zou kunnen zijn om te dienen als biomarker voor CIDP en MMN. Diverse kwantitatieve MRI-parameters worden verkregen middels DTI, T2 mapping en analyse van de vetfractie en zij worden opgevolgd over 1 jaar tijd. De resultaten van deze studie laten zien dat bij patiënten met CIDP verschillende diffusieparameters en de vetfractie veranderen over de tijd. Deze veranderingen correleren helaas niet aan een van de klinische parameters zoals behandelrespons en spierkracht. Patiënten met MMN lieten geen veranderingen zien in een van de kwantitatieve MRI-parameters over de tijd. Op basis van deze studie lijkt kwantitatieve MRI van de plexus brachialis een beperkte prognostische waarde te hebben. Deze studie geeft daarentegen wel richting voor toekomstig onderzoek. Zo zouden toekomstige onderzoekers zich kunnen richten op het gebruik van andere technieken dan beeldvorming.

Samengevat richt dit proefschrift zich op het onderzoeken van de verschillende kenmerken van CIDP en MMN middels meerdere MRI-studies. Het verbeteren van de waarde van MRI binnen de diagnostiek van CIDP en MMN wordt beschreven, alsook het gebruik van MRI voor het bestuderen van de pathofysiologie en als biomarker voor het vervolgen van ziektebeloop en respons op behandeling. Dit proefschrift beschrijft dat MRI van de plexus brachialis betrouwbaar kan worden ingezet voor het stellen van de diagnose CIDP of MMN, mits een kwantitatieve beoordelingsmethode gebruikt wordt. Met name voor CIDP-patiënten is MRI van toegevoegde waarde. Verder laat MRI van de intraspinale zenuwen zien dat er ook morfologische veranderingen zijn in de meest proximale delen van het perifere zenuwstelsel bij patiënten met CIDP en MMN en dat dit lijkt samen te hangen met de neurologische klachten. Geavanceerde, kwantitatieve MRI-technieken, zoals DTI, zijn in staat om verschillen aan te tonen in de plexus brachialis tussen CIDP en MMN, wat erop wijst dat



de primaire onderliggende pathofysiologische processen van deze twee neuropathieën verschillend zijn ondanks gelijke uitkomsten bij zenuwgeleidingsonderzoek, zenuwechografie en kwalitatieve MRI. Wat betreft het voorspellen van ziektebeloop of respons op behandeling lijken de kwantitatieve MRI-technieken onderzocht in dit proefschrift van beperkte waarde en minder geschikt om als biomarker gebruikt te worden in de klinische praktijk.





REVIEW COMITÉ

Prof. dr. N.M. Wulffraat

Professor kinderreumatologie, Universitair medisch centrum Utrecht

Prof. dr. P.A. van Doorn

Professor neuromusculaire ziekten, Erasmus medisch centrum Rotterdam

Prof. dr. D.W.J. Klomp

Professor high precision structural and metabolic imaging, Universitair medisch centrum Utrecht

Prof. dr. N.C. Notermans

Professor neuromusculaire ziekten, Universitair medisch centrum Utrecht

Dr. R.A.J. Nijelstein

Radioloog, Universitair medisch centrum Utrecht





DANKWOORD

Een promotietraject biedt niet alleen de mogelijkheid om je te ontplooiën binnen de wetenschap, maar geeft ook tijd om na te denken over binnen welk specialisme je je medische kennis verder wilt uitbreiden, om uit te vinden welke balans tussen werk en privé het beste past in je leven en om te trainen voor een eerste Nijmeegse Vierdaagse. Ik kijk dan ook terug op een uiteenlopende periode in mijn leven als het gaat om hoe de tijd in de afgelopen drie jaar besteed kon worden en hoe dit op een hele waardevolle, maar ook praktisch nuttige, manier heeft bijgedragen aan de vormgeving van mijn leven. Ik ben daarom dankbaar dat het mij gegeven is om dit mee te mogen maken.

Allereerst heb ik een woord van zeer grote dank voor alle betrokken patiënten en vrijwilligers die de tijd en de bereidheid gevonden hebben om deel te nemen aan mijn MRI-studie en daarmee een enorme bijdrage hebben geleverd aan de totstandkoming van dit proefschrift. Ik vind het erg bijzonder om te zien dat zij vanuit heel Nederland naar Utrecht zijn gekomen voor deelname aan het onderzoek.

Natuurlijk wil ik ook alle collega's, vrienden en familie bedanken die op wat voor manier dan ook hebben bijgedragen aan dit proefschrift, waarvan een aantal in het bijzonder.

Ludo, het was heel prettig om samen te werken met iemand met zoveel kennis op het gebied van inflammatoire neuropathieën en MMN in het bijzonder. Jouw wetenschappelijke ervaring en schrijfvaardigheden waren onmisbaar voor de artikelen in dit proefschrift en hiervoor ben ik je dan ook erg dankbaar. Daarnaast zei jij me ooit dat het in principe niet goed is, als ik het gevoel heb dat het niet goed is, en deze wijsheid zal ik meenemen in mijn verdere carrièrepad maar ook daarbuiten. Verder gaf jij me mee dat het goed is om altijd een vervolgvraag te stellen op een eerder gestelde vraag, ik zal dit proberen toe te passen in de toekomst, bijvoorbeeld tijdens mijn opleiding tot radioloog. Hartelijk dank voor de fijne samenwerking!

Jeroen, ik heb je de afgelopen jaren leren kennen als een onderzoeker die ervan houdt om snelle stappen te nemen en efficiënt om te gaan met de tijd. Dat ligt mij natuurlijk wel. Voor nu zou ik graag een moment stil willen staan om je te bedanken. Je commentaar op de manuscripten drukte telkens weer een radiologische stempel op de neurologische stukken en dat maakte het voor mij zo leuk. Verder wil ik je bedanken voor de aanmoedigingen en complimenten op zijn tijd want het zorgt er oprecht voor dat een PhD-student zin heeft om door te gaan met het volgende project!



Stephan, hartelijk dank voor je enthousiasme en ijver gedurende de gehele looptijd van mijn promotietraject. In de eerste week van mijn onderzoekstijd nam je me op sleeptouw en kruisten we het UMC Utrecht door om handen te schudden met iedereen die potentieel belangrijk zou kunnen zijn voor mijn onderzoek. Dit heeft ertoe geleid dat ik geheel gedesoriënteerd maar met een vliegende start aan mijn onderzoek kon beginnen. Verder zou ik je graag alle succes willen wensen met het begeleiden van de PhD's die na mij zullen komen!

Martijn, tijdens mijn promotietraject was je absoluut laagdrempelig benaderbaar en kon ik je altijd opzoeken voor een vraag of uitleg over MRI-fysica. Meerdere keren heb ik (geloof ik) dezelfde vragen gesteld en elke keer probeerde je het op een andere manier uit te leggen met figuren en filmpjes. Voor deze onderwijsmomenten en het geduld daaromtrent ben ik je erg dankbaar. De samenwerking met iemand met een niet-medische achtergrond heeft mijn blik verder verruimd. Op naar nog meer MRI-onderzoek in de toekomst!

Anouk en Theo, mijn overstap van de neurologie naar de radiologie heb ik grotendeels aan jullie te danken. Voor jullie bereidwilligheid om te helpen bij het scoren van mijn scans ben ik zeer dankbaar en de betogen over de radiologie heb ik in mijn oren geknoopt en hebben me absoluut over de streep getrokken om uiteindelijk te solliciteren voor de opleiding. Anouk, ik kijk ernaar uit om samen te gaan werken binnen de radiologie. Theo, bedankt voor al je wijsheid en geniet van je pensioen!

Leden van de beoordelingscommissie, prof. dr. N.M. Wulffraat, prof. dr. P.A. van Doorn, prof. dr. D.W.J. Klomp, prof. dr. N.C. Notermans en dr. R.A.J. Nievelstein, hartelijk dank voor de tijd die u heeft vrijgemaakt om mijn proefschrift te lezen en te beoordelen.

Paranimfen, Jeroen en Ea, wie had ooit gedacht dat we hier samen zouden staan toen we in 2008 (13 jaar terug) over Herman en de zonnestrallen stonden te zingen in de Gieter? Studeren begon voor ons, samen met Thijs, Nadine en Lisette met biomedische wetenschappen aan de VU. Wat een special stationsensations mooie mensen. Je moet het. Een proefschrift is toch wel echt het officiële einde van de studietijd en het lijkt me dan ook niet meer dan logisch om dit samen met jullie op 4 november 2021 te verdedigen.

Ramona en Diana, Seline, Niels, en de MRI-laboranten, bedankt voor jullie hulp bij de MRI-planning, het protocol, de geïnteresseerde vragen en de laagdrempelige praatjes tussendoor. Ik wil ook de scanner op MR4 bedanken want die heeft mij eigenlijk nooit in de steek gelaten.

Christa, Fay-Lynn en Simone, met jullie helpende hand werd dit onderzoek in goede banen geleid. Christa, ontzettend bedankt voor het versturen van alle brieven, ongeveer tweehonderd telefoontjes naar patiënten en het geduld bij het inplannen van de MRI's. Je was altijd welwillend als er weer een nieuwe inclusieronde bedacht was en jij die vervolgens moest inplannen naast je SMA-

werkzaamheden. Heel knap, het valt mij op dat je veel oog hebt voor het welzijn van de patiënt en dat is een waardevolle eigenschap. Fay-Lynn, voor iemand die de zaken liever vandaag regelt dan morgen (ik), ben jij heel prettig om mee samen te werken. Je bent duidelijk, scheidt hoofd- van bijzaken, geeft grenzen aan en werkt hard. Onze etentjes door heel Utrecht relativeerden de boel op z'n tijd behoorlijk. Veel dank voor je luisterend oor. Simone, hartelijk dank voor de hulp via het ALS-centrum bij het vinden van ALS-patiënten die bereid waren mee te doen met het onderzoek.

Ruben, voor het idee van het beoordelingsmodel uit hoofdstuk 4 verdien jij absoluut de credits! Bedankt voor het delen van je statistische kennis en het stellen van kritische vragen, maar ook voor je engelengeduld bij het uitleggen van mixed models.

Bram, Diederik, Camiel, Chantal, Eva, Ewout, Hannelore, Harold, Ingrid, Janna, Jeroen, Johan, Kevin, Leandra, Loes, Louise, Mark en Vi, oh oh oh, dit is het momentooo. Huts! Het zit erop, onze samenwerking als Polysmals-crew. Covid gooide roet in de gezellige dagen op het lab, maar de periode daarvoor ben ik niet vergeten. Dus: dank voor de kritische gesprekken en de hulp bij presentaties (iedereen), Matlab scripts en andere computerdingen (Hannelore en Harold), maar vooral ook voor de potjes tafelvoetbal (iedereen), de woordgrappen (soms was het best wel grappig, Bram), het leren uitspreken van *immunoglobulins* (Jeroen), gewoon er zijn (Louise, Janna, Loes en Ingrid), fietsen naar Utrecht CS (Mark), het introduceren van een koelkast op het lab (Eva) en de muziek op vrijdagmiddag (iedereen!).

Nens, als bachelor-student zie ik mezelf nog zitten in jullie tuin in Nijmegen-Oost pratend over een "idee dat nog op de plank lag". Ongemerkt was dit voor mij het begin van mijn tocht in 'de wereld van de beeldvorming' en jij hebt me destijds jouw voortvarende manier van onderzoek doen geleerd. Deze enorme efficiëntie heb ik nu zelf toegepast tijdens mijn promotietraject en dat werkte. Dat jij aanwezig was bij mijn presentatie op mijn allereerste congres (Berlijn, 2019) maakte voor mij de cirkel rond. Ik ben dankbaar dat jij, en ook Sigrid, aan het begin staan van mijn wetenschappelijke carrière. Bedankt!

Lieve Eva en Marit, en lieve Anne en Edith, ik voel me gezegend met zulke vriendinnen als jullie. Bedankt voor jullie oprechte interesse in mijn onderzoek de afgelopen jaren maar vooral voor de, minstens zo belangrijke, ontspanning tussendoor tijdens bijvoorbeeld de vierdaagse en carnaval.

Lieve Jopke, Robbert-Jan, Jannick en Kayleigh, tot tweemaal toe heeft de Sint me de afgelopen jaren een surprise gegeven die te maken had met MRI of DTI, dat zegt toch wat. Jullie zijn altijd geïnteresseerd geweest in mijn onderzoek en de vorderingen daaromheen. Bedankt daarvoor. Ik ben blij met zo'n lieve schoonfamilie!



Lieve opa, de afgelopen jaren vroeg je me altijd met aandacht hoe het onderzoek ervoor stond, en vooral wanneer ik tussen de “geleerde heren” zou staan om te promoveren. Het was een van de redenen waarom ik hard werkte, met de hoop dat de tijd ons niet zou inhalen en je erbij zou zijn. Helaas hebben we er geen grip op, en kijk jij nu mee vanaf de andere kant. Ik kom je ooit nog wel eens vertellen hoe het geweest is.

Lieve oma, het is een drukke tijd geweest, en nog steeds, en rust en ontspanning is dan belangrijk. Gelukkig vind ik die altijd als ik bij jou ben, alleen of samen met Jonas. Bij jou in de tuin zitten of even thee op de bank is voor mij al genoeg om daarna weer verder te kunnen werken. Bedankt daarvoor.

Mijn lieve zussen, Brigitte en Anouk, samen hebben wij aan één woord (of letter), blik of beweging genoeg om te begrijpen wat de ander bedoelt. Voor ons drie is het vanzelfsprekend, maar ik heb geleerd dat het heel bijzonder is om zo’n sterke zussenband te hebben. Familie is er voor altijd, en dat beseffen wij alledrie. Bedankt dat jullie, samen met Lennart en Lorenzo, in mijn leven zijn op de momenten die er echt toe doen, en die ervoor zorgen dat ik uitgerust weer verder kon met dit proefschrift, zoals bijvoorbeeld de etentjes bij papa en mama thuis en alle tijd die we samen al hebben mogen doorbrengen aan de Kirchstraße, bij de Ascherhütte en in de Hühnerstall.

Lieve, lieve, lieve Juerd, jij bent mijn grote liefde. Jij bent er iedere dag voor mij en jij zorgt dat ik elke dag met een lach opsta en met een lach weer ga slapen. Altijd blij, altijd positief. Samen met die lieve kleine Jonas hebben wij het bijzonder goed en dat koester ik. Ik voel me gelukkig en sterk met iemand als jij aan mijn zijde en daar ben ik je, vanuit het diepst van mijn hart, dankbaar voor.

Lieve papa en lieve mama, jullie zijn mijn rotsen in de branding en dat zijn jullie altijd al geweest. Niets is te veel als ik, Brigitte en Anouk maar gelukkig zijn. Ik heb dan ook aan niemand zoveel te danken als aan jullie. Bedankt voor jullie vertrouwen, jullie onvoorwaardelijke steun en liefde en alle normen en waarden die jullie mij geleerd hebben. Het helpt me iedere dag. Het heeft er ook toe geleid dat dit proefschrift geworden is zoals het geworden is, en het traject ernaar toe gelopen is zoals het gelopen is. Aan niemand anders wil ik dit proefschrift dan ook opdragen. Alsjeblieft, dit proefschrift is voor jullie!





PUBLICATIELIJST

1. Bhansing KJ, **Van Rosmalen MHJ**, Van Engelen BG, et al. Increased fascial thickness of the deltoid muscle in dermatomyositis and polymyositis: An ultrasound study. *Muscle and Nerve* 2015;52:534–539.
2. Lieba-Samal D, Van Eijk JJJ, **Van Rosmalen MHJ**, et al. Extremely painful multifocal acquired predominant axonal sensorimotor neuropathy of the upper limb. *J. Ultrasound Med.* 2018;37:1565–1574.
3. Van Alfen N, Doorduyn J, **Van Rosmalen MHJ**, et al. Phrenic neuropathy and diaphragm dysfunction in neuralgic amyotrophy. *Neurology* 2018;91:e843–e849.
4. **van Rosmalen MHJ**, Lieba-Samal D, Pillen S, van Alfen N. Ultrasound of peripheral nerves in neuralgic amyotrophy. *Muscle and Nerve* 2019;59:55–59.
5. **van Rosmalen MHJ**, Goedee HS, Gijp A, et al. Low interrater reliability of brachial plexus MRI in chronic inflammatory neuropathies. *Muscle Nerve* 2020;61:779–783.
6. Herraets I, **van Rosmalen MHJ**, Bos J, et al. Clinical outcomes in multifocal motor neuropathy: A combined cross-sectional and follow-up study. *Neurology* 2020;95:e1979–e1987.
7. **van Rosmalen MHJ**, Goedee HS, van der Gijp A, et al. Quantitative assessment of brachial plexus MRI for the diagnosis of chronic inflammatory neuropathies. *J. Neurol.* 2020;268:978–988.
8. **van Rosmalen MHJ**, Goedee H, Derks R, et al. Quantitative MRI of the brachial plexus shows specific changes in nerve architecture in chronic inflammatory demyelinating polyneuropathy, multifocal motor neuropathy and motor neuron disease. *Eur. J. Neurol.* 2021;28:2716–2726.
9. **van Rosmalen MHJ**, Froeling M, Mandija S, et al. MRI of the intraspinal nerve roots in patients with chronic inflammatory neuropathies: abnormalities correlate with clinical phenotypes. *J. Neurol.* 2021;Accepted
10. **van Rosmalen MHJ**, Goedee HS, van Eijk RPA, et al. Quantitative MRI of the brachial plexus in CIDP and MMN: a longitudinal cohort study. 2021;Submitted





CURRICULUM VITAE

Marieke Helena Johanna van Rosmalen is geboren op 27 maart 1990 te Rosmalen. In 2008 voltooide zij het gymnasium aan het Jeroen Bosch College te 's-Hertogenbosch. Zij studeerde vervolgens biomedische wetenschappen aan de Vrije Universiteit te Amsterdam, waarna zij in 2009 naar Nijmegen verhuisde om daar te starten met de studie geneeskunde aan de Radboud Universiteit. Tijdens haar studie werkte zij als student-onderzoeker op de afdeling klinische neurofysiologie van het Radboudumc onder begeleiding van dr. N. van Alfen. Zij leerde hier zenuwechografie van de perifere zenuwen en de plexus brachialis te verrichten, definieerde normaalwaarden voor zenuwdikte en onderzocht de diagnostische waarde van zenuwechografie voor patiënten met neuralgische amyotrofie. De interesse voor beeldvorming was hiermee gewekt.

Na haar artsexamen in 2016 besloot zij te gaan werken op de afdeling neurologie in het Amphia ziekenhuis te Breda en later in het Onze Lieve Vrouwe Gasthuis te Amsterdam. De interesse voor wetenschappelijk onderzoek bleef bestaan en zij begon in 2018 met haar promotieonderzoek op de afdeling neuro-musculaire ziekten en de afdeling radiologie van het Universitair Medisch Centrum (UMC) Utrecht naar de waarde van magnetic resonance imaging (MRI) in de diagnostiek, pathofysiologie en de prognose voor patiënten met chronische inflammatoire neuropathieën onder begeleiding van prof. dr. W.L. van der Pol en prof. dr. J. Hendrikse. De resultaten van het promotieonderzoek staan in dit proefschrift beschreven. Tevens heeft zij de resultaten van dit onderzoek gepresenteerd op het MyoMRI congres in 2019 in Berlijn, op het Spierziektencongres van Spierziekten Nederland in 2018, 2019 en 2020, op een bijeenkomst van de Belgisch-Nederlandse neuro-musculaire studieclub in 2020 en op een internationaal congres over neuromusculaire beeldvorming (ICCNMI) in september 2021. Na haar promotieonderzoek is zij in het UMC Utrecht en in het Gelre ziekenhuis te Apeldoorn gestart met de opleiding tot radioloog onder begeleiding van dr. R.A.J. Nievelstein en drs. K.E. Droogh – de Greve. Marieke is getrouwd met Juerd Wijntjes en zij wonen samen met hun zoon in Berlicum, een natuurrijk Brabants dorp onder de rook van 's-Hertogenbosch.



